

AD743762

NAVAL POSTGRADUATE SCHOOL

Monterey, California



THESIS

RECEIVED
13 1972
SLOTTED
A

THE THERMAL DECOMPOSITION OF RDX

by

Kenneth Kinard Miles

Thesis Advisor:

J. E. Sinclair

March 1972

Reproduced by
NATIONAL TECHNICAL
INFORMATION SERVICE
Springfield, Va. 22151

Approved for public release; distribution unlimited.

89

The Thermal Decomposition of RDX

by

Kenneth Kinard Miles
Lieutenant, United States Navy
B.S., United States Naval Academy, 1965

Submitted in partial fulfillment of the
requirements for the degree of

MASTER OF SCIENCE IN AERONAUTICAL ENGINEERING

from the

NAVAL POSTGRADUATE SCHOOL
March 1972

Author

Kenneth K. Miles

Approved by:

James Sinclair

Thesis Advisor

Carl L. ...

Chairman, Department of Aeronautics

Milton H. ...

Academic Dean

DOCUMENT CONTROL DATA - R & D

(Security classification of title, body of abstract and indexing annotation must be entered when the overall report is classified)

1. ORIGINATING ACTIVITY (Corporate author) Naval Postgraduate School Monterey, California 93940		2a. REPORT SECURITY CLASSIFICATION Unclassified	
		2b. GROUP	
3. REPORT TITLE The Thermal Decomposition of RDX			
4. DESCRIPTIVE NOTES (Type of report and inclusive dates) Master's Thesis; March 1972			
5. AUTHOR(S) (First name, middle initial, last name) Kenneth Kinard Miles			
6. REPORT DATE March 1972	7a. TOTAL NO. OF PAGES 90	7b. NO. OF REFS 10	
8a. CONTRACT OR GRANT NO.		8b. ORIGINATOR'S REPORT NUMBER(S)	
a. PROJECT NO.			
c.	8d. OTHER REPORT NO(S) (Any other numbers that may be assigned this report)		
d.			
10. DISTRIBUTION STATEMENT Approved for public release; distribution unlimited.			
11. SUPPLEMENTARY NOTES		12. SPONSORING MILITARY ACTIVITY Naval Postgraduate School Monterey, California 93940	
13. ABSTRACT <p>Cyclotrimethylenetrinitramine (RDX or Cyclonite) exists in two polymorphic species, α and β. The α-form is stable under normal conditions, whereas β-RDX is formed by recrystallization from high boiling solvents. It immediately transfers to the α-form in the presence of excess α-RDX, and it is therefore assumed that RDX as it exists in its normal state consists solely of the α polymorph.</p> <p>The thermal decomposition of RDX has been comprehensively studied at Picatinny Arsenal by means of quantitative measurements of the decomposition products. The thermal stability of explosive compositions has also been investigated by measuring the rate of gas evolution during decomposition.</p> <p>It was the purpose of this work to obtain thermal and kinetic data for RDX using Differential Thermal Analysis (DTA) experimental methods. These results and techniques were compared with those obtained using the other methods and with theoretical values. The favorable results lend credibility to the DTA method and suggest that further development in the technique will prove useful in providing a fast and reasonably accurate method of characterizing the thermal and kinetic properties of new explosives and propellants.</p>			

14. KEY WORDS	LINK A		LINK B		LINK C	
	ROLE	WT	ROLE	WT	ROLE	WT
autocatalytic cyclotrimethylenetrinitramine (RDX) differential thermal analysis explosive induction time thermal decomposition time-to-deflagration						

ABSTRACT

Cyclotrimethylenetrinitramine (RDX or Cyclonite) exists in two polymorphic species, α and β . The α -form is stable under normal conditions, whereas β -RDX is formed by recrystallization from high boiling solvents. It immediately transfers to the α -form in the presence of excess α -RDX, and it is therefore assumed that RDX as it exists in its normal state consists solely of the α polymorph.

The thermal decomposition of RDX has been comprehensively studied at Picatinny Arsenal by means of quantitative measurements of the decomposition products. The thermal stability of explosive compositions has also been investigated by measuring the rate of gas evolution during decomposition.

It was the purpose of this work to obtain thermal and kinetic data for RDX using Differential Thermal Analysis (DTA) experimental methods. These results and techniques were compared with those obtained using the other methods and with theoretical values. The favorable results lend credibility to the DTA method and suggest that further development in the technique will prove useful in providing a fast and reasonably accurate method of characterizing the thermal and kinetic properties of new explosives and propellants.

TABLE OF CONTENTS

I.	INTRODUCTION	8
II.	THERMAL DECOMPOSITION OF EXPLOSIVES	10
III.	REACTION KINETICS IN DTA	12
IV.	EXPERIMENTAL PROCEDURE	16
	A. APPARATUS	16
	B. SAMPLE PREPARATION	23
	C. VARIABLE HEATING RATE EXPERIMENT	25
	D. ISOTHERMAL EXPERIMENT	27
V.	RESULTS AND DISCUSSION	29
VI.	CONCLUSIONS AND RECOMMENDATIONS	33
APPENDIX A.	HEATING RATE VS. PEAK TEMPERATURE, 500.00-530.50 °K	81
APPENDIX B.	HEATING RATE VS. PEAK TEMPERATURE, 500.00-530.50 °K	82
APPENDIX C.	RATE CONSTANT VS. ISOTHERMAL TEMPERATURE, 470.00-550.00 °K	83
APPENDIX D.	RATE CONSTANT VS. ISOTHERMAL TEMPERATURE, 470.00-550.00 °K	85
	LIST OF REFERENCES	87
	INITIAL DISTRIBUTION LIST	88
	FORM DD 1473	89

LIST OF TABLES

I.	Experimental data, variable heating rate thermal analysis --	37
II.	Kinetic parameters -----	38
III.	Heating rate data comparison -----	38
IV.	Rate constant data comparison -----	38
V.	Experimental data, isothermal analysis -----	39
VI.	Isothermal analysis, induction time data -----	39
VII.	Isothermal analysis, time-to-deflagration data -----	40
VIII.	Isothermal results using reciprocal time and MAA methods --	40

LIST OF ILLUSTRATIONS

1.	DuPont 900 Differential Thermal Analyzer -----	17
2.	Remote cell assembly -----	18
3.	Differential thermocouple -----	16
4.	DTA system schematic -----	19
5.	Heating block and thermocouple arrangement -----	20
6.	DTA thermogram, inert sample -----	21
7.	DTA thermogram, active sample -----	22
8.	Transition temperatures -----	22
9.	DTA thermogram, RDX sample heated at $20^{\circ}\text{C}/\text{min}$ -----	41
10.	DTA thermogram, Ammonium Nitrate sample heated at $20^{\circ}\text{C}/\text{min}$ -----	42
11-17.	DTA thermograms, RDX samples, heating rates varied from $2.43\text{-}30.00^{\circ}\text{C}/\text{min}$ -----	43-49
18-36.	Series of plots of $T^{\circ}\text{K}$ versus time in seconds for each heating rate -----	50-68
37.	Plot of $\ln [\phi/T_m^2]$ versus $1000/T_m$, variable heating rate data -----	69
38.	DTA thermogram showing reproducibility, three runs made with RDX samples at heating rates of $6^{\circ}\text{C}/\text{min}$ -----	70
39.	DTA thermogram showing sample size effects, two runs made with RDX samples at heating rates of $4^{\circ}\text{C}/\text{min}$ -----	71
40-44.	DTA thermograms, RDX samples, isothermal runs at temperatures of $467.25\text{-}483.00^{\circ}\text{K}$ -----	72-76
45.	Isothermal data plot using induction time data, $\ln[1/t_0]$ versus $1000/T$ -----	77
46.	Isothermal data plot using induction time data, $\ln[t_0/T^2]$ versus $1000/T$ -----	78
47.	Isothermal data plot using time-to-deflagration data, $\ln [1/\tau]$ versus $1000/T$ -----	79
48.	Isothermal data plot using time-to-deflagration data, $\ln [\tau/T^2]$ versus $1000/T$ -----	80

TABLE OF SYMBOLS

A	= Arrhenius frequency factor.
c	= Heat capacity.
dq/dt	= Chemical energy generated by decomposition.
DTA	= Differential Thermal Analysis.
dx/dt	= Rate of reaction.
E_a	= Activation energy, calories/mole.
k	= Rate constant.
MAA	= Microimmersion Autocatalytic Analysis.
n	= Empirical order of reaction.
R	= Gas constant, 1.987 calories/mole °K.
T	= Temperature in degrees Kelvin.
T_m	= The sample temperature at which the peak in the DTA thermogram occurs.
T_o	= Temperature at the outside of the sample or reference cylinder.
T_r	= Temperature of the reference material.
T_s	= Temperature of the sample material.
t_o	= Induction time.
x	= Fraction of material reacted.
θ	= Differential temperature ΔT .
κ	= Thermal conductivity.
ρ	= Sample density.
τ	= Time-to-deflagration.
ϕ	= dT/dt , heating rate supplied to sample explosive, °K/min.

ACKNOWLEDGMENT

The author wishes to express his gratitude to Professor J. E. Sinclair for his help and guidance and to Professor G. F. Kinney and Assoc. Prof. J. W. Schultz of the Department of Material Science and Chemistry and Asst. Prof. D. W. Netzer of the Department of Aeronautics for their timely advice. The technical assistance provided by R. F. Edwards and R. C. Smith was greatly appreciated.

I. INTRODUCTION

Explosives undergo thermal decomposition at temperatures far below those at which spontaneous explosion may occur. The decomposition reaction is important in determining the stability of the explosive. A considerable amount of heat energy is liberated in the decomposition process. This highly exothermic reaction accelerates to a high velocity culminating in deflagration or detonation when the rate of heat production is greater than the rate of heat loss to the surroundings by conduction and convection. Explosives in their normal state are metastable, the free energy of the explosive being considerably higher than its decomposition products. For an explosive to remain stable at ordinary temperatures, its decomposition reaction must depend on relatively high activation energies.

Kinetic studies are therefore important in the study of explosive reaction mechanisms. The Differential Thermal Analysis technique is one of several that is used to study reaction kinetics. When a reaction occurs in DTA, the change in heat content and in the thermal properties of the sample is indicated by a deflection in the thermogram. For reactions that possess activation energies and thereby proceed at a rate varying with temperature, the position of the peak varies with the heating rate. The activation energy and Arrhenius frequency factor can be determined from this experimental information.

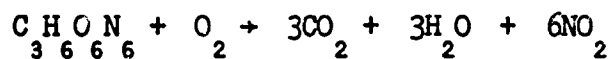
Cyclotrimethylenetrinitramine (RDX or Cyclonite) is an important explosive used in many military composite explosives. RDX melts at 203°C, and the decomposition of liquid cyclonite follows the unimolecular rate

equation over the range of temperatures 213-299°C. [Robertson 1949]. The Arrhenius frequency factor is large, and the activation energy is of the order of 50 kcal/mole. The high value of the Arrhenius frequency factor is a possible indication of self heating.

The purpose of this work was to investigate the thermal decomposition of RDX using DTA experimental techniques. In the decomposition of 1,3,5,7-Tetranitro-1,3,5,7-Tetrazacyclooctane (HMX), three separate peaks were observed in the DTA thermogram, and three separate activation energies obtained from the DTA data [Hondee 1971]. It was of interest to determine whether these phenomena were evident in the decomposition of RDX, to detect any evidence of self-heating, and to compare the kinetic data obtained with that found in the literature.

II. THERMAL DECOMPOSITION OF EXPLOSIVES

The investigation of the thermal behavior of explosives involves both the study of chemical kinetics and the theory of transport properties. The chemical kinetics of explosive reactions are not fully understood due to the high reaction rates and temperatures involved and the complexity of the products of the reaction. The decomposition of RDX may be written:



This reaction may be accurate for detonation but is unlikely to occur thermally due to the large number of bonds which must be broken in the parent molecule. Attempts to study these reactions require that measurements of the decomposition rates be made at relatively low temperatures.

Thermal decomposition is essentially a heat-balance problem. The heat loss to the surroundings and the accumulation of heat in the explosive equals the chemical energy generated by the decomposition of the explosive.

$$\kappa \nabla^2 T + \rho c \dot{\phi} = dq/dt$$

This can be written simply as $F + G = H$. The chemical energy generated by the decomposition, H , increases exponentially with temperature. The heat loss, F , consists of thermal conduction, which is proportional to the thermal gradient, and radiation, which follows the Stefan-Boltzmann T^4 law. The heat loss therefore increases at a slower rate, especially since the heats of activation of explosives are of the order of 50 kcal/mole. The accumulation of heat in the explosive, G , becomes more important as the temperature increases, causing acceleration of the decomposition.

Some explosives liberate energy in their interior due to a slow chemical reaction that is often a decomposition reaction. This is known as self-heating and causes the temperature of the material to increase, resulting in an increase in the rate of reaction. Dynamic equilibrium is reached when the heat is removed as fast as it is generated. If heat is generated faster than it can be removed, the temperature increases more rapidly and the reaction accelerates. The maximum temperature of the surroundings for which a steady state is possible is called the critical temperature for the explosive. Above this temperature, the material will self-heat until ignition or explosion occurs [Longwell 1961].

Decomposition reactions are sometimes autocatalytic or catalyzed by small amounts of impurities. The decomposition products or impurities in the explosive may act as a catalyst in that the reaction rate is increased as more products are produced. The decomposition rates of these materials then become a function of the duration or extent of the decomposition.

III. REACTION KINETICS IN DTA

The material of this section is a summary of Kissinger's work on the theory of differential thermal analysis [Ref. 2]. DTA techniques produce a deflection or peak (ΔT) in the thermogram due to a change in heat content and thermal properties of the active sample during a reaction. This peak temperature is affected by experimental technique, and is often higher than known transition or decomposition temperatures.

The temperature of maximum deflection is defined by kinetic constants and the heating rate. If a reaction possesses an activation energy, it will proceed at a rate varying with temperature and the position of the peak will vary with the heating rate. The temperature of maximum deflection in DTA is also the temperature at which the reaction rate is a maximum. The temperature distribution of the sample explosive obeys the general heat flow equation;

$$\frac{\partial T}{\partial t} - \frac{\kappa}{\rho c} \nabla^2 T = \frac{1}{\rho c} \frac{dq}{dt} \quad (1)$$

where the rate of heat generated due to chemical reaction per unit volume of the sample is equal to zero in the inert reference. The temperature distribution in the reference material is then given by;

$$\frac{\partial T}{\partial t} = \frac{\kappa}{\rho c} \nabla^2 T \quad (2)$$

Assuming the sample to be a cylinder of radius a and of infinite length, integration of equation 2 yields;

$$T_r = T_o + \phi t - \frac{\phi \rho c a^2}{4\kappa} \quad (3)$$

where $\phi = dT/dt$ and the outside temperature is given by $T = T_o + \phi t$.

The rate of heat generated due to chemical reaction is a function of

temperature in the active sample. Equation 1 is therefore a non-linear partial differential equation. Assuming that the temperature of the outside of the tube rises at a linear rate, the solution for the temperature at the center of the sample will be of the form;

$$T_s = T_h + \phi t - f(dq/dt) \quad (4)$$

where $f(dq/dt)$ is a function of the reaction rate and includes secondary effects of the reaction such as changes in volume, density and thermal properties.

The differential temperature is the difference between temperatures at the centers of the two samples;

$$\theta = f\left(\frac{dq}{dt}\right)_{\text{sample}} - \left(\frac{\phi \rho c a^2}{\kappa}\right)_{\text{reference}} \quad (5)$$

and is a maximum at the temperature of maximum deflection where $d\theta/dt$ is zero.

$$d\theta/dt = f'(dq/dt) d^2q/dt^2 \quad (6)$$

When the derivative of the rate of heat absorption is zero it can be seen from Equation 6 that $d\theta/dt$ is also zero. Since the rate of heat absorption is proportional to the rate of reaction, Equation 6 shows that the peak differential deflection occurs when the reaction rate is a maximum. It should be noted that the heating rate must be constant for this to hold and that Equation 6 is valid for a sample of any shape.

The rate law for the thermal decomposition of explosives can be described by the equation;

$$\left(\frac{\partial x}{\partial t}\right)_T = k_T (1-x)^n \quad (7)$$

where $k_T = A \exp(-E_a/RT)$ and temperature is a function of time.

$$\frac{dx}{dt} = \left(\frac{\partial x}{\partial t}\right)_T + \left(\frac{\partial x}{\partial T}\right)_t \frac{dT}{dt} \quad (8)$$

The rate of change of x with respect to temperature, with the time coordinates fixed, is equal to zero because the number and positions of the particles of the reactant are also fixed with time. The only effect of instantaneous change in temperature is in the velocities of thermal motion of the reactant particles. Equation 7 can now be written;

$$dx/dt = A(1-x)^n \exp(-E_a/RT) \quad (9)$$

which holds for any temperature as long as the fraction of reactant decomposed and temperature are measured at the same instant. It is assumed that the empirical order of the reaction remains constant through the greater part of the reaction.

When the temperature rises during the reaction, the reaction rate will rise to a maximum value, then return to zero as the reactant is exhausted. This maximum rate occurs when $d/dt(dx/dt)$ is zero. Providing the temperature rises at a constant rate, the differentiation of Equation 9 yields;

$$\frac{d}{dt} \left(\frac{dx}{dt} \right) = \frac{dx}{dt} \left[\frac{E_a \phi}{RT^2} - An(1-x)^{n-1} e^{-E_a/RT} \right] \quad (10)$$

Setting this equation equal to zero defines the temperature at which the maximum rate occurs.

$$\frac{E_a \phi}{RT_m^2} = An(1-x)_m^{n-1} e^{-E_a/RT_m} \quad (11)$$

T_m is the sample temperature at which the peak in the DTA thermogram occurs. The quantity of material left unreacted, $(1-x)_m$, is not determined by the DTA method.

To obtain the extent of reaction as a function of temperature, Equation 9 can be integrated. The resulting exponential integral does

not yield a simple expression. Previous work has resulted in a satisfactory approximation by successive integration by parts. Higher order terms were neglected, and the simplified expression becomes;

$$n(1-x)_m^{n-1} = 1 + (n-1) \frac{2RT_m}{E_a} \quad (12)$$

The heating rate does not appear except as a result of T_m , which varies with heating rate. The product $n(1-x)_m^{n-1}$ is independent of heating rate and nearly equal to unity. Equation 11 now becomes;

$$\phi = \frac{AR T_m^2}{E_a} e^{-E_a/RT_m} \quad (13)$$

Taking the natural logarithm of both sides and differentiating;

$$\begin{aligned} \frac{d \ln(\phi/T_m^2)}{d(1/T_m)} &= \frac{d \ln (AR/E_a e^{-E_a/RT_m})}{d(1/T_m)} \\ &= \left(\frac{E_a}{AR}\right) e^{+E_a/RT_m} \left(\frac{AR}{E_a}\right) \left(\frac{-E_a}{R}\right) e^{-E_a/RT_m} \\ \frac{d \ln(\phi/T_m^2)}{d(1000/T_m)} &= \frac{-E_a}{R} \end{aligned} \quad (14)$$

By experimentally obtaining DTA thermograms at different heating rates, the activation energy for the decomposition reaction can be determined by Equation 14, regardless of reaction order.

IV. EXPERIMENTAL PROCEDURE

A. APPARATUS

The differential thermal analysis reaction was obtained by use of the DuPont 900 Differential Thermal Analyzer shown in Figure 1. A remote cell unit, shown in Figure 2, was used in this work due to the nature of the samples being studied.

DTA uses a differential thermocouple arrangement consisting of two thermocouples wired in opposition as shown in Figure 3.

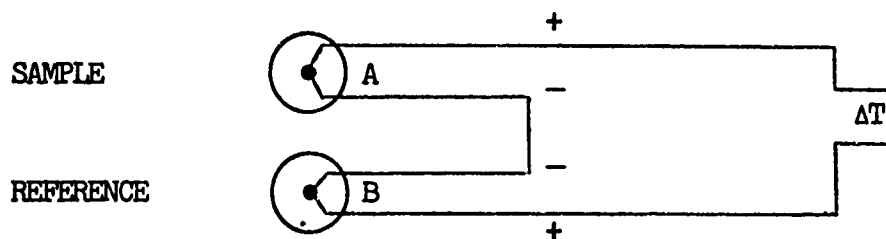


FIGURE 3 DIFFERENTIAL THERMOCOUPLE

Thermocouple A is placed in the sample to be analyzed. Thermocouple B is placed in an inert reference material. When the temperature of the sample equals the temperature of the reference, the thermocouples produce identical voltage, and the net voltage output, ΔT , is zero. When a physical or chemical reaction occurs in the sample, a differential signal is received and recorded. Figure 4 shows a schematic of the DTA system.

A silver heating block is mounted in the remote cell assembly. This block contains the sample, reference, and controlling chromel-alumel thermocouples as shown in Figure 5. The block is designed to provide for equal heating rates for both the reference and sample materials. The temperature of the reference is less than the temperature

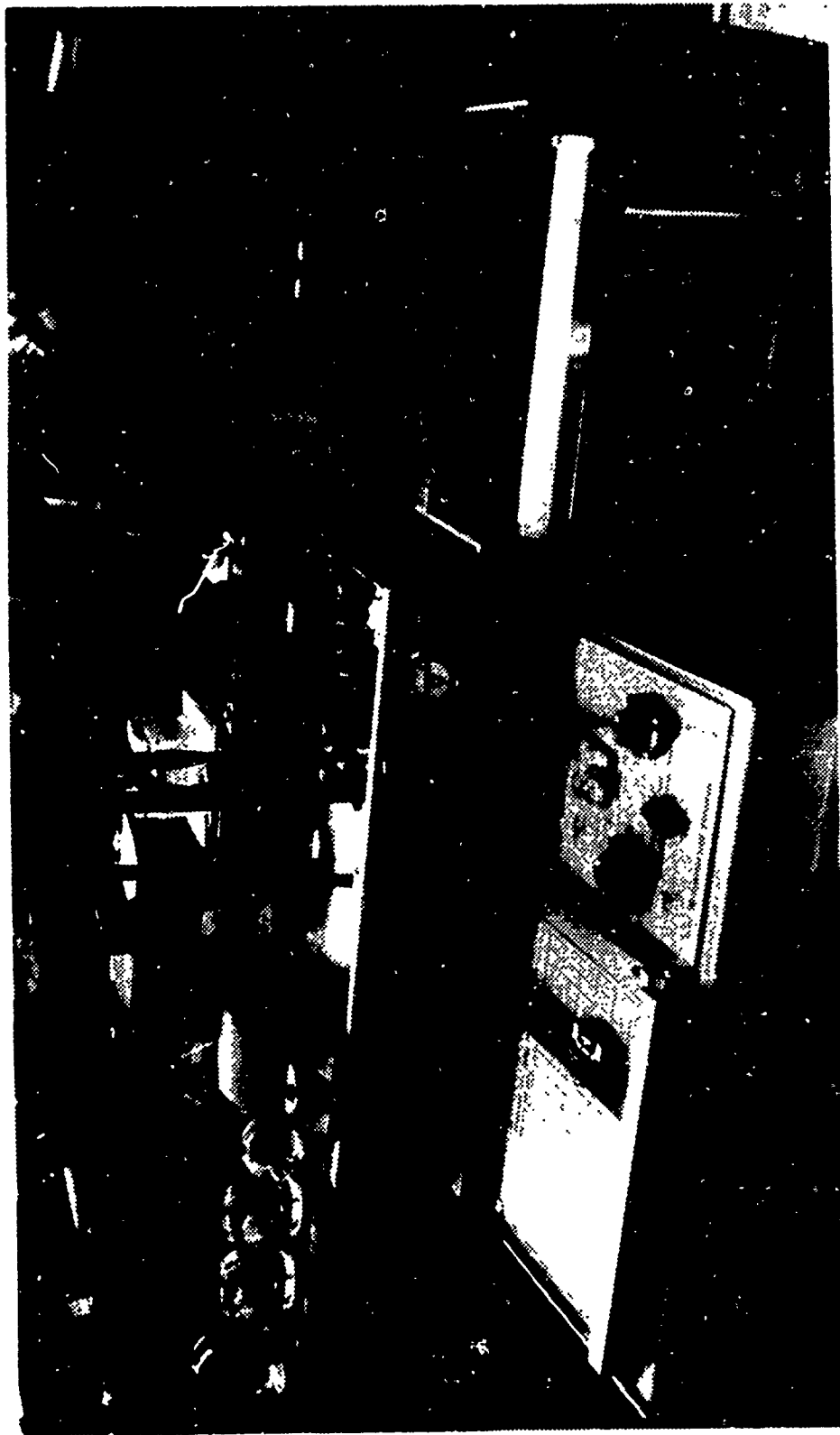


FIGURE 1: DuPont 900 Differential Thermal Analyzer

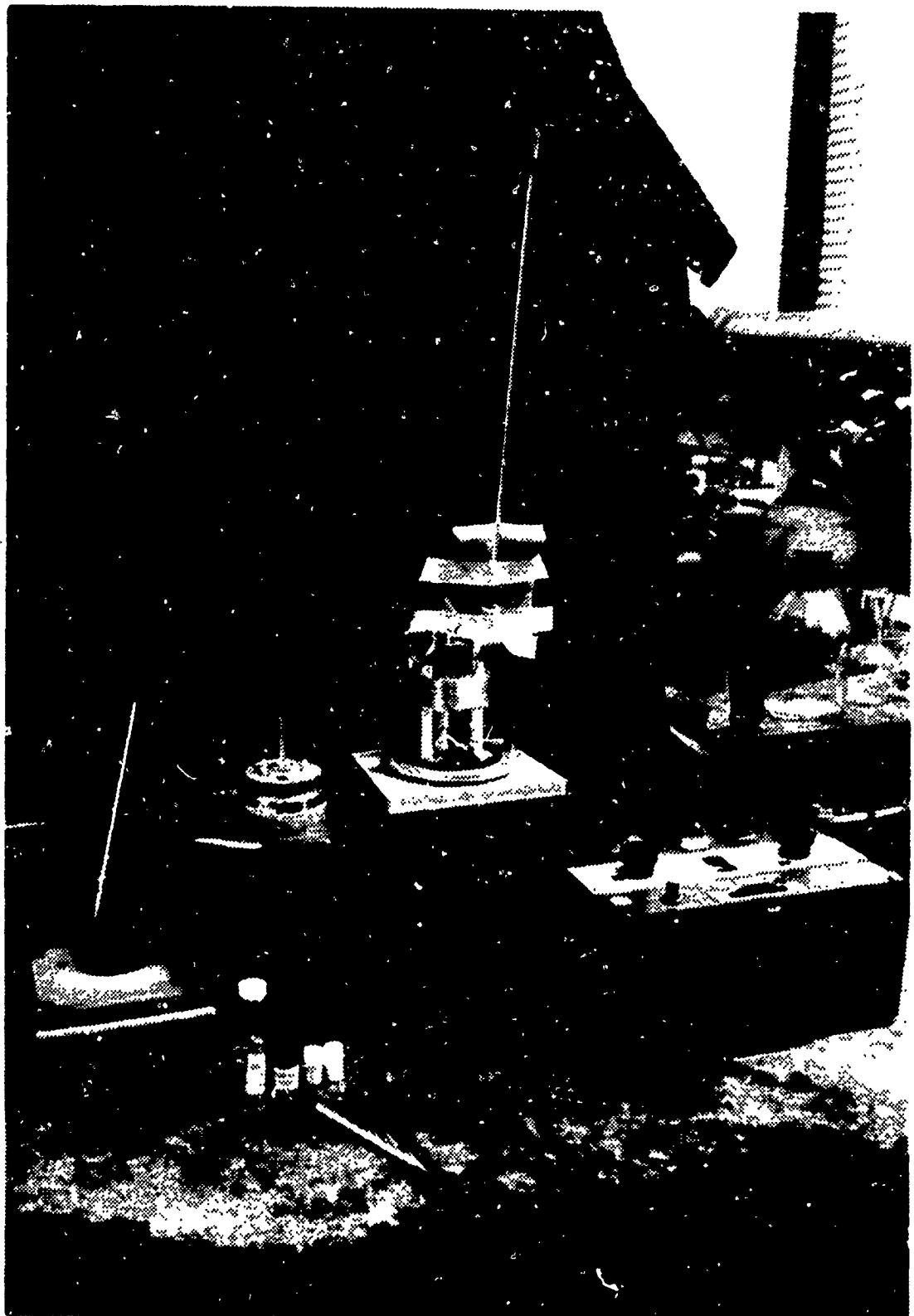


FIGURE 2: Remote Cell Assembly

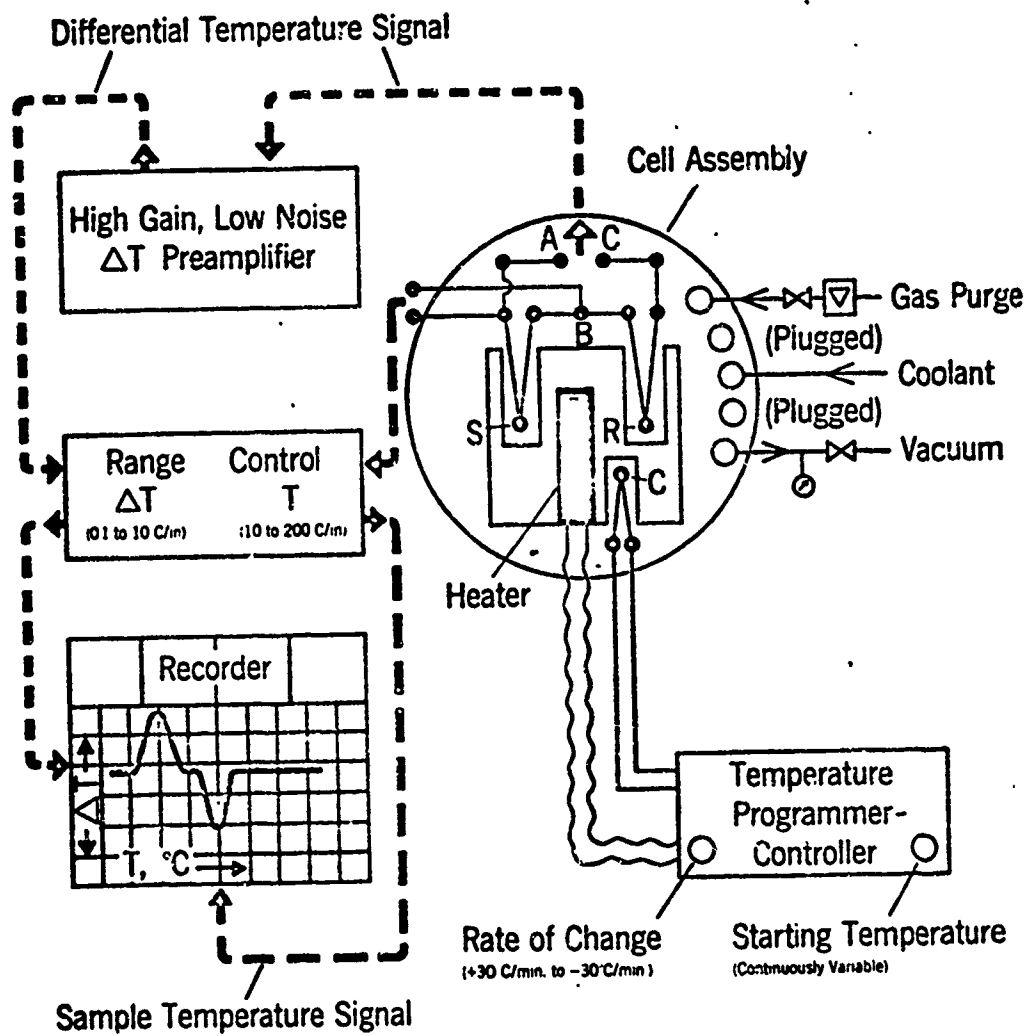


FIGURE 4: DTA System Schematic

(taken from ref. 10, pg. 3-2)

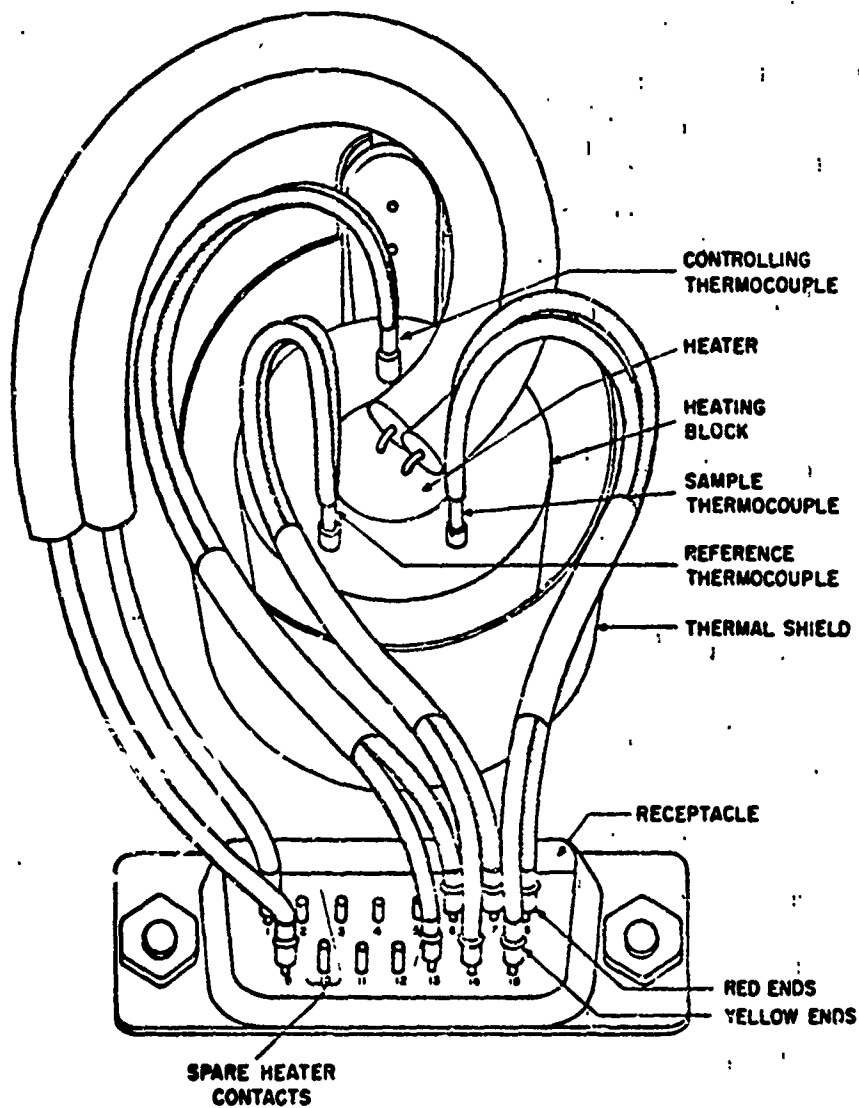


FIGURE 5: Heating Block and Thermocouple Arrangement
 (taken from ref. 10, pg. 3-4)

of the block by a constant amount that is directly proportional to the heating rate, weight and heat capacity of the reference material, and inversely proportional to the thermal conductivity of the reference material, plus a complex exponential function which can be neglected for simplification.

$$T_R = T_B - \phi_R (Wc/\kappa)_R$$

Assuming a thermally inert sample,

$$T_S = T_B - \phi_S (Wc/\kappa)_S$$

T = temperature
 ϕ = heating rate
 W = weight
 c = heat capacity

κ = thermal conductivity
 S = sample
 R = reference
 B = block

The differential temperature is:

$$\Delta T = T_S - T_R = \phi_R (Wc/\kappa)_R - \phi_S (Wc/\kappa)_S$$

The heating block in the DuPont 900 is designed such that $\phi_S = \phi_R$:

$$\Delta T = (Wc/\kappa)_R - (Wc/\kappa)_S$$

If the weight, heat capacity and thermal conductivity of the sample and reference material are the same, ΔT is zero. The ΔT signal as a function of sample temperature is sent to the X-Y recorder. Any change in the properties of the sample results in a positive or negative value for ΔT as shown in Figure 6.

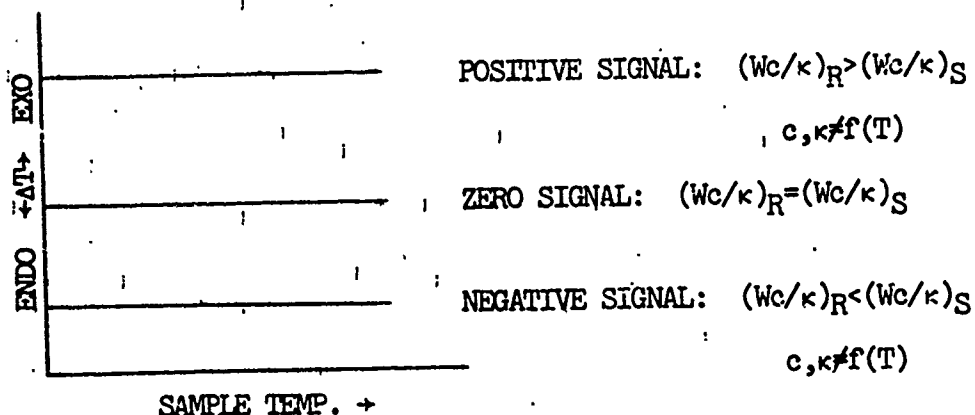


FIGURE 6 DTA THERMOGRAM

A thermally active material will experience a change in heat capacity and thermal conductivity over a temperature range. The ΔT trace will be a sloping straight line if the properties change linearly with temperature, and curved if the change with temperature is quadratic or of higher order. Figure 7 exhibits this relationship, where the curved line would have a positive slope if $(Wc/\kappa)_R > (Wc/\kappa)_S$.

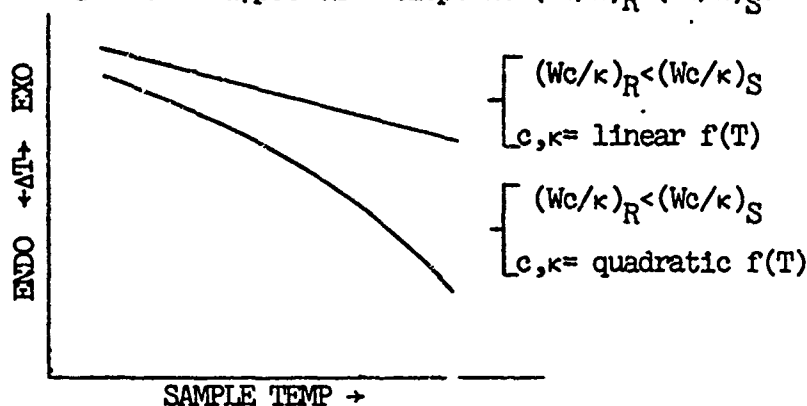


FIGURE 7 DTA THERMOGRAM

The DTA thermogram of a thermally active sample will exhibit endotherms and exotherms where the temperatures of interest are defined in Figure 8.

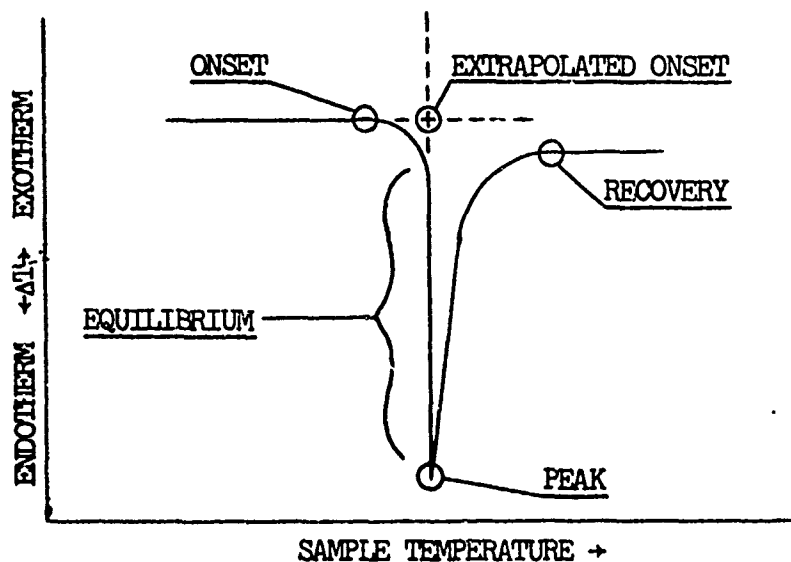


FIGURE 8 TRANSITION TEMPERATURES

TRANSITION TEMPERATURE DEFINITIONS USED IN FIGURE 8.

ONSET: The temperature at which the thermogram starts to depart from the base line.

EXTRAPOLATED ONSET: The temperature corresponding to the intersection of extrapolations of the base line and the longest straight-line section of the low-temperature side of the peak.

PEAK: The temperature of reversal.

RECOVERY: The temperature at which the thermogram returns to either the same or a different base line.

EQUILIBRIUM: The region where the state or form of the sample before transition is in equilibrium with its state or form after transition.

For the purposes of this work, a fourth well was drilled in the silver heating blocks to cross check the temperature scale on the DTA 900 X-Y plotter. A single chromel-alumel thermocouple was set in inert glass beads and connected to a Varian recorder. This gave a millivolt versus time chart to check the heating block temperatures and heating rate. The Varian thermocouple was calibrated with a millivolt potentiometer and temperatures were verified through the use of a hot oil bath. The temperature scale of the DTA thermogram is calibrated to the chromel-alumel millivolt output to give direct temperature readings in degrees centigrade.

B. SAMPLE PREPARATION

The samples of RDX that were used in the experimental runs were prepared by drying a small quantity of pure RDX that was stored in water. The sample appeared to be pure RDX as its melting temperature of 204°C compared favorably with listed values.

Two separate heating blocks were used in the experimental work. In the variable heating rate runs, a silver block with wells to accept two

millimeter diameter capillary tubes was used. The RDX sample was tapped down into one of the four capillary tubes to a depth of four millimeters, which was calculated to be 19.3 milligrams of RDX. The three remaining capillary tubes contained equal levels of inert finely ground glass beads .05 millimeters in diameter. These tubes contained the reference, controlling, and Varian recorder chromel-alumel thermocouples. All four capillary tubes were then cut to 1-1/8 inch. Care was taken when placing the thermocouples to insure that they were pushed to the full depth of the material. The capillary tubes were then placed in their respective wells, and the thermocouple leads were folded under the rim of the remote cell unit to insure that they remained completely seated throughout the run. This was especially important in the case of the RDX sample since the reactant gases given off during the exothermic decomposition tended to push the thermocouple out of the tube. The sample depth of four millimeters was critical for satisfactory results. A quantity larger than this would push the thermocouple out of the tube, giving erroneous readings. A smaller quantity would not provide complete coverage of the thermocouple probe. The fineness or texture of the sample in this work was not considered since the reactions occurred above the melting temperature, or in all cases for the variable heating rate runs, in the liquid phase.

The second silver heating block was identical to the first with the exception of the sample and reference wells which were designed to hold four millimeter diameter test tubes. The RDX sample was measured in the same manner as before to a depth of four millimeters, which in

this case gave a sample of 43.32 milligrams of RDX. The second four millimeter test tube contained an equal volume of inert glass beads and served as the reference. Both four millimeter tubes were covered with small metal caps through which the thermocouples were inserted. This reduced losses to the atmosphere during reaction. The controlling and Varian thermocouples were inserted in the remaining two small capillary wells in the same manner as in the variable heating rate block. This second heating block was used in the isothermal portion of the experimental work.

C. VARIABLE HEATING RATE EXPERIMENT

The DTA 900 control panel contains dials to set starting temperatures and heating rates. It was determined that there was no apparent difference in the thermogram presentation for a sample that was heated from room temperature at an established rate through decomposition or for one which was heated at an accelerated rate (50°C/min.) to 200°C, then slowed to the established rate through the decomposition reaction. In order to expedite the runs, this latter procedure was adopted.

The full range of the DTA 900 heating rate capability was utilized. In order to establish consistency in the procedure, an outline was set down and followed in each run.

EXPERIMENTAL PROCEDURE FOR VARIABLE HEATING RATE EXPERIMENT

- (1) Turn DTA 900 power knob to STANDBY, allow five minute warm up.
- (2) Place inert reference and sample material in the capillary tubes, tap and measure to a depth of four millimeters. Cut to 1-1/8 inch.
- (3) Insert corresponding thermocouples, insuring that the thermocouple probe is completely immersed in the material. A new thermocouple is used for the RDX sample in each run.

- (4) Insert capillary tubes into the correct wells of the heating block.
- (5) Bend the leads of the thermocouples under the remote cell rim.
- (6) Insure that the zero temperature ice bath reference thermocouples are fully inserted into their glass tubes, which in turn are immersed in the ice and distilled water solution at 0°C.
- (7) Place a thermogram grid on the X-Y plotter.
- (8) Set the pen to room temperature on the T-scale.
- (9) Set the DTA 900 upper panel knobs:
 - (a) T-zero shift.
 - (b) T-scale, °C/in.
 - (c) ΔT -zero shift.
 - (d) ΔT -scale, °C/in.
 - (e) Baseline slope.
- (10) Set the DTA 900 lower panel dials:
 - (a) Temperature heating rate, range 0-30°C/min.
 - (b) Set starting temperature dial to minimum setting to get the minimum voltage reading on the heater voltage indicator.
- (11) Set the program mode to HEAT.
- (12) Push RESET to erase previous program memory.
- (13) Place recorder pen to the DOWN position.
- (14) Place power knob to RECORD.
- (15) Start timer and Varian recorder.

Figure 9 shows a sample thermogram for a heating rate of 20°C/min. beginning at room temperature. The endotherm at 204°C shows transformation to the liquid phase, followed immediately by the exothermic decomposition with the peak in the exotherm at 251°C. Figure 10 shows a thermogram for ammonium nitrate. The endotherm at 40°C shows a transition from rhombic I to rhombic II. At 91°C, a crystalline change to tetragonal occurs, then to cubic at 130°C. Melting occurs at 174°C followed by decomposition in the liquid phase. This run was made to

check the calibration of the machine, to give an indication of the sensitivity of the analyzer, and for use in a method of estimating the heat of reaction of RDX, to be described in the recommendations. The thermogram was compared with the ammonium nitrate thermogram presented on page 5-7 of the DTA Instruction Manual [Ref. 10]. The comparison showed a disparity in temperature for the peak exotherm, where that of Figure 10 showed a temperature approximately 10°C higher than that of the reference thermogram. This was corroborated by the Varian recorder, and subsequent temperature readings were taken from the Varian recorder.

D. ISOTHERMAL EXPERIMENT

A time base adaptor for the DTA 900 provides for maintaining the heating block at set temperatures over long periods of time. The X-Y plotter now provides for time in minutes on the abscissa and as before, ΔT on the ordinant. Experimental runs were made using the four millimeter test tube macro heating block. A variation of a method used in determining the effects of thermal aging of propellants was followed [Kuletz and Pakulak 1962]. This technique is known as microimmersion autocatalytic analysis (MAA). In this work, the sample of RDX was dropped into the well of the macro heating block after the block had been established at a desired temperature. The procedure followed is listed below.

EXPERIMENTAL PROCEDURE FOR ISOTHERMAL EXPERIMENT

- (1) Turn DTA 900 power knob to STANDBY, allow one to two hours warm up.
- (2) Place inert reference material in both 4mm test tubes, tap and measure to a depth of four millimeters.
- (3) Place metal thermocouple holder caps over test tubes and insert thermocouples, insuring complete immersion.

- (4) Insert reference and sample 4mm test tubes in the large wells of the macro heating block. Two small capillary tubes are used for the controlling and Varian recorder thermocouples.
- (5) Bend the thermocouple leads under the remote cell rim.
- (6) Check the zero temperature ice bath and thermocouples.
- (7) Place a thermogram grid on the X-Y plotter.
- (8) Set the time base adaptor to TIME.
- (9) Set the DTA 900 upper panel knobs:
 - (a) T-zero shift.
 - (b) T-scale, Min./in.
 - (c) ΔT -zero shift.
 - (d) ΔT -scale.
 - (e) Baseline slope.
- (10) Set the DTA 900 lower panel dials:
 - (a) Set temperature heating rate at zero.
 - (b) Set the starting temperature dial according to the scale of Figure 3G of section 3, DTA Instruction Manual [Ref. 10].
- (11) Set the program mode to ISOTHERMAL.
- (12) Allow the temperature to stabilize at the desired setting and record the Varian reading.
- (13) Place a sample test tube of RDX in the macro heating block and reset the corresponding thermocouple. (Wear protective shield)
- (14) Push RESET to start zero time at the left end of the scale.
- (15) Place recorder pen to the DOWN position.
- (16) Record time and start timer.
- (17) Monitor Varian recorder.

The resulting thermogram plots ΔT versus time.

V. RESULTS AND DISCUSSION

The series of thermograms obtained from the variable heating rate method using RDX samples are reproduced in Figures 11-17. During each of these runs, temperatures were recorded at 5°C intervals and at significant points on the thermogram (melting, peak exotherm) with the corresponding time in seconds. This data is plotted in Figures 18-36. An n^{th} order regression analysis program of the WANG 700 was used to calculate the least squares fit to the data points, the slope of which is the actual heating rate for that run. The resulting equation gives the temperature at any time during each run for the programmed heating rate. The calculated heating rates, along with the sample temperature of the peak in the exotherm T_m , are the required data for determining the kinetic parameters of the decomposition by Kissinger's method [Ref. 2]. These data are summarized in Table I.

The kinetic data for the decomposition reaction of RDX were determined from the plot of the variable heating rate experimental data of Table I. The natural logarithm of the rate factor ϕ/T_m^2 was plotted versus the reciprocal of the Kelvin temperature of the heating block, as shown in Figure 37. The WANG 700 was used to calculate a least squares fit to the experimental data points. The slope of this line determines the activation energy which was calculated to be 49.4713 kcal/mole. The Arrhenius frequency factor was determined from Equation 13, averaged over the temperature range of the experiment. The average value was 6.9199×10^{20} , which varied from the fastest heating rate value by 1.1501×10^{20} and from the lowest by 0.1415×10^{20} . These values compare favorably with those of previous works [Rauch and

Wainright 1969, Robertson 1948]. The kinetic parameters are summarized in Table II. There is a 1.6% error in the value for the activation energy when compared with that of Rauch and Wainright's work for Picatinny Arsenal.

Appendix A is an IBM 360 computer readout which tabulates values for the heating rate with incremental increase in the peak temperature T_m . The experimentally determined values of activation energy and Arrhenius frequency factor were used in Equation 13 to generate values of the heating rate ϕ . Appendix B tabulates the same information for comparison using the kinetic data determined by Rauch and Wainright. This data is presented in Table III along with values from the experimental runs for comparison. At higher heating rates, the experimental and calculated data differ to a larger extent. This is probably due to experimental time lag at the higher heating rates which caused lower temperature readings at the higher rates. Although the values of activation energies compare favorably, Table III shows that the experimentally determined temperatures of the peak in the exotherms at the various heating rates would have to be approximately 30°C higher to give heating rates comparable to the Picatinny data.

The rate constant k over the experimental temperature range was calculated using the Arrhenius equation. Appendix C tabulates values of k using the experimentally determined values of E_a and A . Appendix D presents the same data using the kinetic data determined in the study made for Picatinny Arsenal. These values are compared in Table IV. The smaller values for the rate constant resulting from the Picatinny data correspond with the lower heating rate values shown in Table III.

Some variation existed in the peak temperature of the exotherms as evidenced in Table I. This resulted in the scatter noted in Figure 37. An attempt to reproduce the peak temperature at a given heating rate was made over three consecutive runs using the standard experimental technique. Results are shown in Figure 38, where the three runs were carried out at a heating rate of 6°C/min. The maximum variation in the peaks was 4°C. This compares with the variation in temperatures for the experimental and calculated values of T_m shown in Table III. The maximum deviation approaches .8% error, which is well within the accuracy of the experiment. There is a definite increase in T_m with heating rate as proposed by the DTA kinetic theory [Kissinger 1957]. The effect of sample size appeared to be only an increase in the quantity of heat liberated, as shown in Figure 39. The peak temperature did not vary to any greater degree than in the normal manner with equivalent volumes of material.

The isothermal data gave somewhat less conclusive results. The thermograms, Figures 40-44, show a definite exothermic decomposition reaction which occurs at a constant block temperature after an induction time which decreases with increased temperature. A temperature range of 192-210°C was investigated. The time elapsed to initiation of the exothermic reaction, or induction time, and the time elapsed to the peak in the exotherm, the time-to-deflagration, were observed and recorded. Table V summarizes the isothermal data. It was noted that although these reactions occur at or below the normal melting temperature they occurred in the liquid phase. A physical observation during one of the runs confirmed a liquid phase decomposition with decomposition gases bubbling off. The sample at 192°C showed no evidence of

reaction after six and one-half hours. Near the melting temperature (204°C) and above, the sample changed to the liquid phase immediately upon reaching block temperature with the exothermic decomposition ensuing. The microimmersion autocatalytic analysis (MAA) method was used to determine kinetic data from the isothermal phase of the experiment. This method is based on the equation;

$$\frac{T^2}{\tau} = \frac{AQE_a}{cR} e^{-E_a/RT} \quad (15)$$

where Q is the heat of reaction. A plot of the natural logarithm of the rate factor (τ/T^2) versus the reciprocal of the constant block temperature gives a slope equal to E_a/R . In addition, an Arrhenius plot using the reciprocal of the time data versus $1000/T$ was made [Kuletz and Pakulak 1962]. Both induction time and time-to-deflagration data were used. Table VI lists the induction time data. Two plots were made using these data. The natural logarithm of the reciprocal of the induction time versus the reciprocal of the isothermal block temperature in degrees Kelvin is presented in Figure 45. The MAA procedure, plotting the natural logarithm of the rate factor (t_0/T^2) versus $1000/T^\circ K$, is shown in Figure 46. This was done again using the time-to-deflagration. The data for time-to-deflagration are listed in Table VII. The plots of these data are shown in Figures 47 and 48 respectively. The results are shown in Table VIII. In all cases the WANG 700 was used to determine a least squares fit to the data points and the resulting slopes. It can be seen that both the reciprocal time and MAA rate factor methods produce nearly identical results. The values obtained for E_a are far too high for activation energies.

VI. CONCLUSIONS AND RECOMMENDATIONS

Experimental work done on HMX [Suryamarayana and Graybush 1967] suggested that materials which exhibit sigmoid pressure-time curves generally involve three stages in the decomposition reaction. The first stage is the induction period. This is followed by an acceleration period where the rate reaches a maximum. The material is consumed in the decay period. Even with this mass spectrometric study, the conclusions were limited due to the several decomposition products formed. It was observed that each product reached a constant rate of formation after an acceleratory stage which appeared due to autocatalysis. It was found that HMX exhibited different modes of decomposition. The kinetic data changed in different discrete temperature ranges. These findings were supported in a DTA analysis of HMX [Hondee 1971], where three separate activation energies were found during three discrete stages of the decomposition process.

Causes for acceleration of the decomposition of HMX to a constant rate can be attributed to [Suryamarayana and Graybush 1967]:

- (1) Progressive melting as a result of lowered melting point by the decomposition products.
- (2) Self-heating.
- (3) Autocatalysis by products.
- (4) Acceleration due to structural factors such as the increase in the number of nuclei.

During this experimental study of the decomposition of RDX there was no evidence of different activation energies since the heating rate in all runs remained constant over the entire decomposition. The peak exotherm, although somewhat variable, did not exhibit more than one sharp peak. The thermograms for the variable heating rate experiments

(Figures 11-17) show that the exothermic decomposition reached a peak which was in most cases followed by a second peak. This second peak is probably a result of the capillary action of the liquid sample causing the thermocouple to rise in the tube, then drop back down just before the reaction completes causing another jump in the thermogram.

The isothermal experiment thermograms (Figures 40-44) show a definite decomposition reaction after an induction time at lower temperatures. This is in agreement with previous studies which have found evidence of self-heating and autocatalysis in the decomposition of RDX and other explosives. These data can be applied to estimates of the sensitivity of explosives and propellants.

Several reasons may be proposed for the discontinuities in the variable heating rate experiment. Although the RDX sample was assumed homogeneous and pure, it may well have been nonuniform in nature and composition. Possible water content in the samples was neglected. DTA results vary between laboratories due to the difference in experimental techniques and equipment as well as in the interpretation of the results. Standardization of method would be beneficial.

Explosive decomposition rates vary rapidly with temperature and for ideal results the temperature of the sample should at all times be uniform. This is not the true situation due to thermal conduction in the sample and self-cooling or self-heating effects arising from the reaction. Robertson [Ref. 9] showed that errors in the values of the kinetic parameters occur due partly to autocatalysis and self-heating. Autocatalysis increases the activation energy value by approximately 2000 cal/mole as a maximum error and causes a corresponding

variation in the Arrhenius frequency factor by as much as a factor of 10. Errors due to self-heating are also incurred and tend to increase E_a and A as well. This effect increases with increased temperature.

Experimental errors are also induced by the apparatus. The accuracy of the DTA method depends on the precision with which a uniform heating rate can be maintained. Although the DTA 900 provides for a constant rate to the heating block, the exterior of the sample is hotter than the interior and reacts sooner and faster. This causes additional autocatalytic and self-heating effects which are accentuated by an increased heating rate. Another source of error in this work was the uncontrolled atmosphere. This provides for possible variations in the data from day to day. Bubbles of the decomposition gases which formed on the thermocouples caused the high intensity chatter on the thermograms. Capillary action of the melt during decomposition caused it to climb the walls of the tube surrounding the thermocouple sleeve. This drew the material away from the thermocouple probe. Care had to be taken to keep the level of the liquid below the sleeve in order to minimize this effect.

Notwithstanding these adverse and random effects, the dominant factor in controlling the shape and position of the endotherms and exotherms is the nature of the reaction itself. The favorable results obtained lend credibility to the DTA method and suggest that further development in the technique will prove useful in providing a fast and reasonably accurate method of characterizing the thermal and kinetic properties of new explosives and propellants.

Areas for further study are wide and varied. Considerably more information as to the mechanisms of the reaction can be obtained by

combining the DTA method with one or more of several more precise analytical techniques such as thermogravimetry, infrared spectrometry, mass spectrometry, X-ray measurements, and visual observations.

More information may be determined from the DTA thermograms themselves. It has been shown that the area under the peak in the thermogram is proportional to the heat of reaction [Rivette and Besser 1961]. This provides a means to quickly estimate the heats of reaction of the sample. The shape of the exotherm provides a means to estimate the reaction order [Kissinger 1957]. Rough estimations using this method showed the reaction order to vary from 0.2 to 0.8 over the range of heating rates considered. Further analysis of the isothermal thermograms appears warranted to discover the significance of the two slopes on the low temperature side of the exotherm and the shape and extent of the decay pattern on the high temperature side, as well as the significance of the high values obtained for E_a from the Arrhenius and MAA plots of the induction time and time-to-deflagration data.

TABLE I
EXPERIMENTAL DATA, VARIABLE HEATING RATE THERMAL ANALYSIS

<u>RUN #</u>	<u>ϕ, °C/MIN</u>	<u>T_m °K</u>	<u>$\ln(\phi/T_m^2)$</u>	<u>$(1/T_m) \times 10^3$</u>
1	2.431	504.00	-11.5601	1.9802
2	2.880	501.00	-11.3754	1.9960
3	3.333	509.00	-11.2610	1.9646
4	3.8571	513.00	-11.1306	1.9493
5	4.3636	505.25	-10.9768	1.9792
6	4.6957	509.00	-10.9183	1.9646
7	5.1940	510.50	-10.8233	1.9589
8	5.6552	514.50	-10.7538	1.9436
9	6.2069	515.25	-10.6636	1.9408
10	6.8182	513.00	-10.5610	1.9493
11	7.9149	517.25	-10.4283	1.9333
12	8.8696	510.75	-10.2891	1.9579
13	9.7143	511.50	-10.2011	1.9550
14	10.5556	512.75	-10.1229	1.9503
15	11.6471	519.00	-10.0488	1.9268
16	16.5217	517.00	-9.6914	1.9342
17	21.0000	524.50	-9.4804	1.9066
18	26.0769	523.25	-9.2591	1.9111
19	30.0000	528.00	-9.1370	1.8939

TABLE II
KINETIC PARAMETERS

	E_a (kcal/mole)	A (sec ⁻¹)	
EXPERIMENTAL	49.5	6.9×10^{20}	$10^{20.8}$
RAUCH & WAINRIGHT	48.7	1.7×10^{19}	$10^{19.2}$
ROBERTSON	47.5	3.16×10^{18}	$10^{18.5}$

TABLE III
HEATING RATE DATA COMPARISON

PEAK TEMPERATURE	HEATING RATE ϕ			
	T_m	EXPERIMENTAL	CALCULATED	PICATINNY
504.00		2.4310	2.4817	0.1338
509.00		4.6957	4.1122	0.2200
513.00		6.8182	6.1167	0.3253
524.50		21.0000	18.5317	0.9694
528.00		30.0000	25.7247	1.3391

TABLE IV
RATE CONSTANT DATA COMPARISON

PEAK TEMPERATURE	RATE CONSTANT k (sec ⁻¹)		
	T_m	EXPERIMENTAL	PICATINNY
504.00		0.2433	0.0129
509.00		0.3952	0.0208
513.00		0.5787	0.0303
524.50		1.6772	0.0864
528.00		2.2974	0.1177

TABLE V
EXPERIMENTAL DATA, ISOTHERMAL ANALYSIS

RUN #	T (°C)	T (°K)	INDUCTION TIME		DEFLAGRATION		ΔT_{max}	
			t_0 (min)	t_0 (sec)	τ (min)	τ (sec)		
1	192.00	465.00	EXCESS OF 6-1/2 HRS.					
2	194.25	467.25	192.0	11,520	238.5	14,310	.39	
3	196.75	469.75	130.0	7,848	145.6	8,736	.30	
4	198.00	471.00	85.0	5,100	107.5	6,450	.66	
5	198.50	471.50	37.5	2,250	58.5	3,510	1.30	
6	199.50	472.50	15.0	900	34.8	2,088	1.50	
7	204.50	477.50	10.8	648	19.2	1,152	1.60	
8	206.75	479.75	0.0	0	0.0	0	3.20	

TABLE VI
ISOTHERMAL ANALYSIS, INDUCTION TIME DATA

RUN #	$1000/T$	t_0 sec	$1/t_0$	$\ln(1/t_0)$	$\ln(t_0/T^2)$
2	2.1402	11,520	$.8681 \times 10^{-4}$	-9.3518	-2.9419
3	2.1288	7,848	$.1274 \times 10^{-3}$	-8.9680	-3.3364
4	2.1231	5,100	$.1961 \times 10^{-3}$	-8.5370	-3.7727
5	2.1209	2,250	$.4444 \times 10^{-3}$	-7.7187	-4.5932
6	2.1164	900	$.1111 \times 10^{-2}$	-6.8024	-5.5137
7	2.0964	648	$.1543 \times 10^{-2}$	-6.4739	-5.8611

TABLE VII
ISOTHERMAL ANALYSIS, TIME-TO-DEFLAGRATION

<u>RUN #</u>	<u>1000/T</u>	<u>1/τ(sec⁻¹)</u>	<u>ln(τ/T²)</u>	<u>ln(1/τ)</u>
2	2.1402	.6988x10 ⁻⁴	-6.8194	-5.4744
3	2.1288	.1145x10 ⁻³	-7.3235	-4.9809
4	2.1231	.1550x10 ⁻³	-7.6322	-4.6775
5	2.1209	.2849x10 ⁻³	-8.2428	-4.0690
6	2.1164	.4789x10 ⁻³	-8.7665	-3.5496
7	2.0964	.8681x10 ⁻³	-9.3801	-2.9549

TABLE VIII
ISOTHERMAL RESULTS

	INDUCTION TIME		TIME-TO-DEFLAGRATION	
	<u>1/t₀</u>	<u>t₀/T²</u>	<u>1/τ</u>	<u>τ/T²</u>
E _a (kcal/mole)→	159.0282	160.9012	131.0144	132.8778

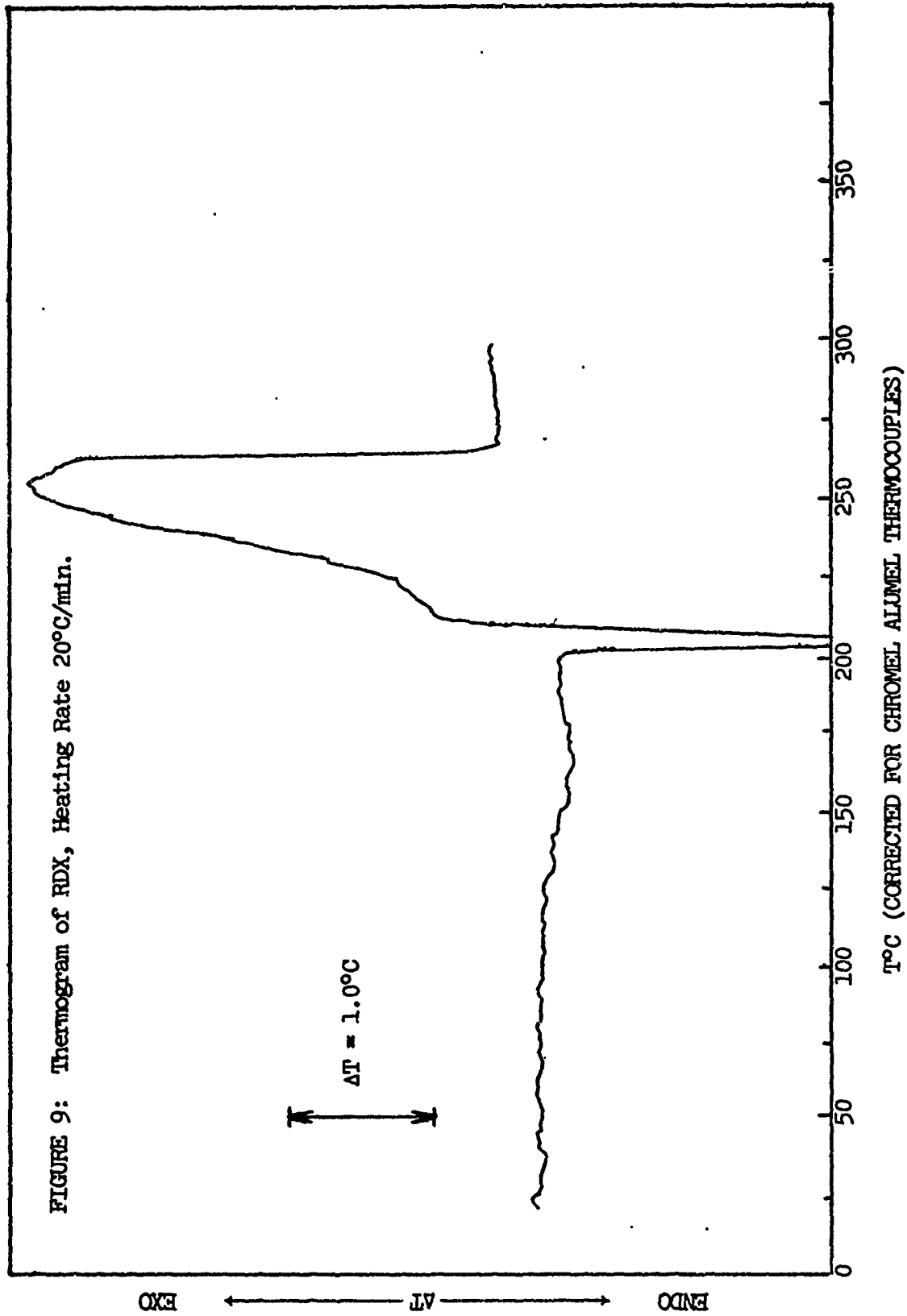
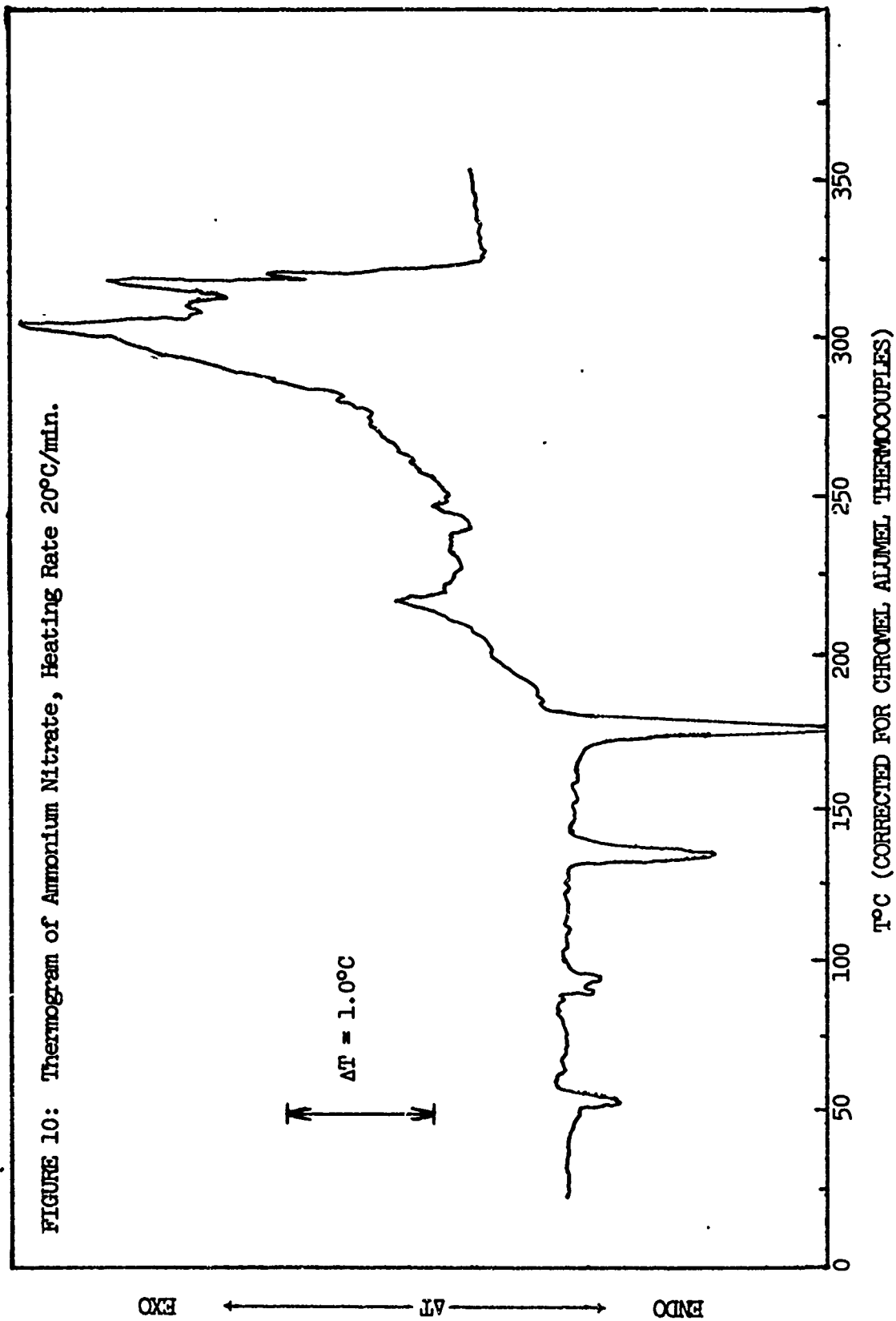


FIGURE 9: Thermogram of RDX, Heating Rate 20°C/min.



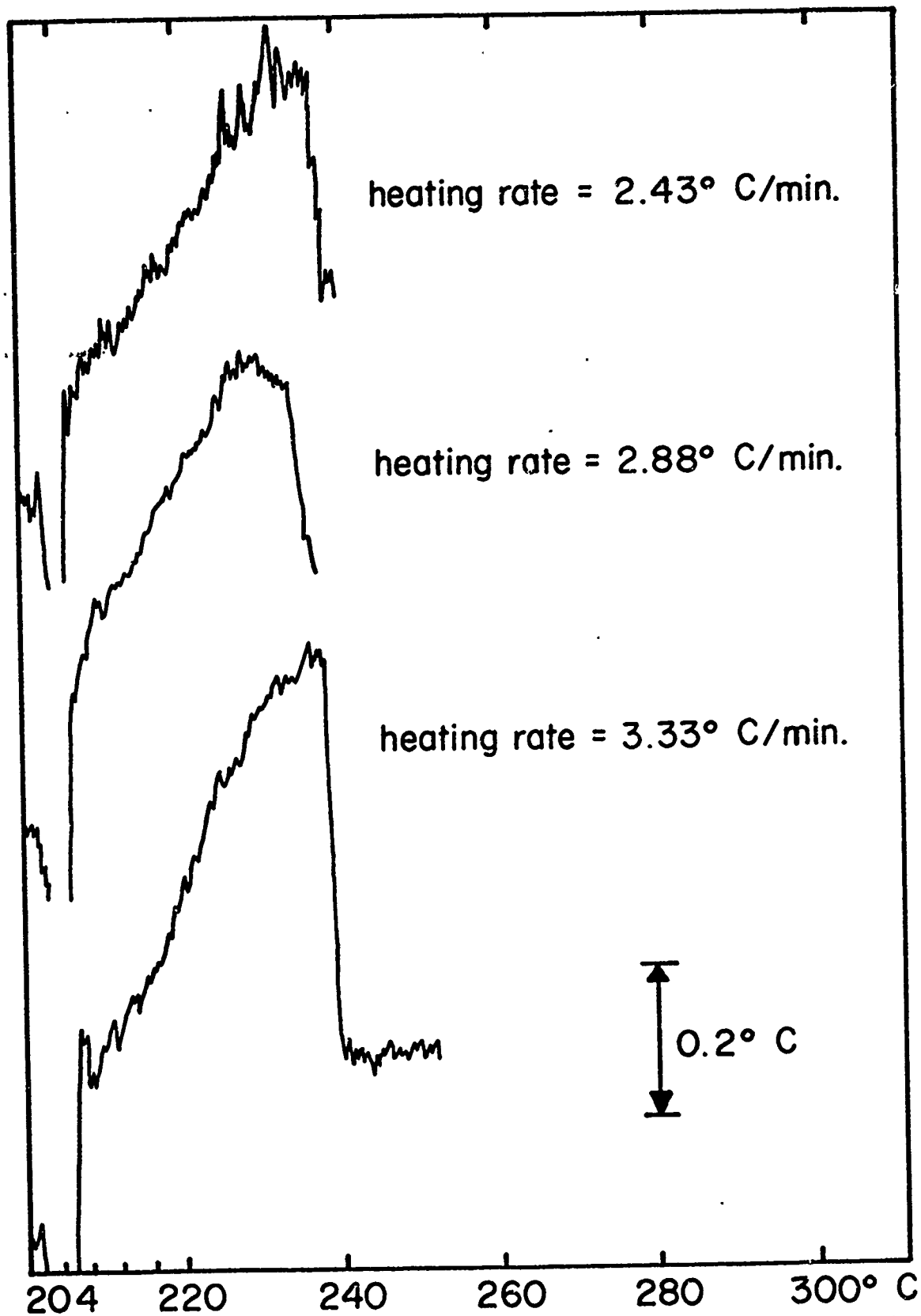


Figure II. Variable Heating runs 1-3.

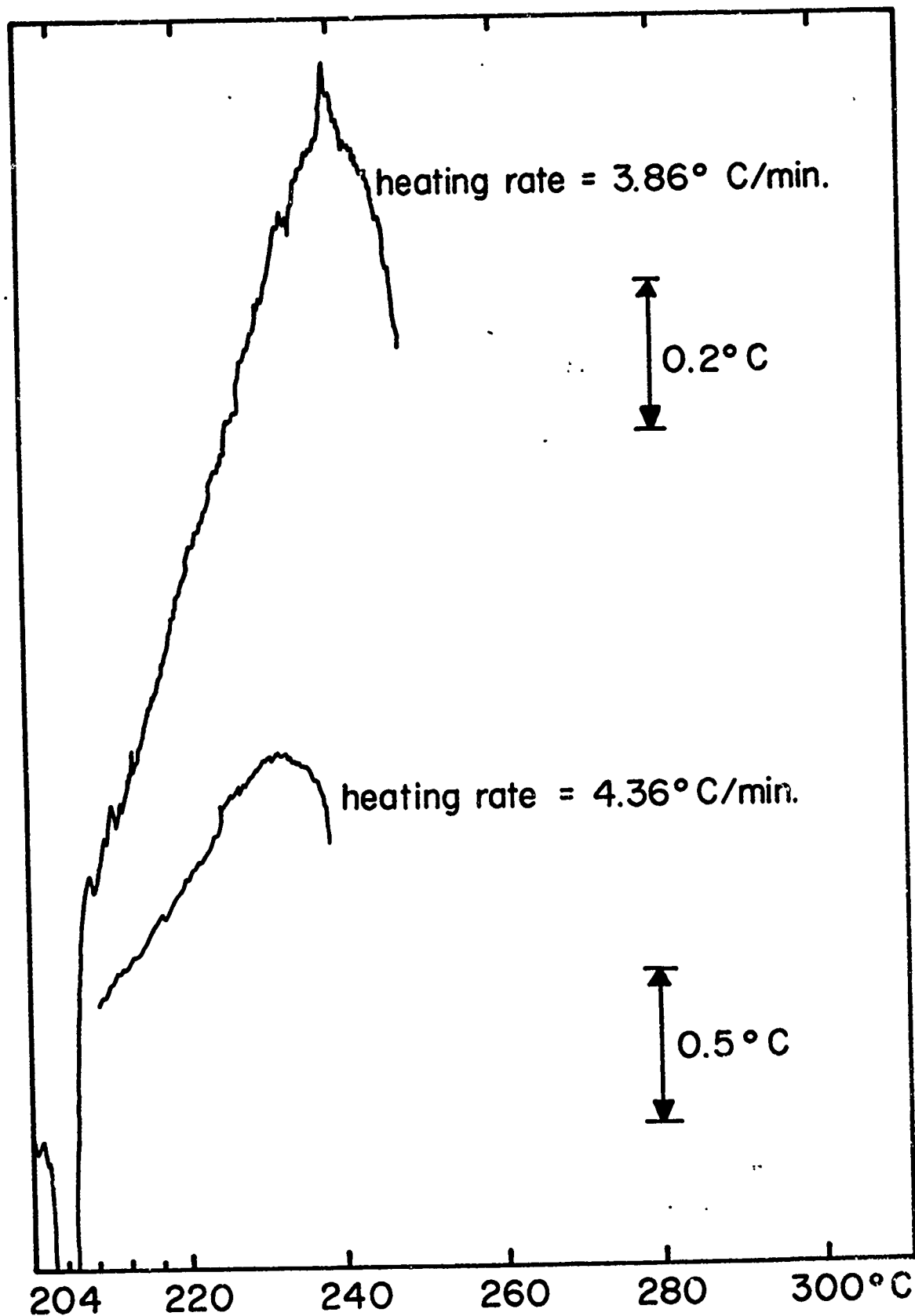


Figure 12. Variable Heating rate runs 4 & 5.

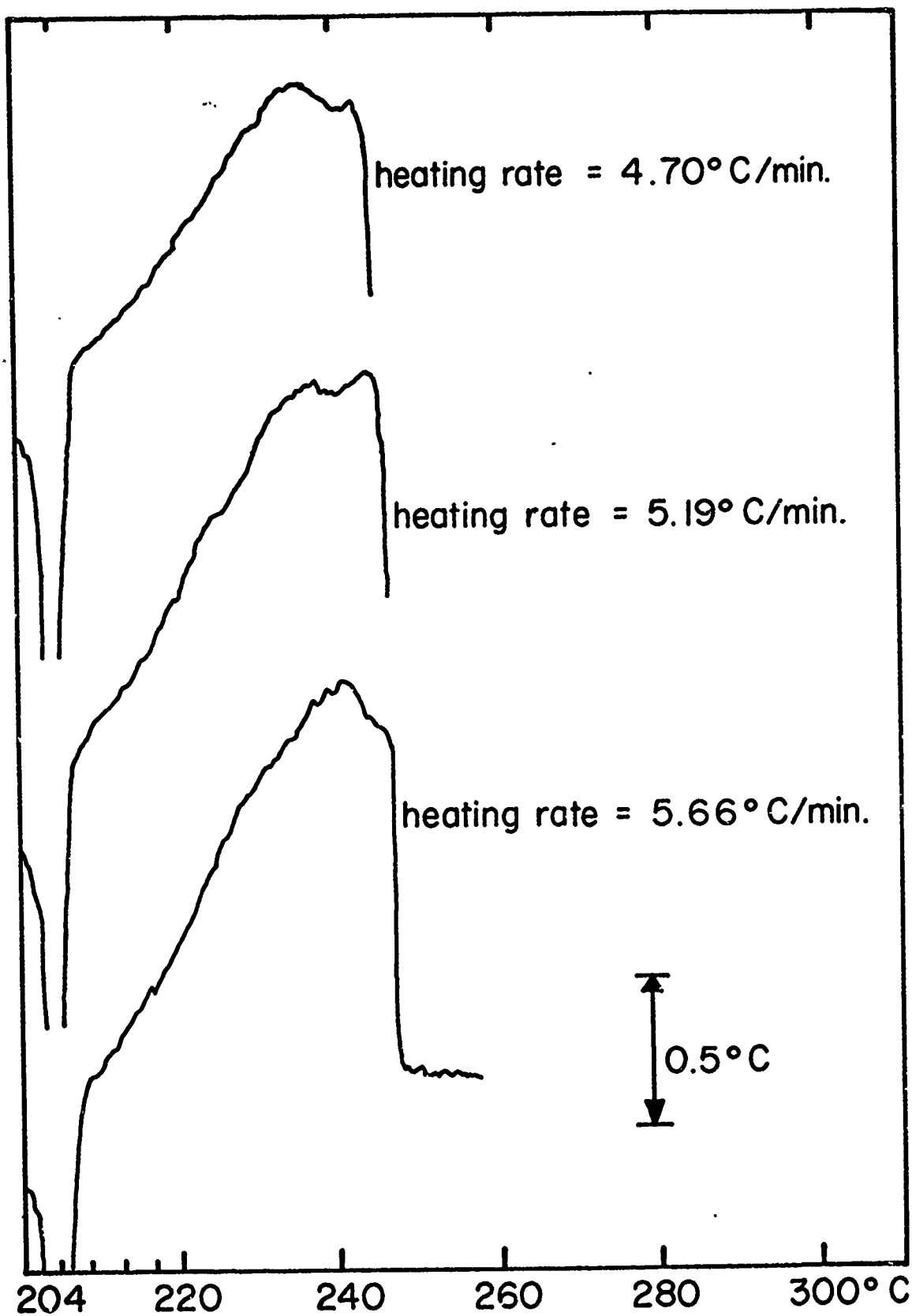


Figure 13. Variable Heating Rate Runs 6-8.

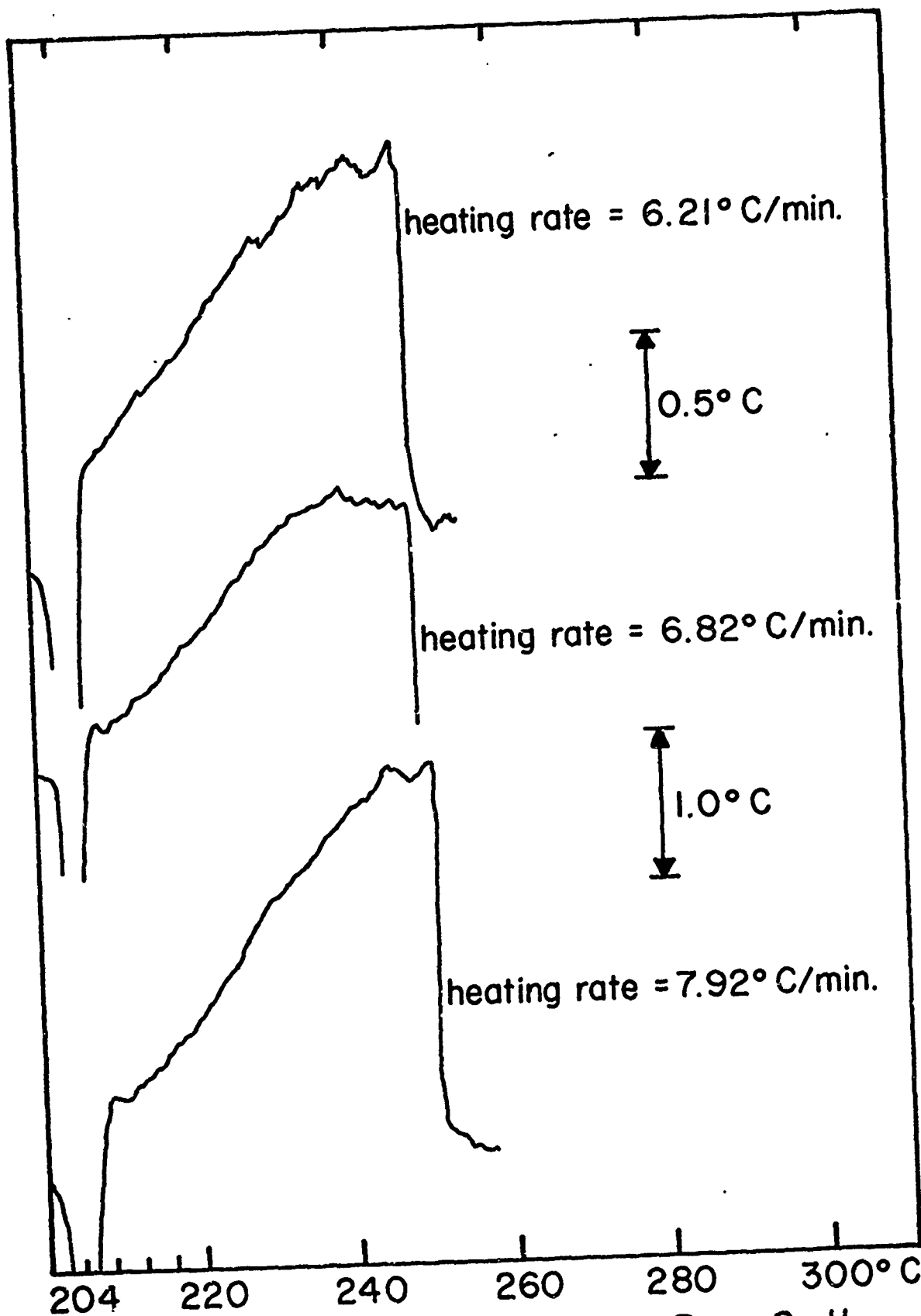


Figure 14. Variable Heating Rate Runs 9-11.

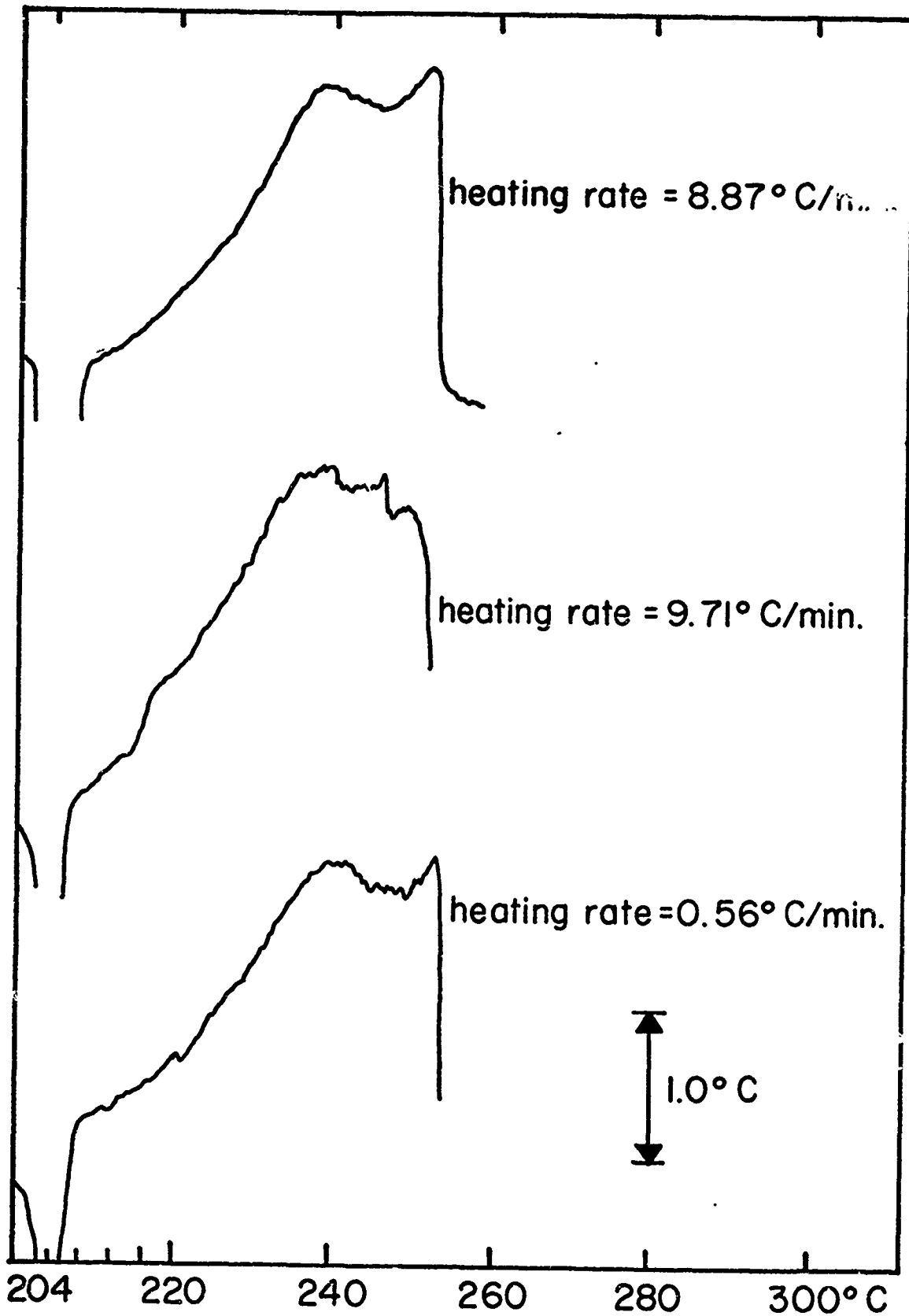


Figure 15. Variable Heating Rate Runs 12-14.

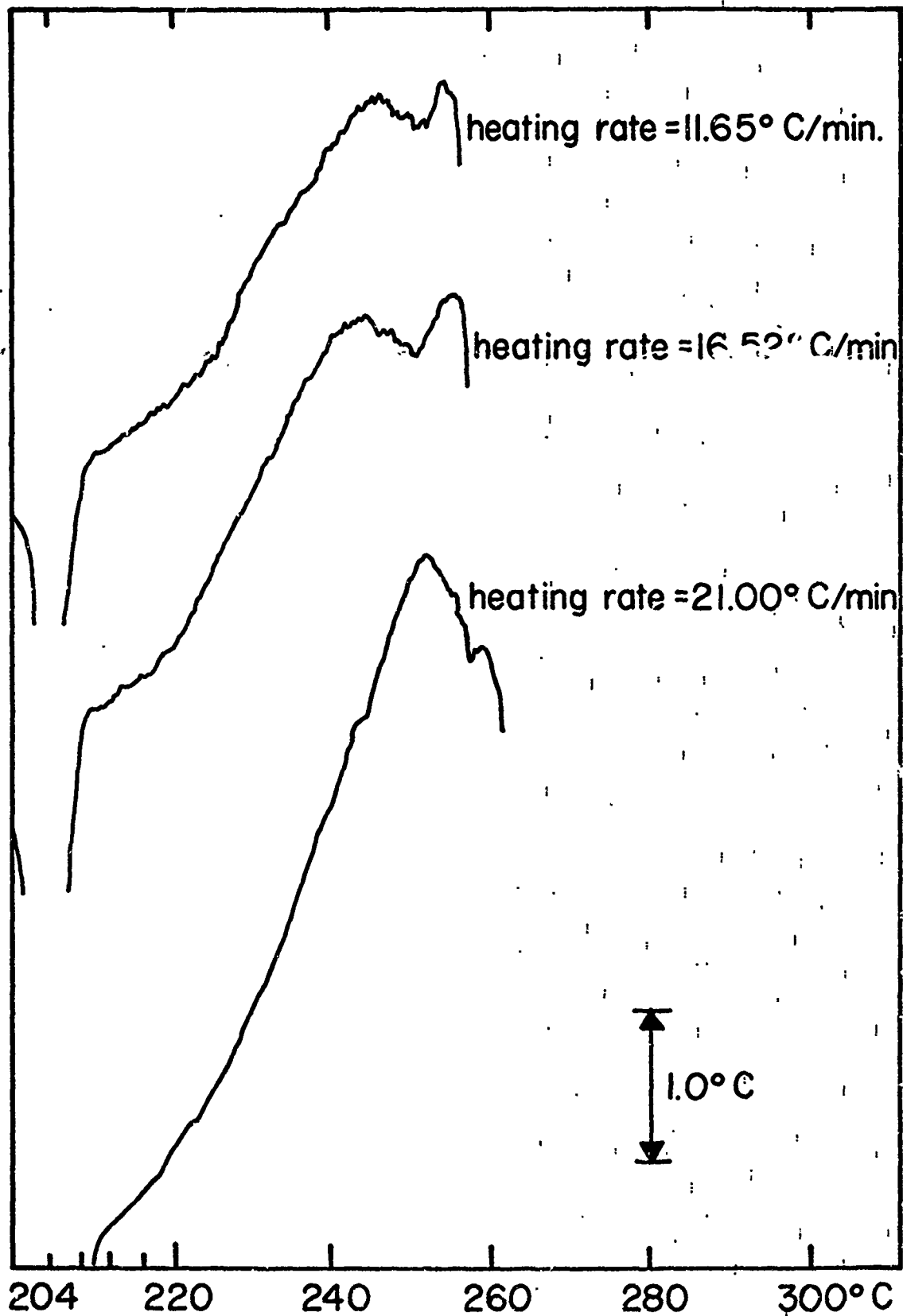


Figure 16. Variable Heating Rate, Runs 15-17.

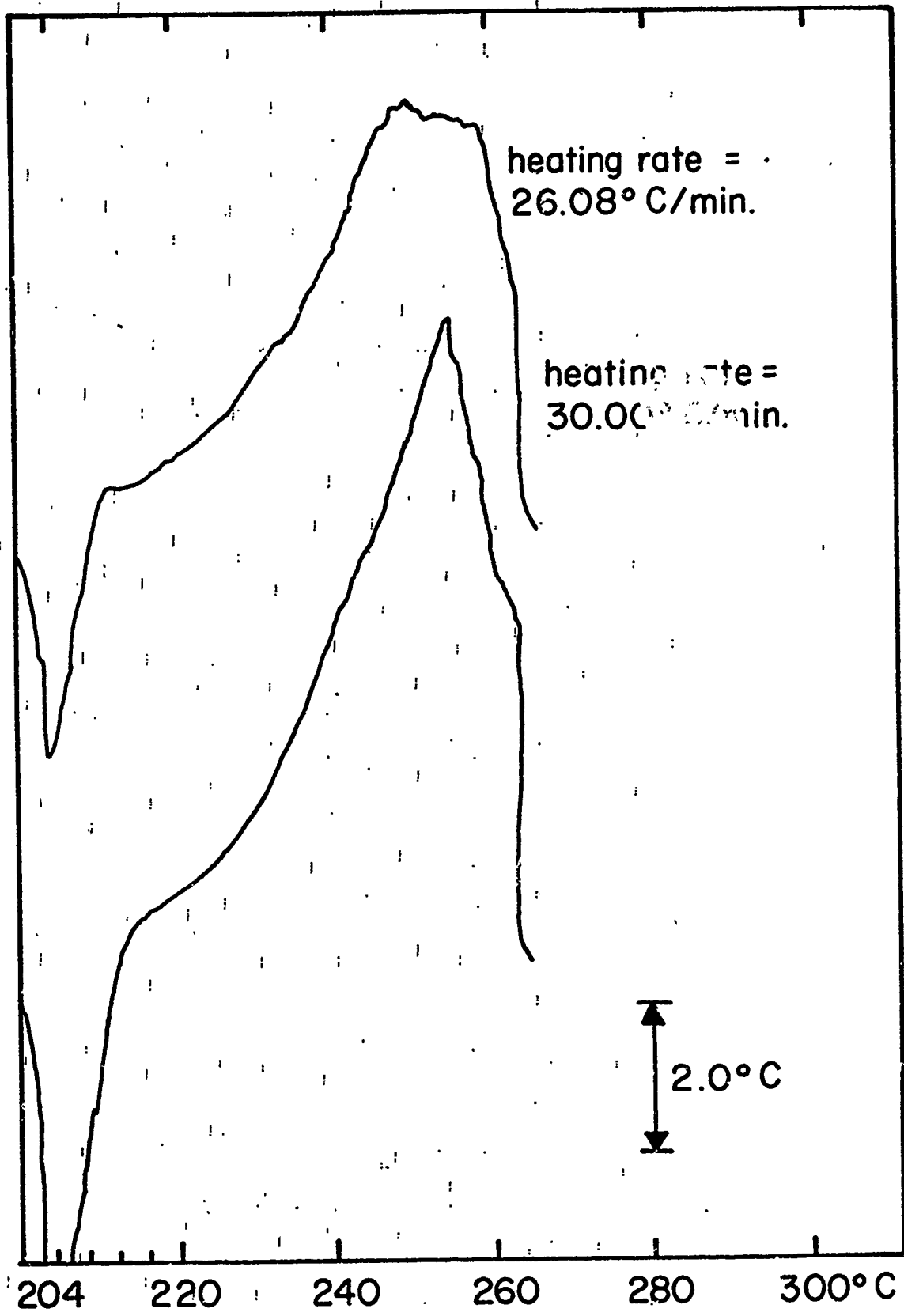


Figure 17. Variable Heating Rate Runs 18 & 19.

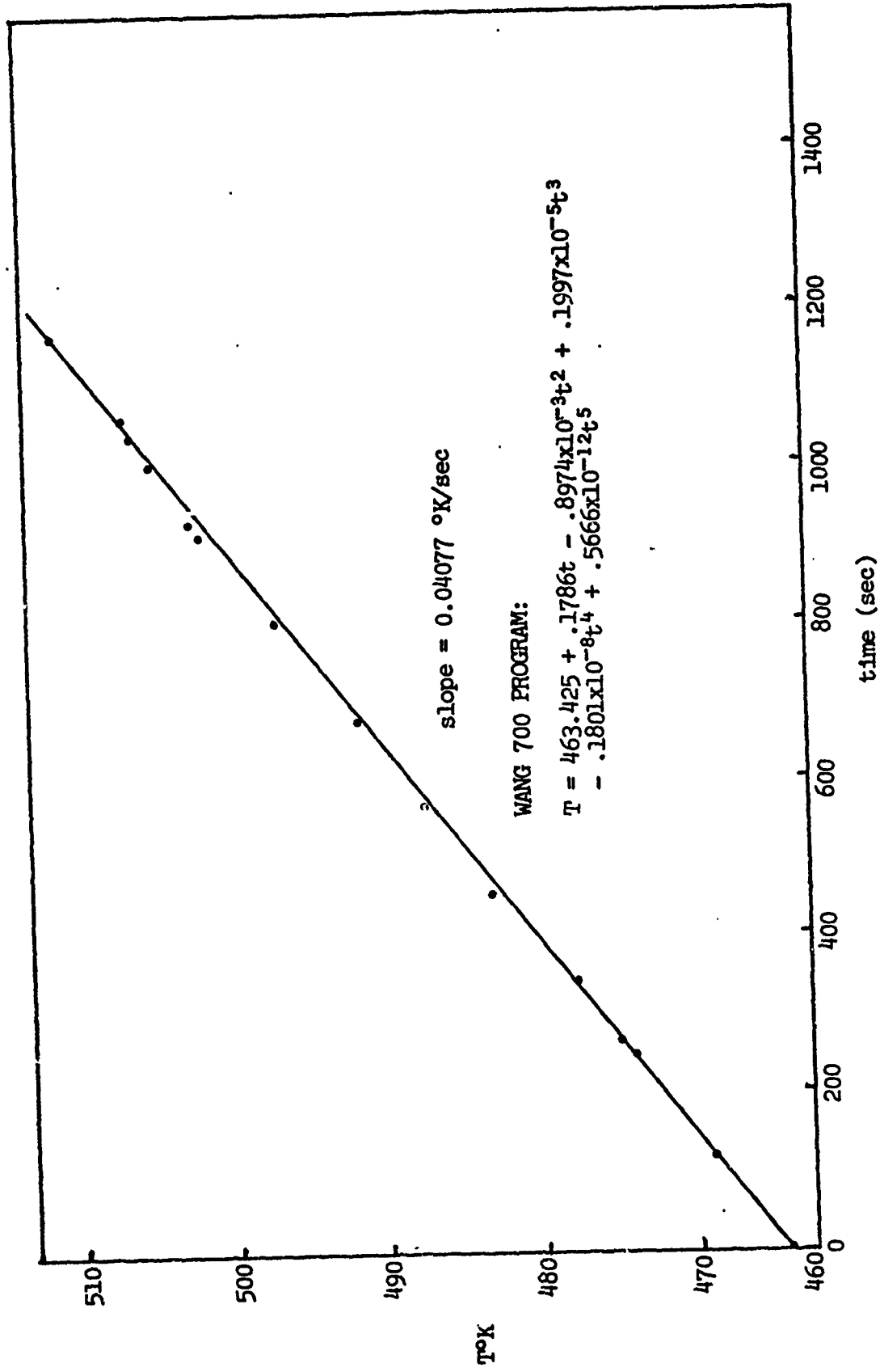


FIGURE 18: T°K vs. time, heating rate 2.43°C/min.

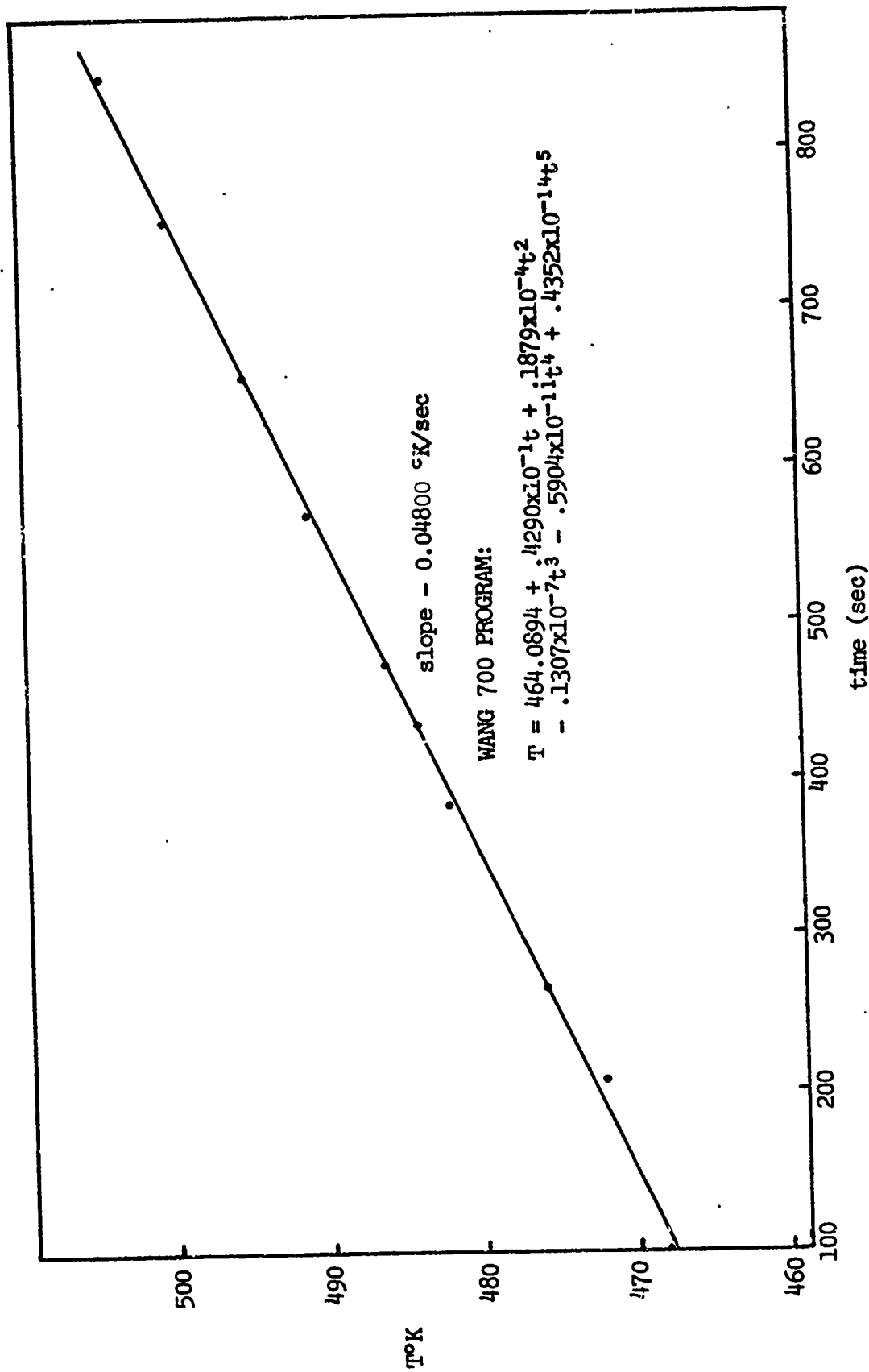


FIGURE 19: T°K vs. time, heating rate 2.88°C/min.

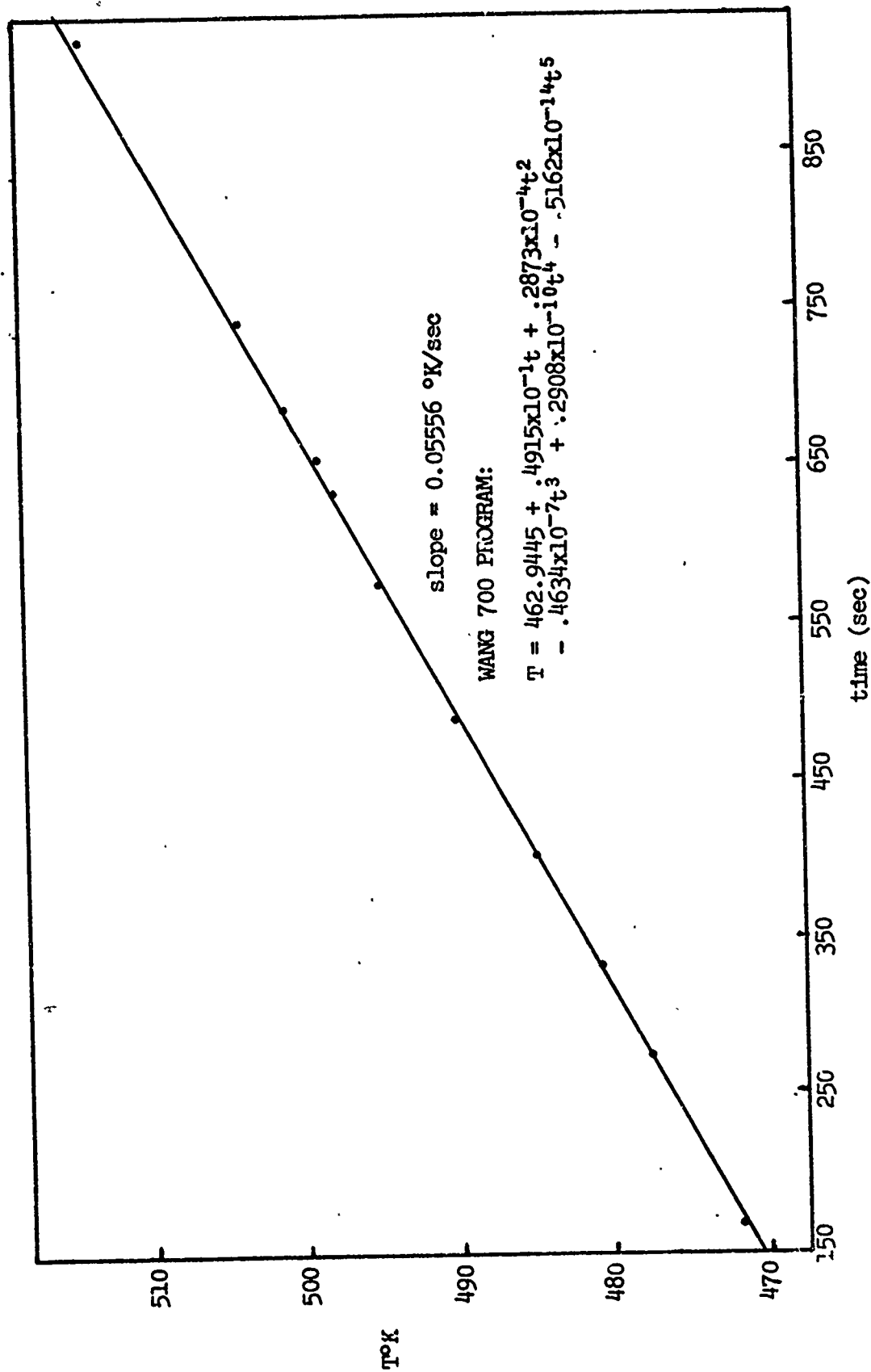


FIGURE 20: T°K vs. time, heating rate 3.33°C/min.

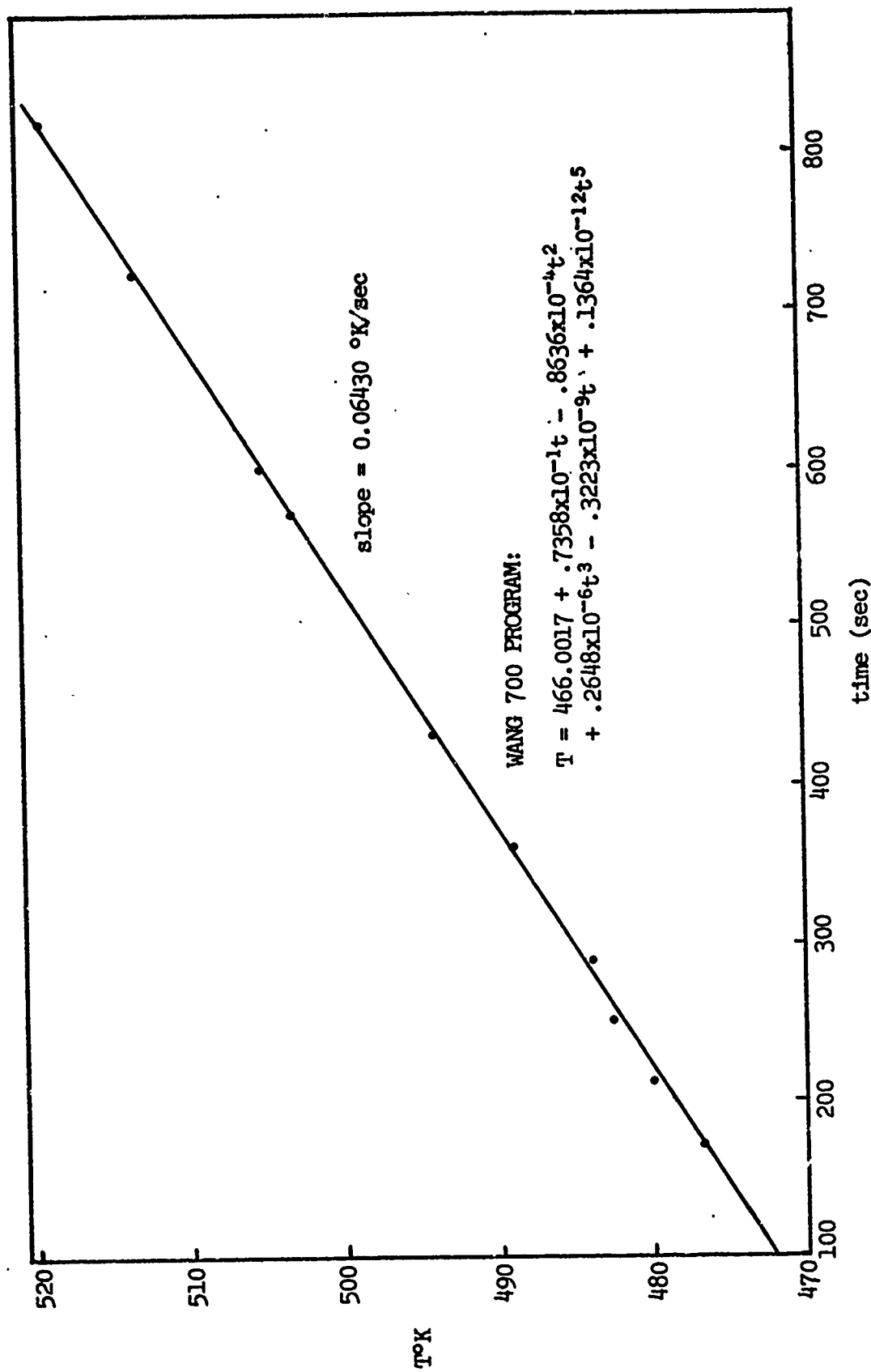


FIGURE 21: T°K vs. time, heating rate 3.86°C/min.

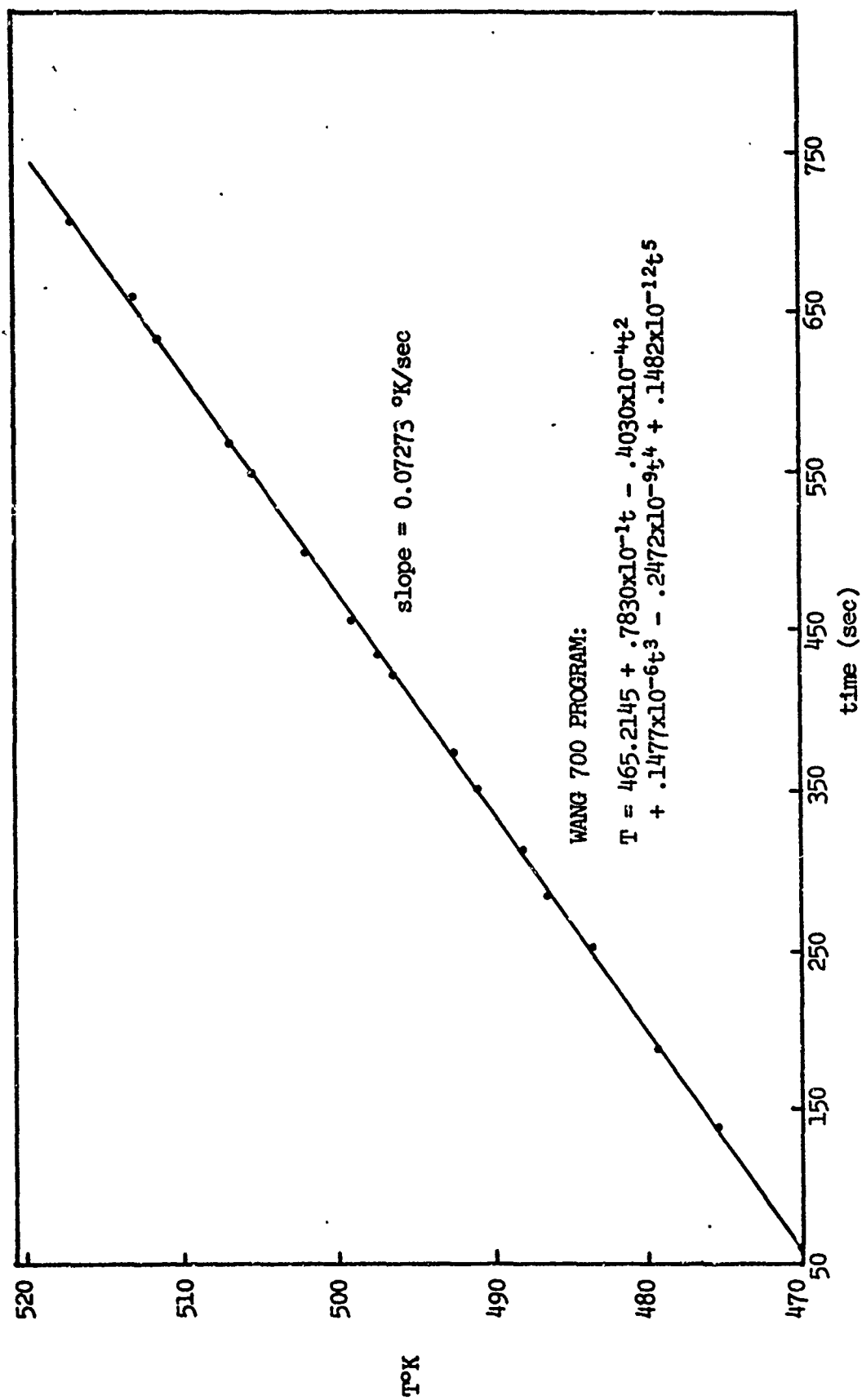


FIGURE 22: T°K vs. time, heating rate 4.36°C/min.

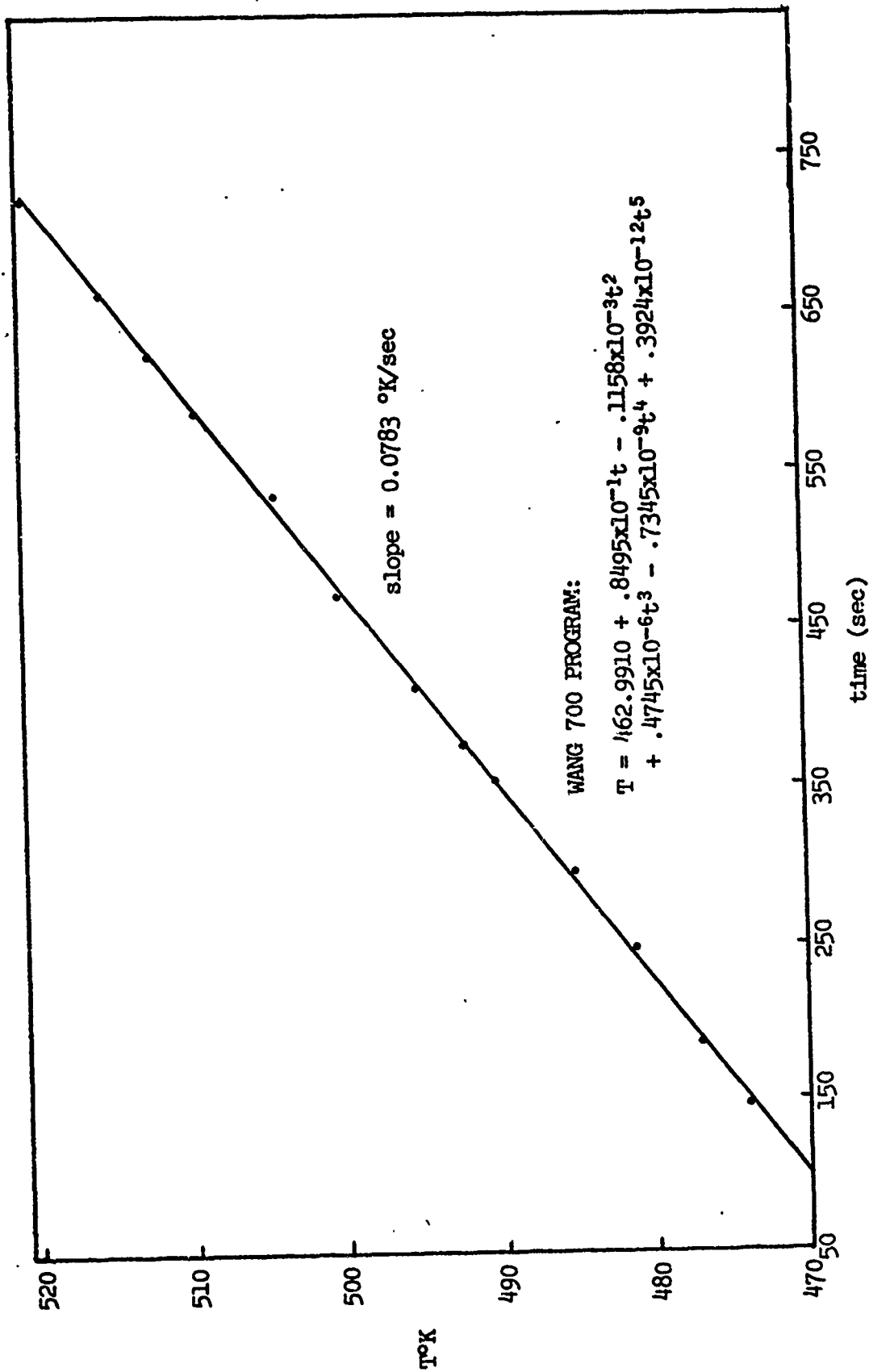


FIGURE 23: T°K vs. time, heating rate 4.70°C/min.

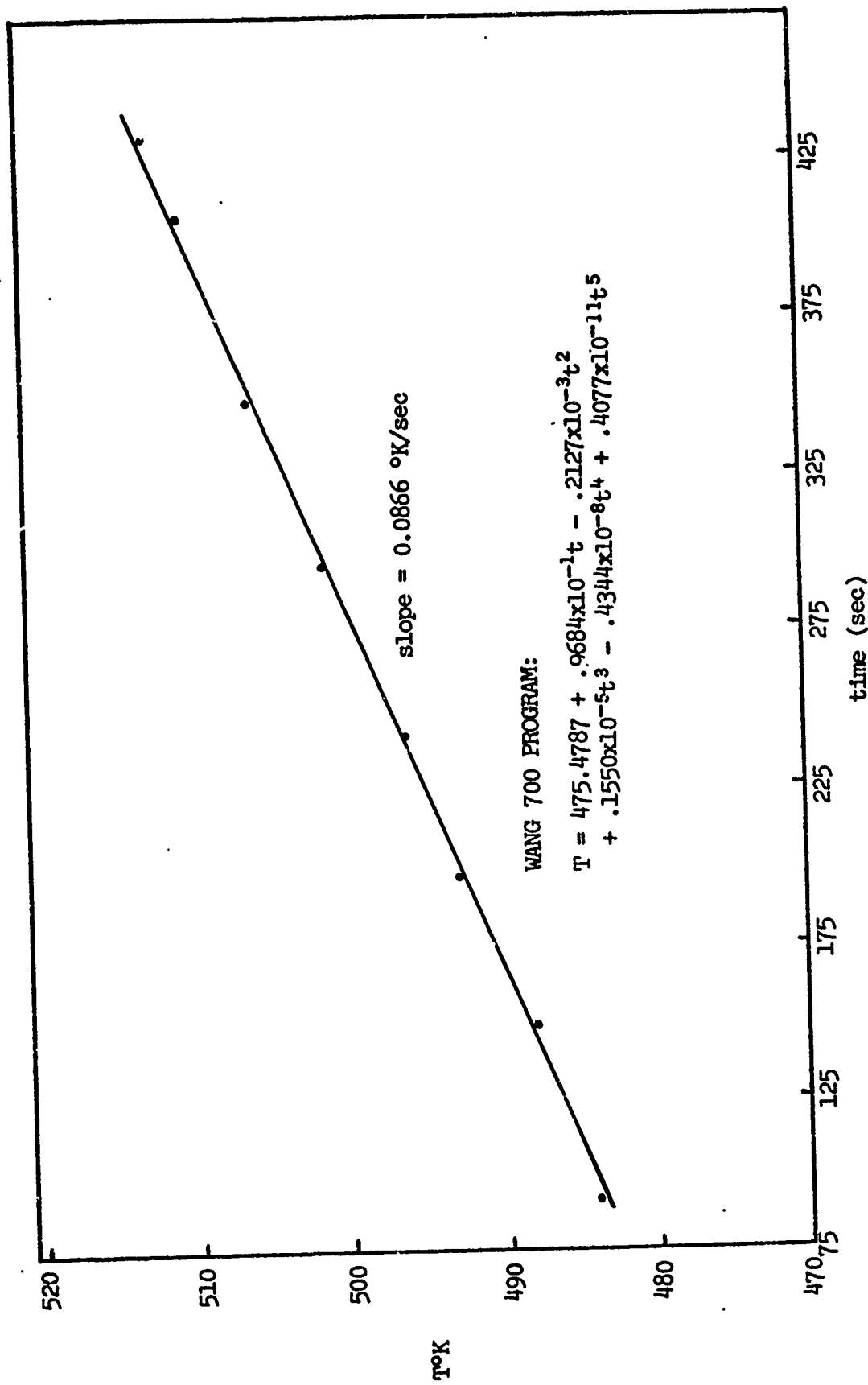


FIGURE 24: T°K vs. time, heating rate 5.19°C/min.

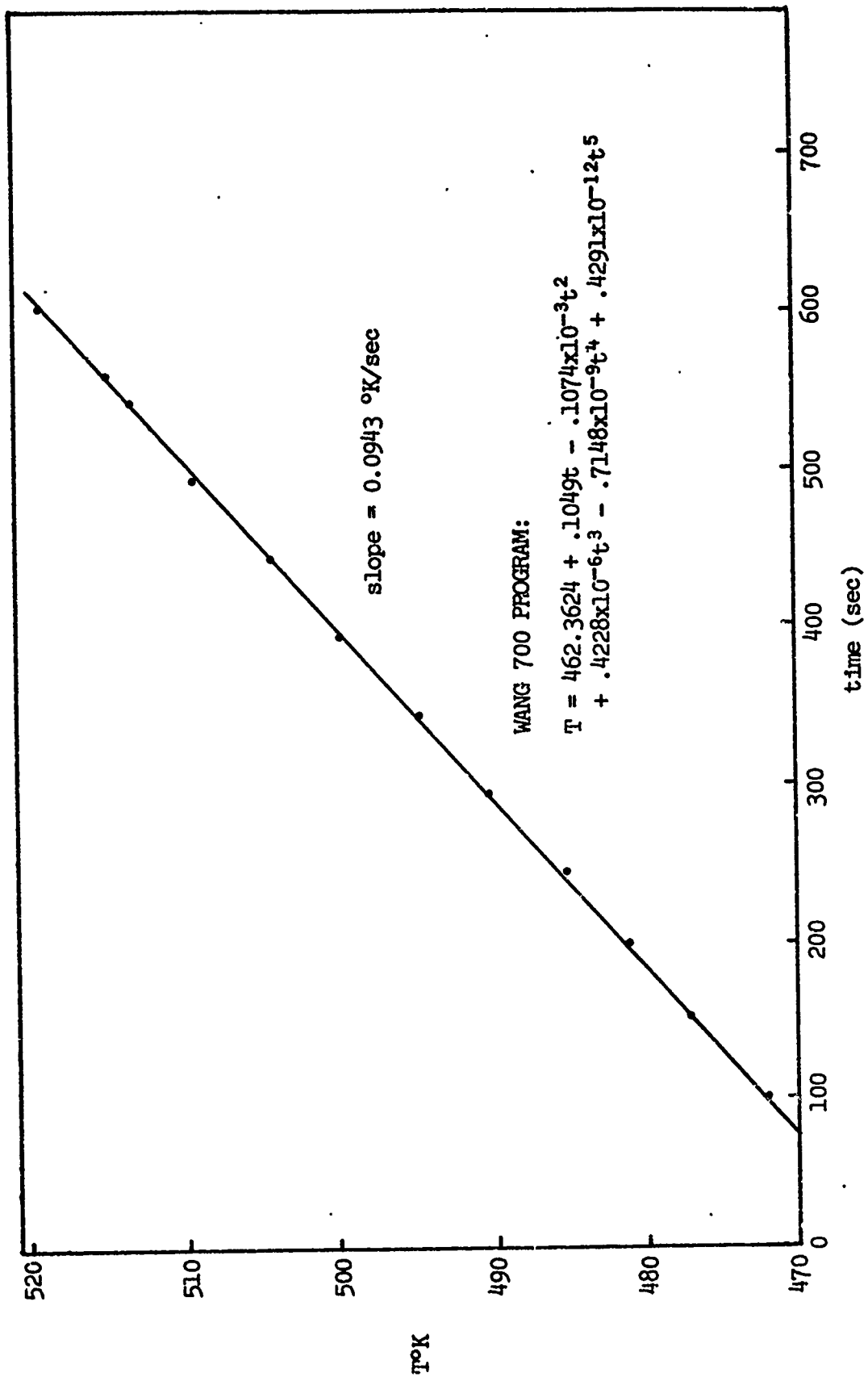


FIGURE 25: T°K vs. time, heating rate 5.66°C/min.

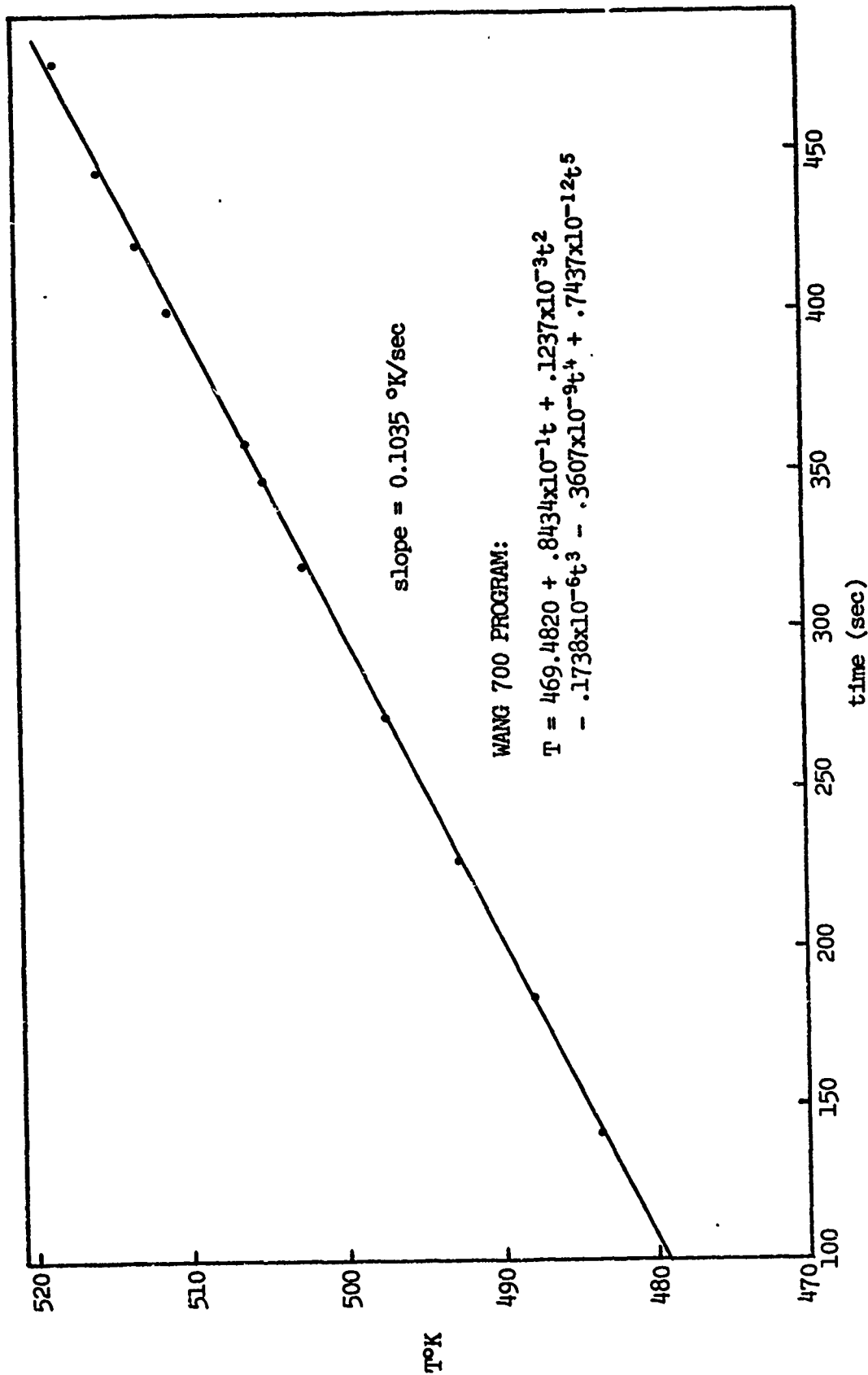


FIGURE 26: T°K vs. time, heating rate 6.21°C/min.

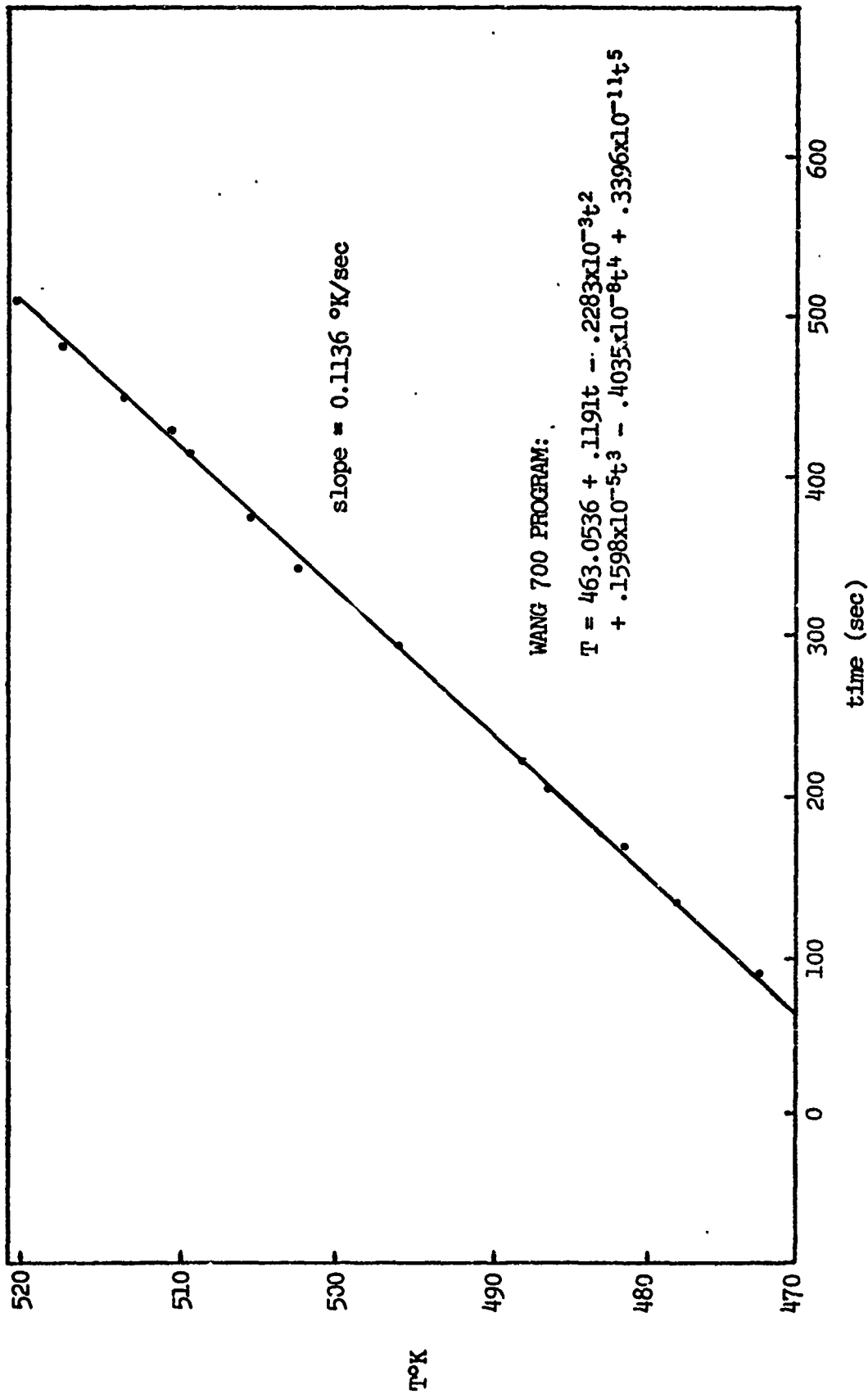


FIGURE 27: T°K vs. time, heating rate 6.92°C/min.

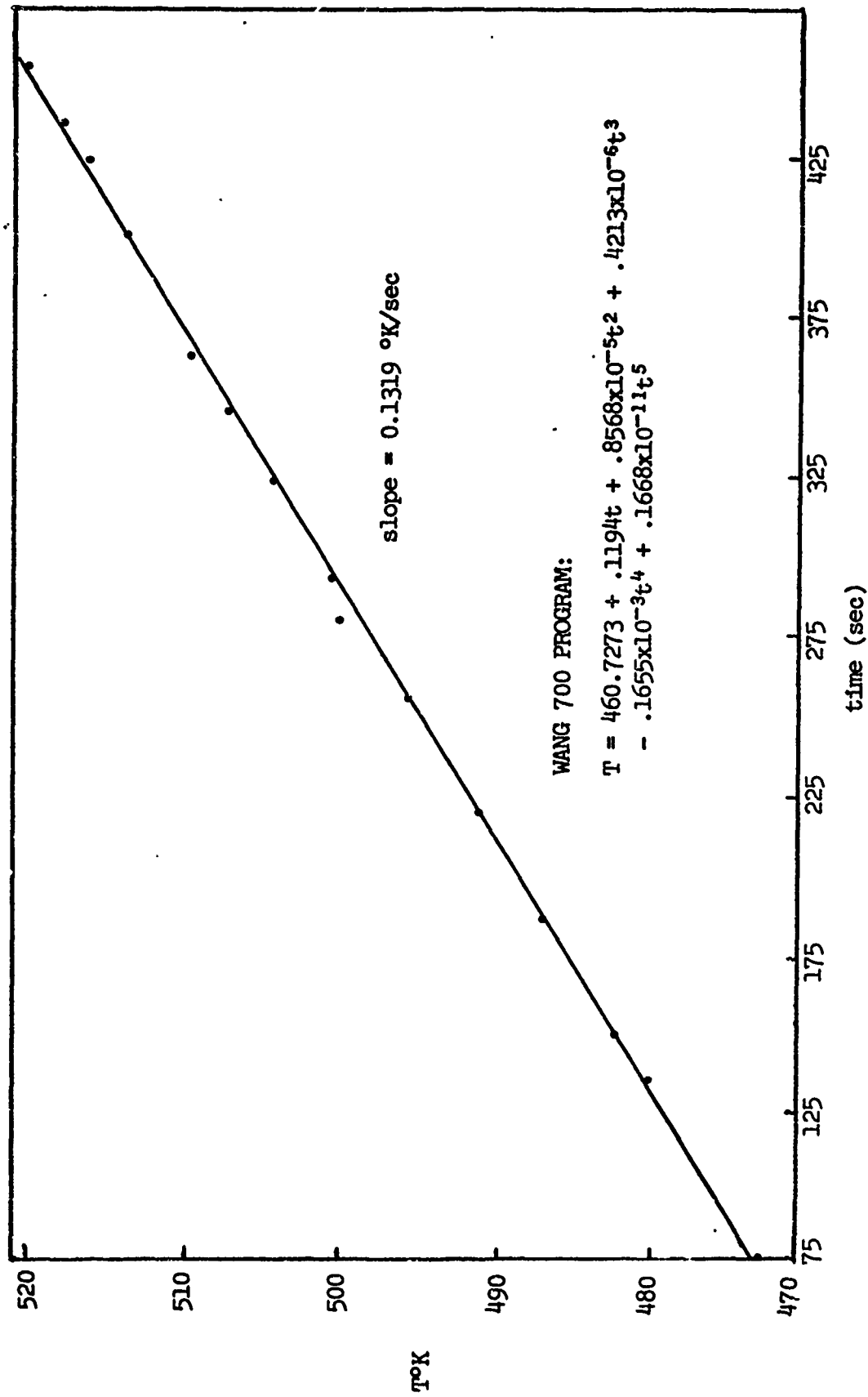


FIGURE 28: T°K vs. time, heating rate 7.92°C/min.

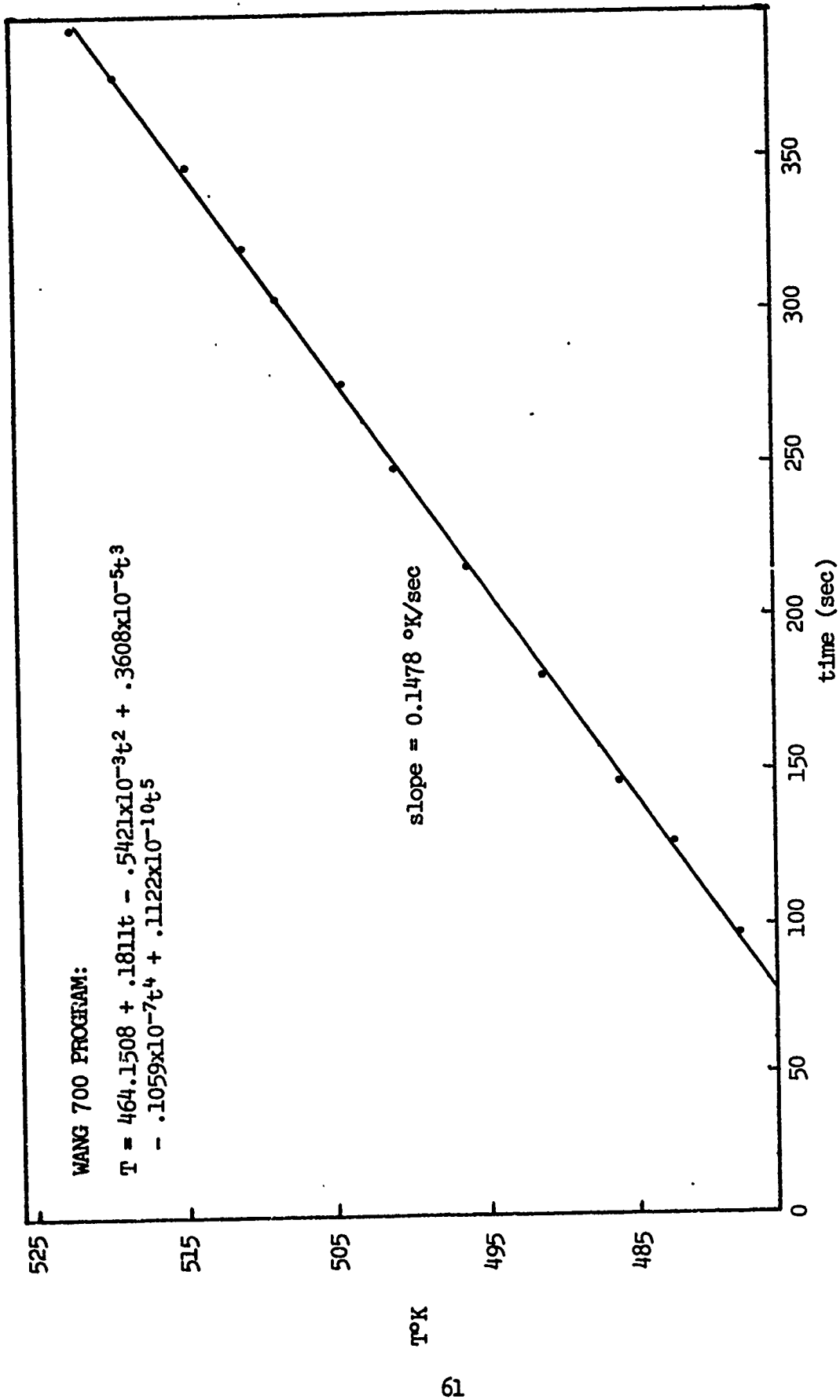


FIGURE 29: °K vs. time, heating rate 8.87°C/mdn.

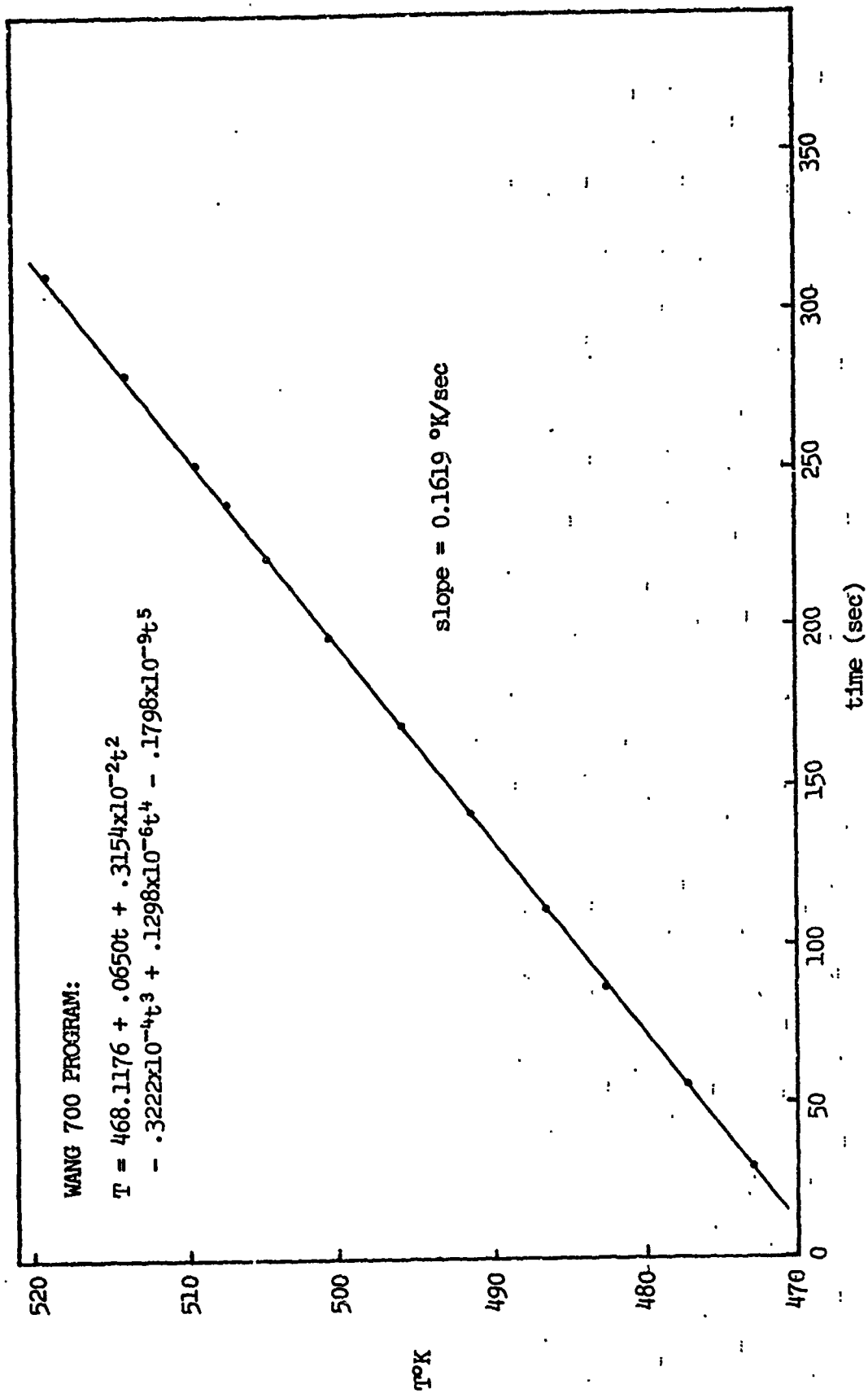


FIGURE 30: T°K vs. time, heating rate 9.71°C/min.

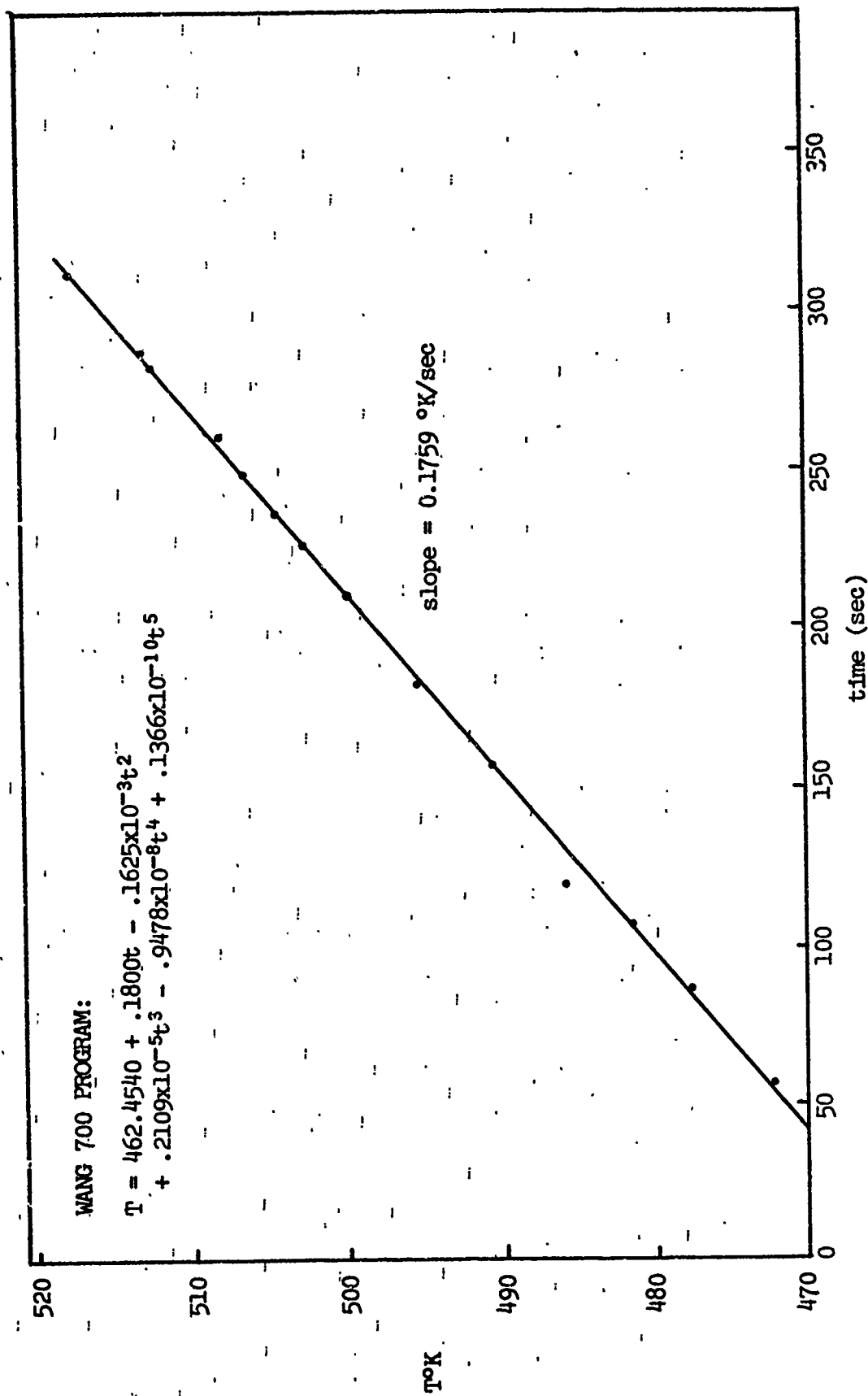


FIGURE 31: T°K vs. time, heating rate 10.56°C/min.

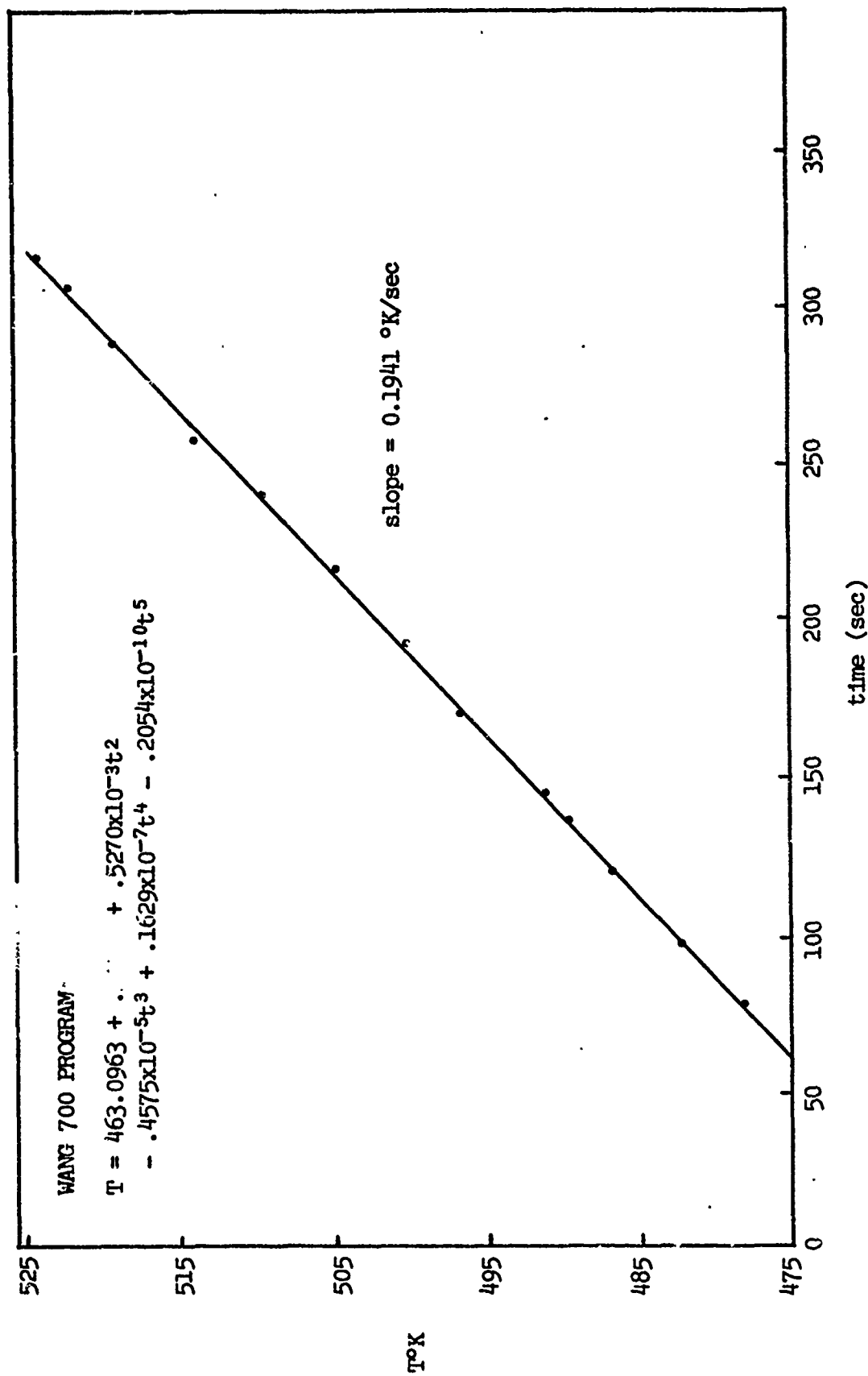


FIGURE 32: T°K vs. time, heating rate 11.65°C/min.

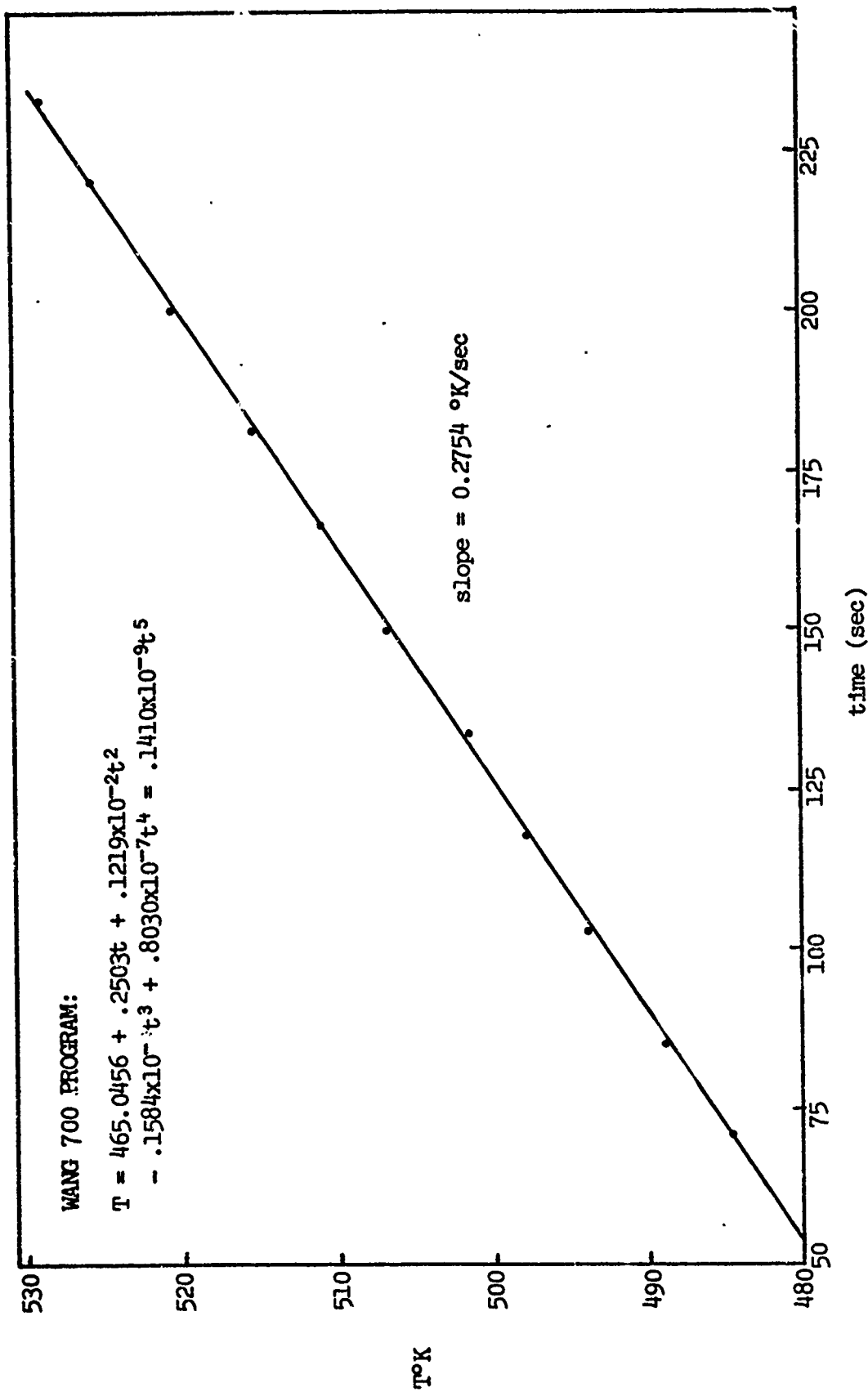


FIGURE 33: T°K vs. time, heating rate 16.52°C/min.

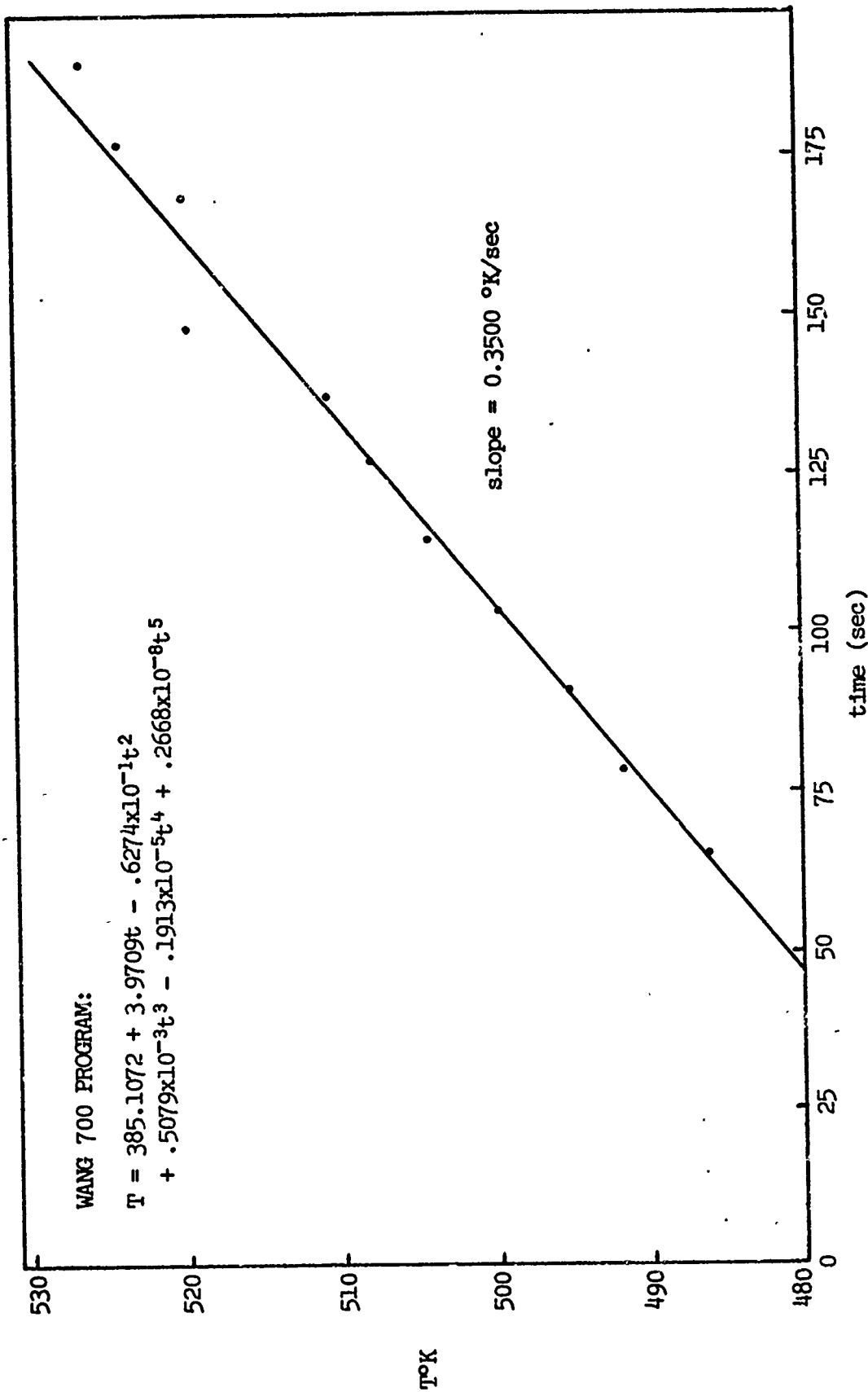


FIGURE 34: T°K vs. time, heating rate 21.00°C/min.

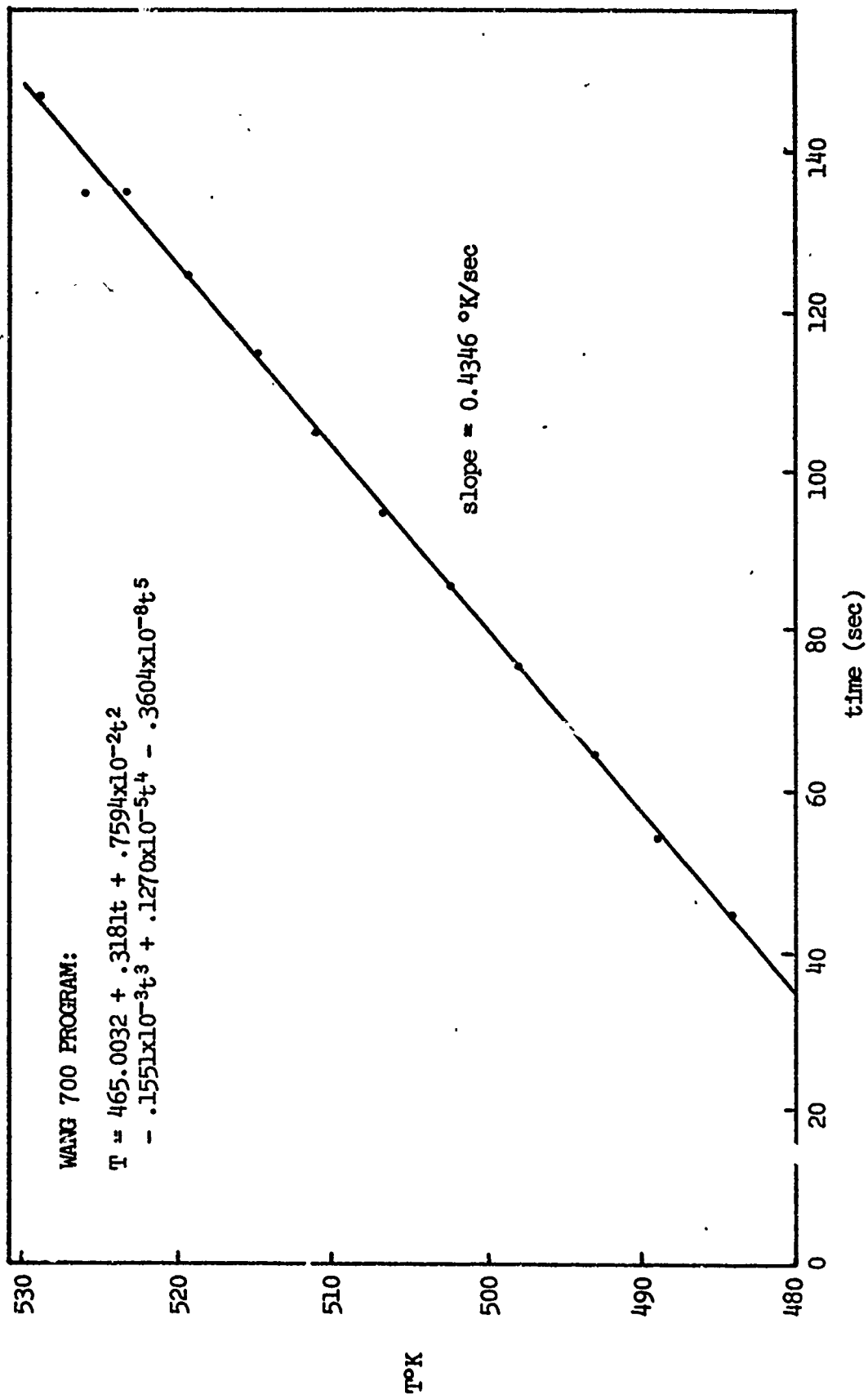


FIGURE 35: T°K vs. time, heating rate 26.08°C/min.

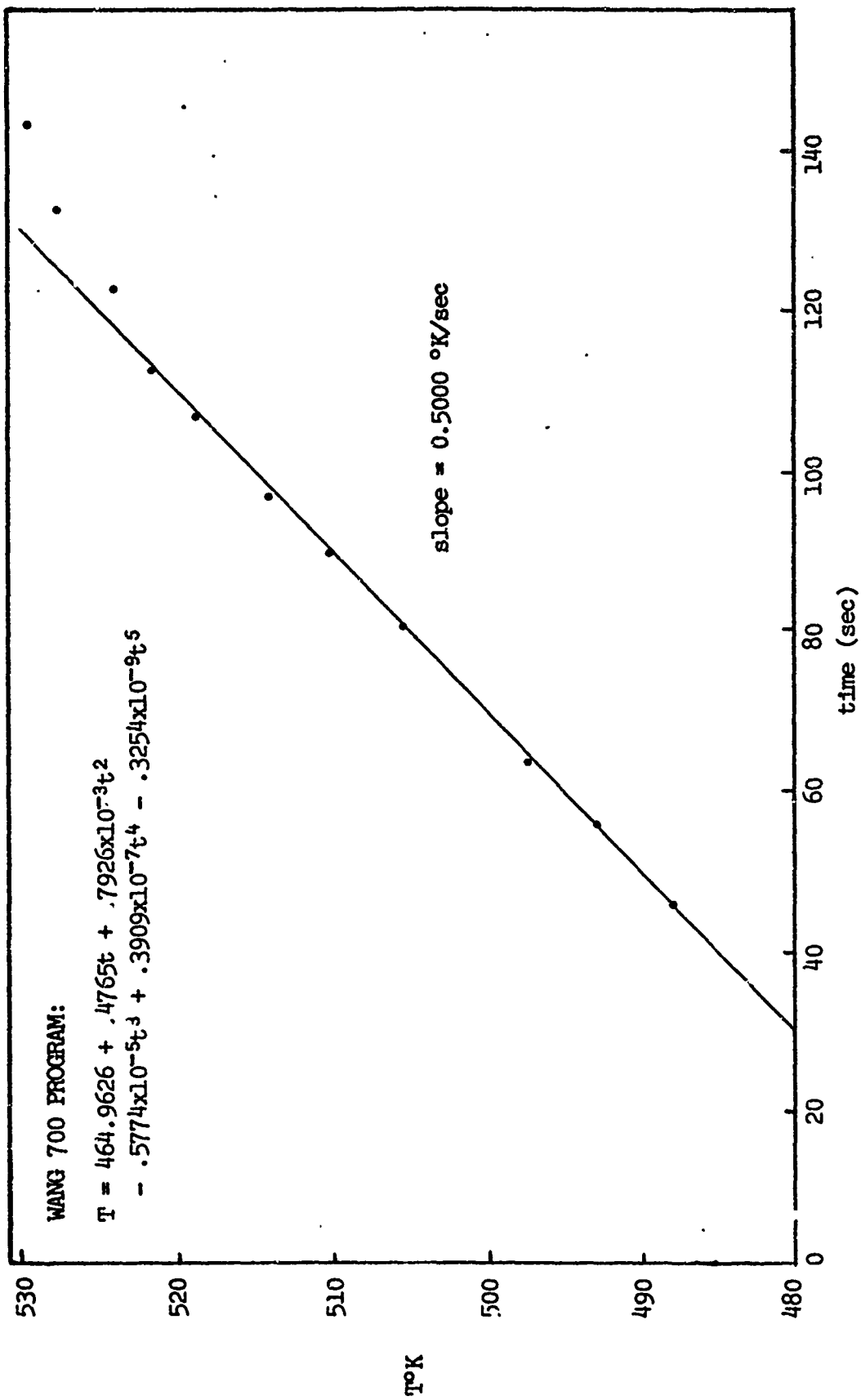


FIGURE 36: T°K vs. time, heating rate 30.00°C/min.

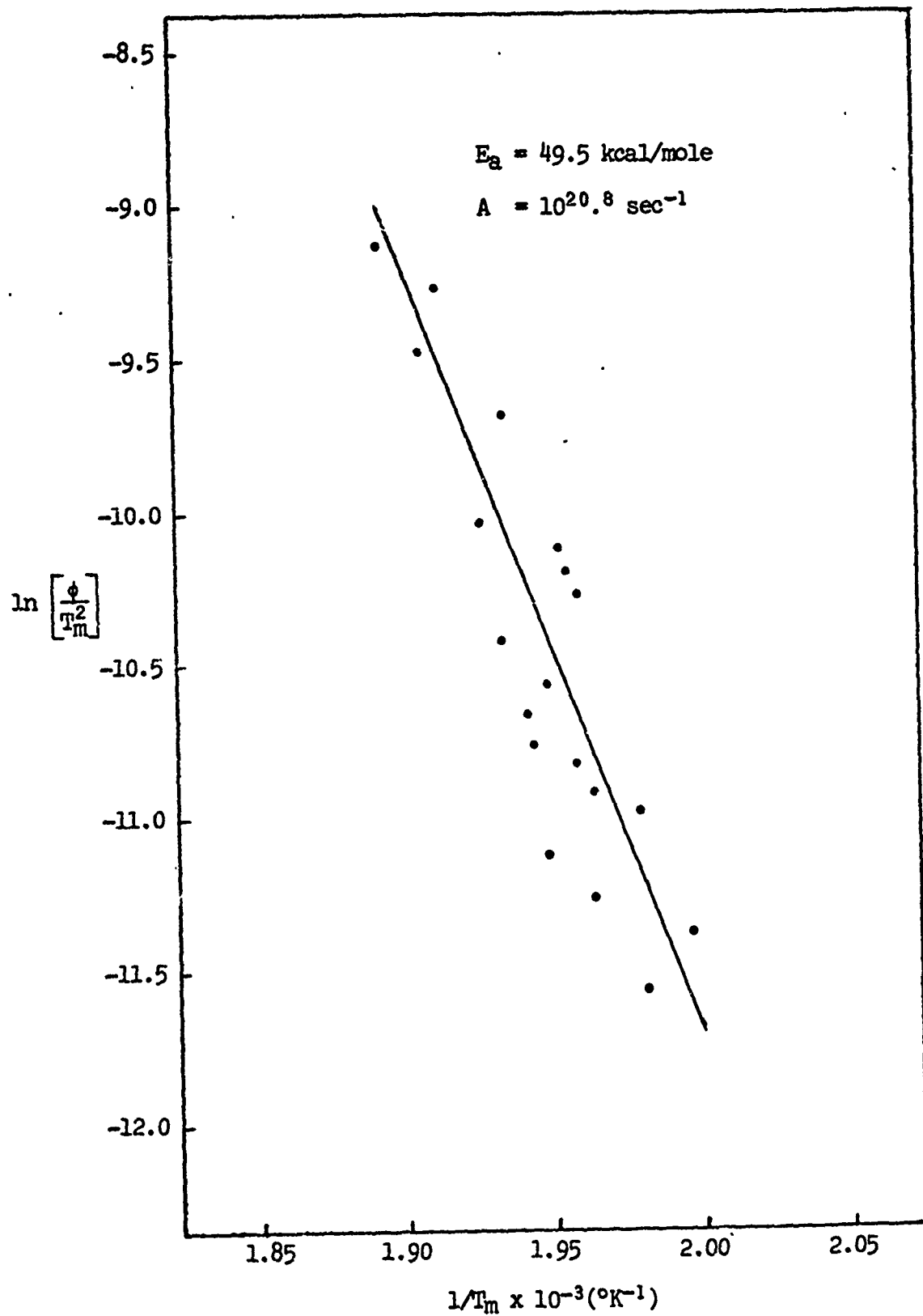
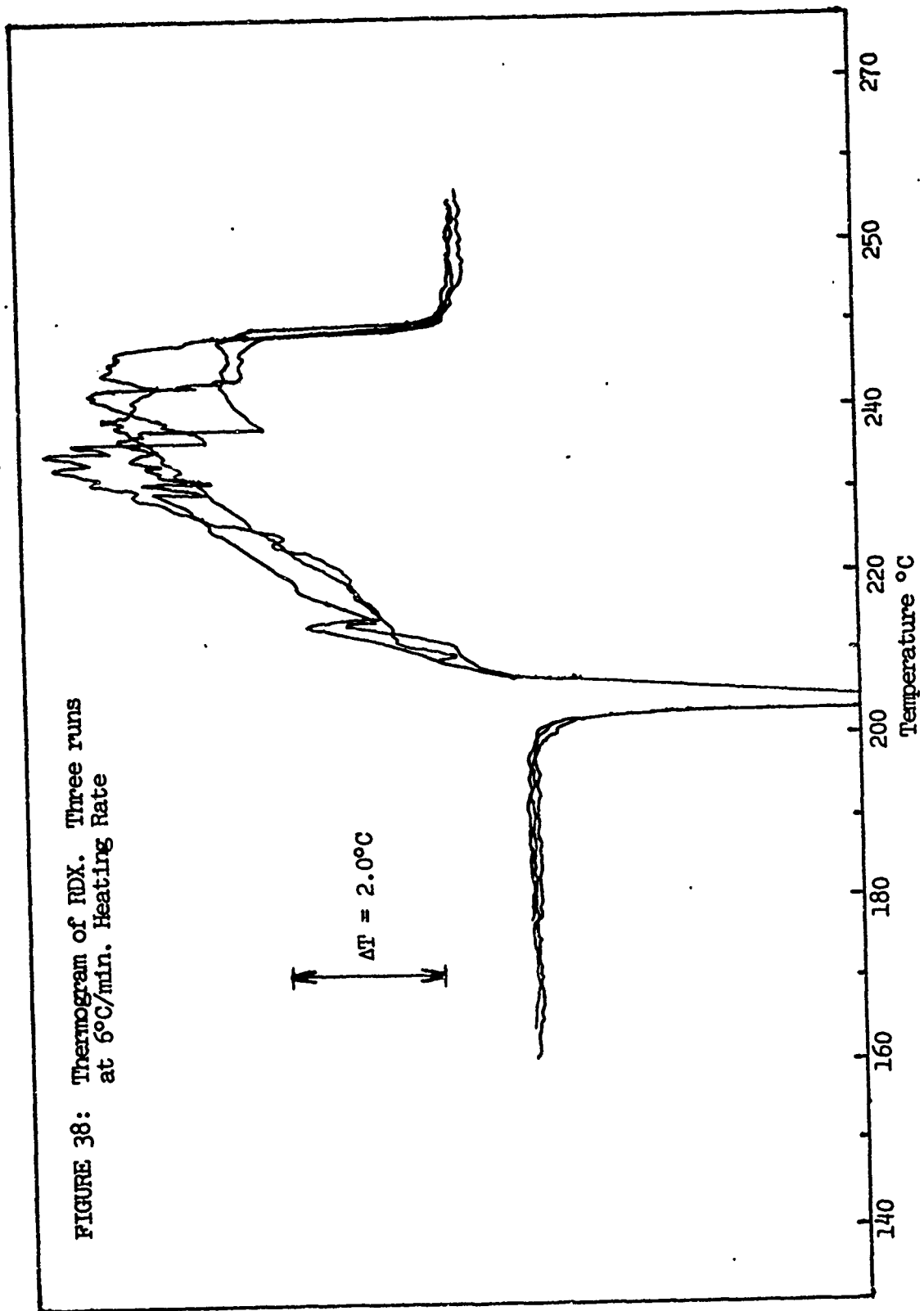


FIGURE 37: Variable heating rate plot of $\ln \left[\frac{\phi}{T_m^2} \right]$ vs. $1000/T_m$

FIGURE 38: Thermogram of RDX. Three runs
at 5°C/min. Heating Rate



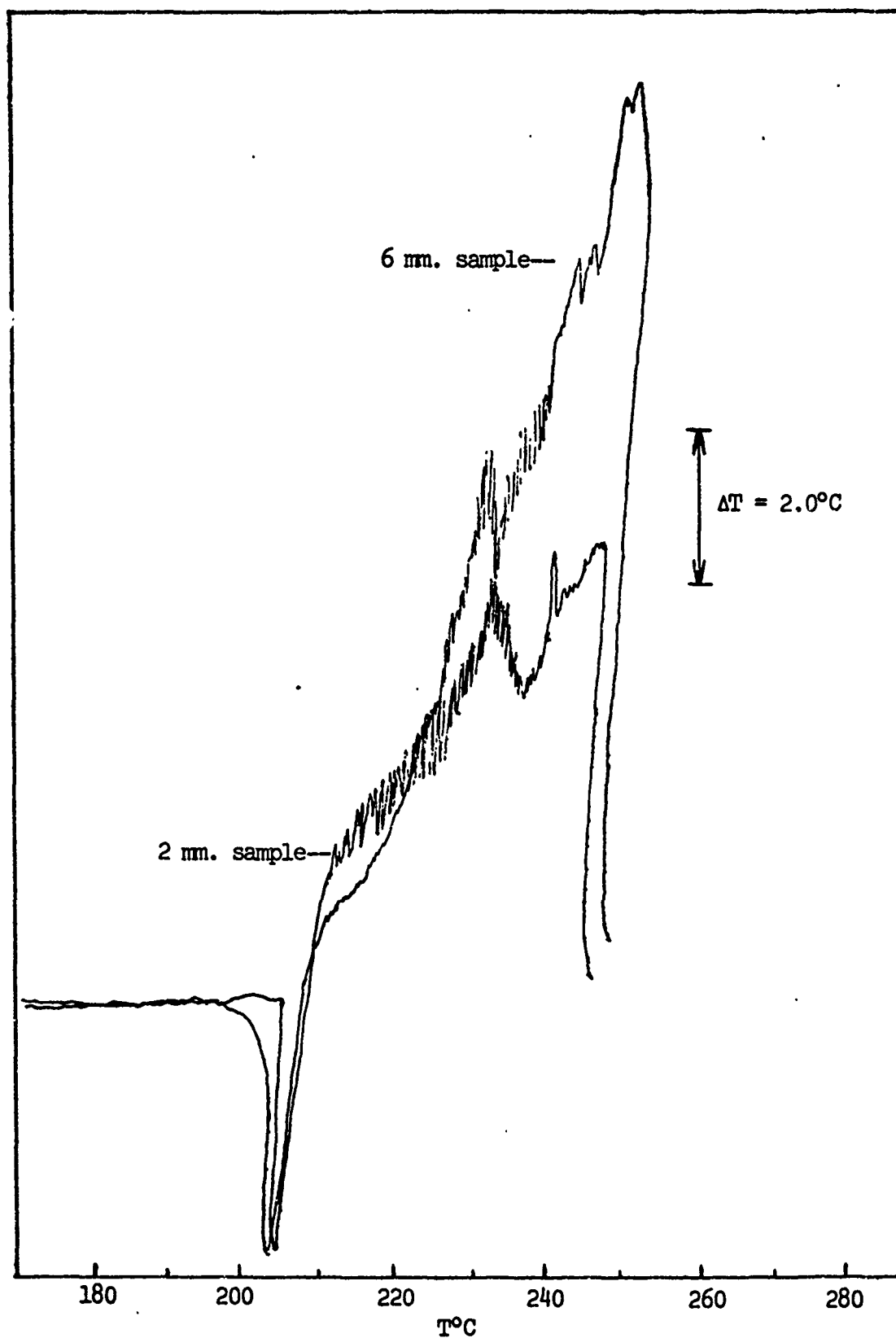


FIGURE 39: Thermogram of RDX, $4^{\circ}\text{C}/\text{min}$.

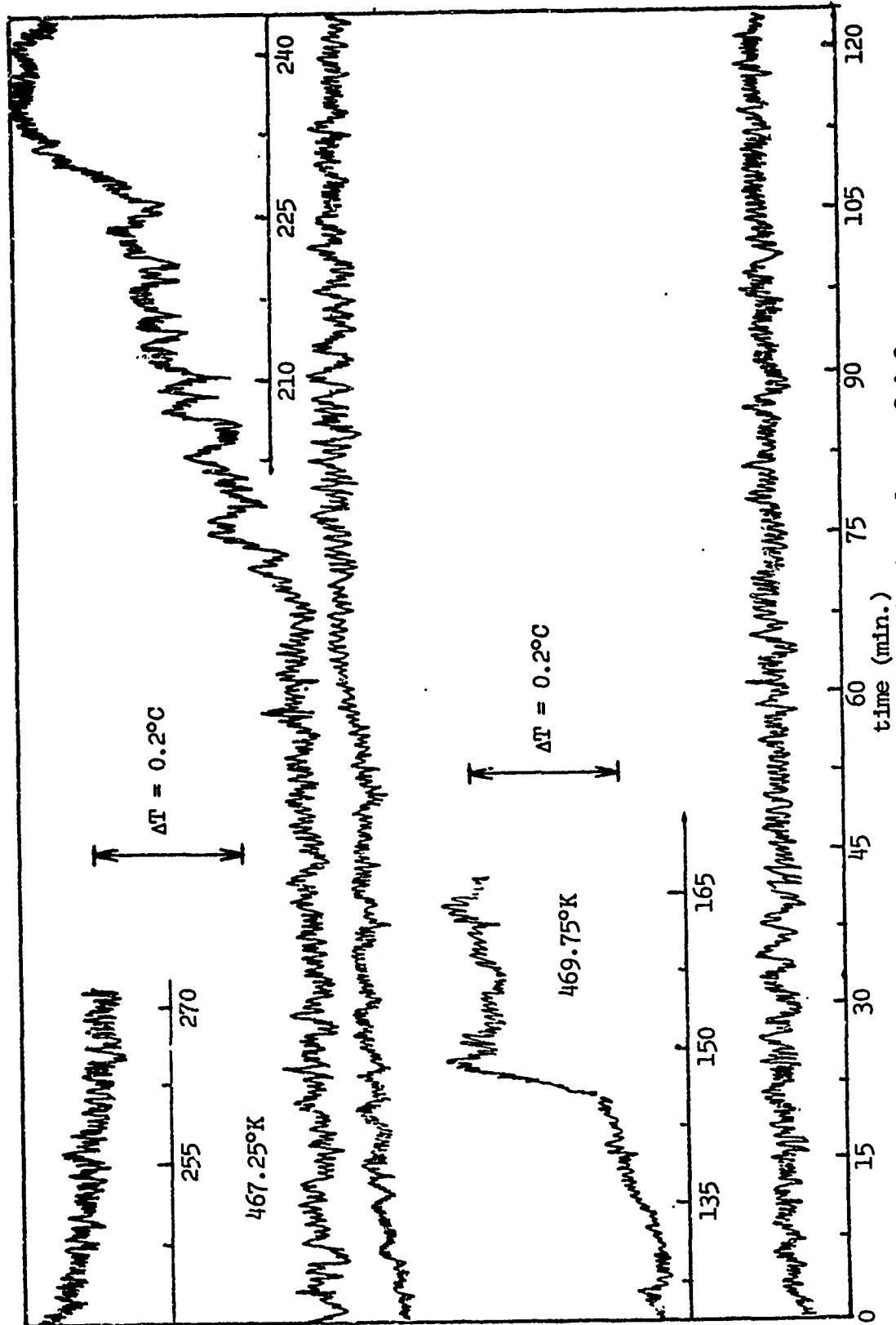


FIGURE 40: Thermograms of RDX, Isothermal runs 2 & 3.

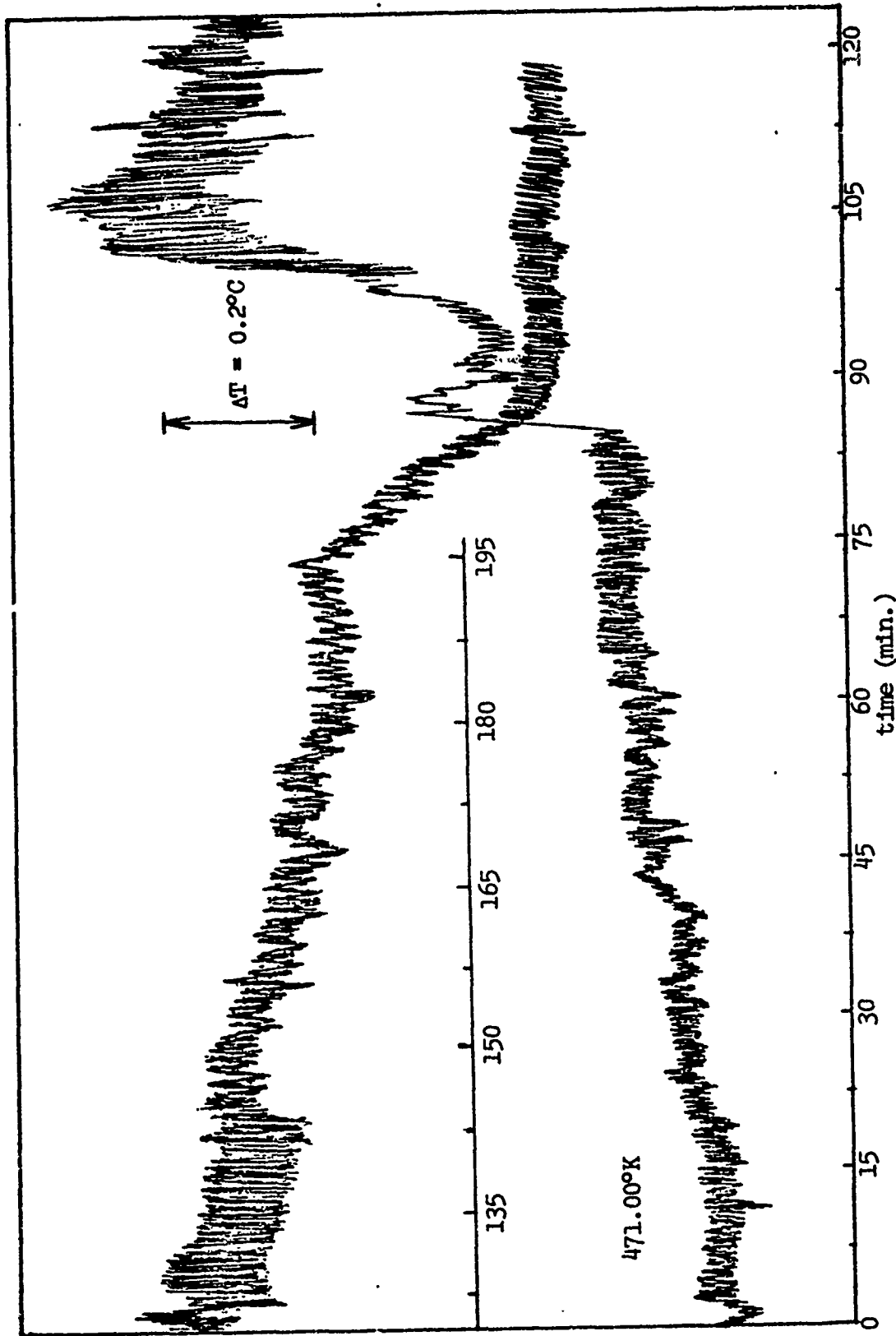


FIGURE 41: Thermogram of KDX, Isothermal run 4.

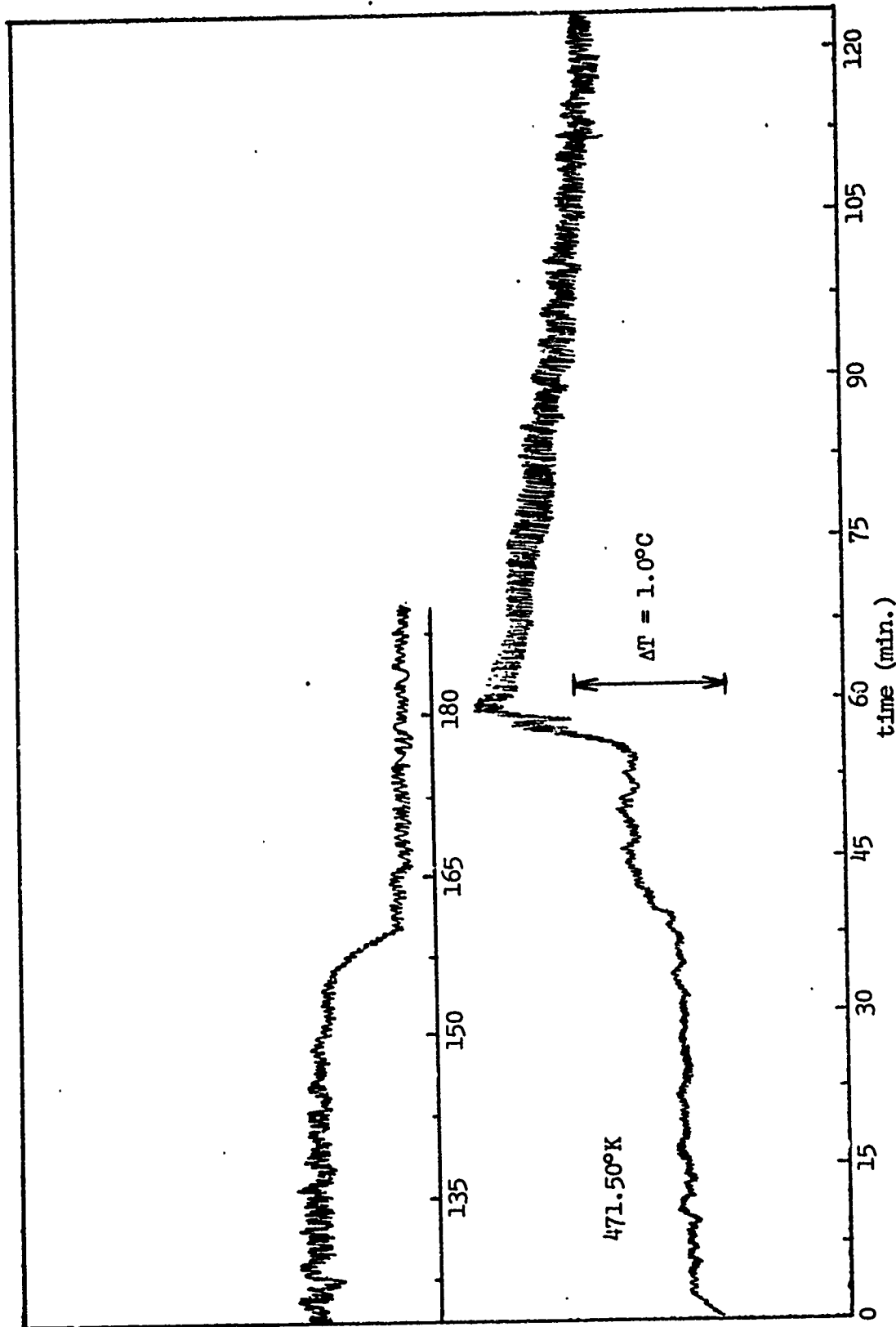


FIGURE 42: Thermogram of RDX, Isothermal run 5.

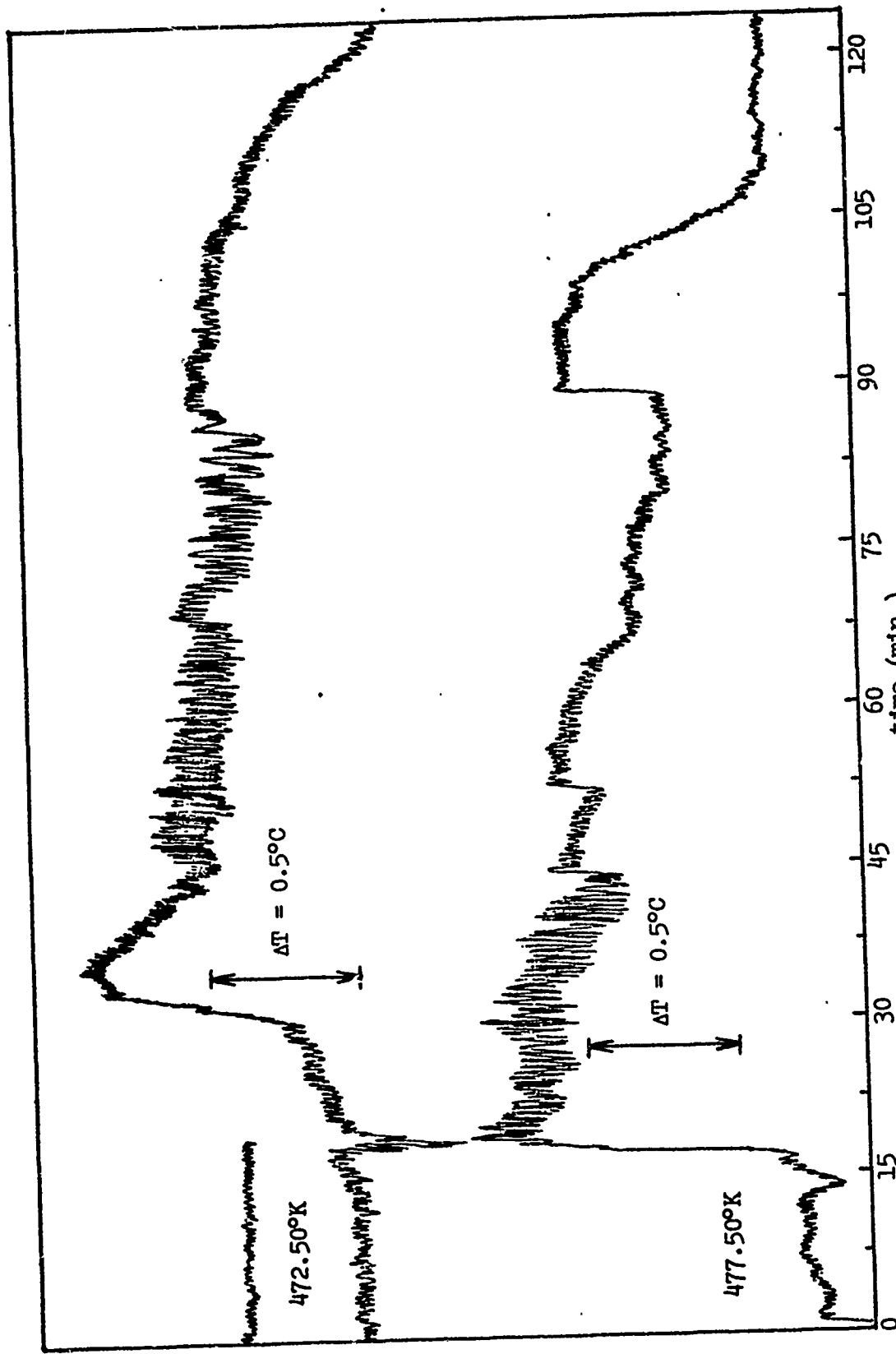


FIGURE 43: Thermograms of RDX, Isothermal runs 6 & 7.

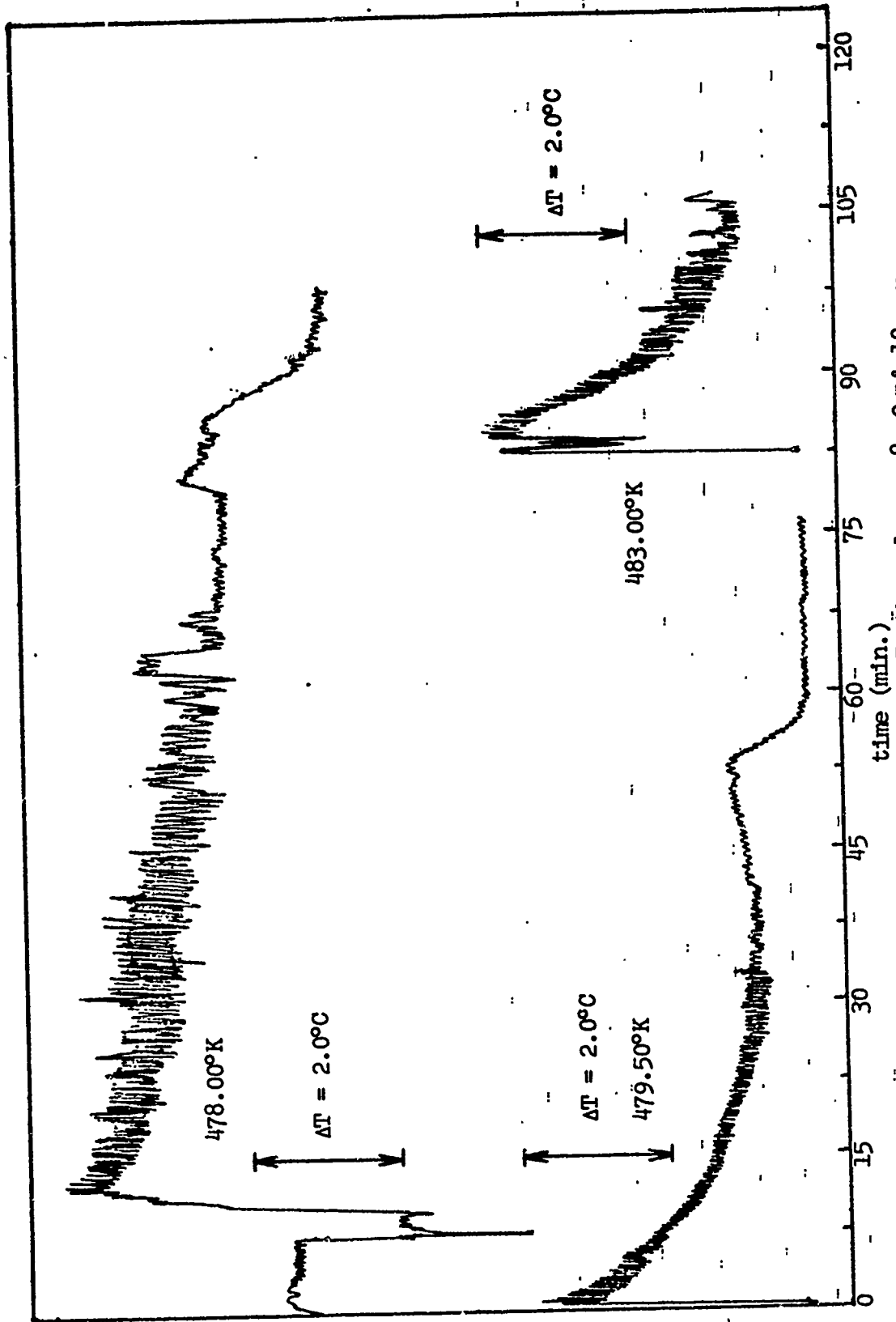


FIGURE 44: Thermograms of RDX, Isothermal runs 8, 9, & 10.

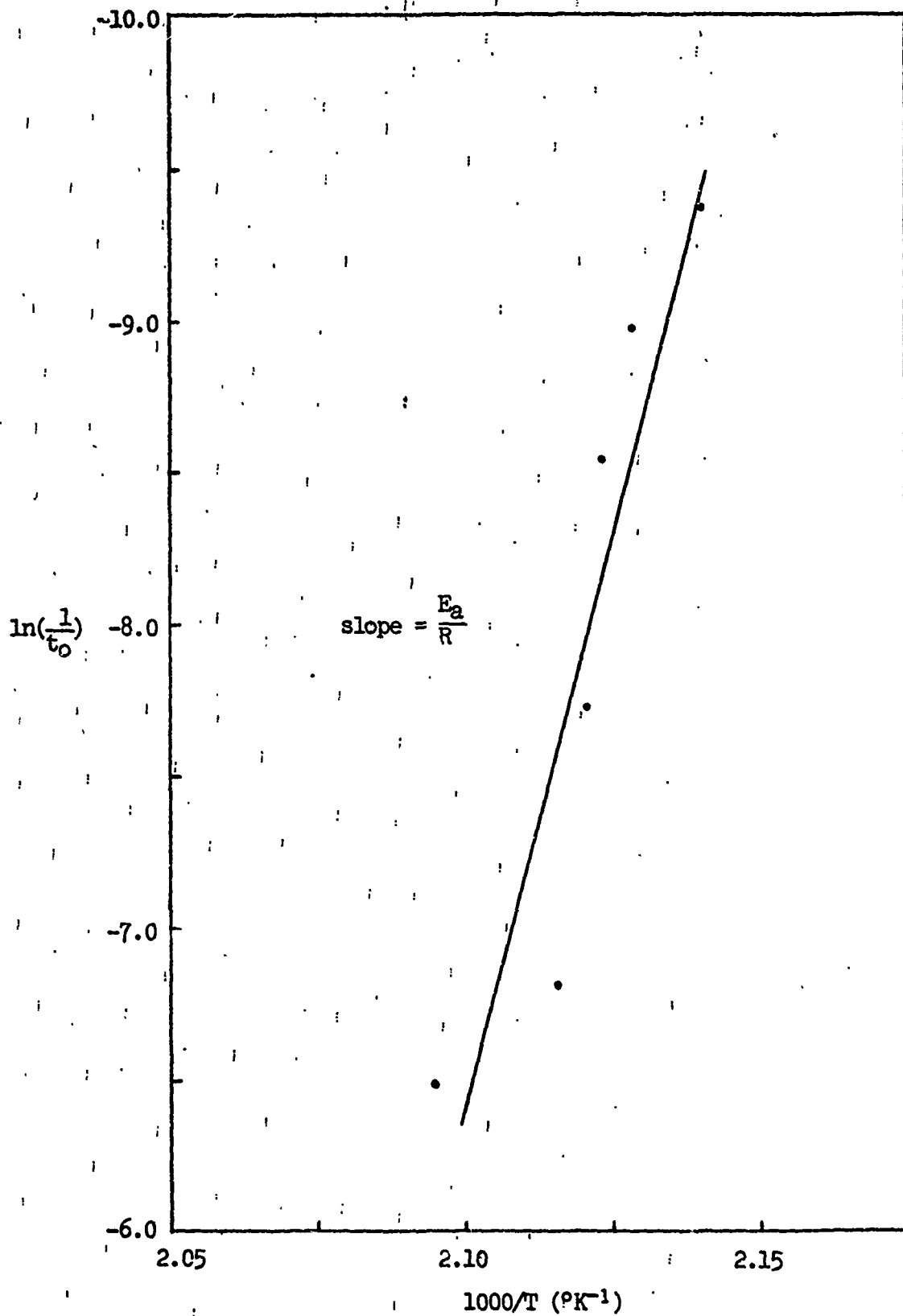


FIGURE 45: $\ln(1/t_0)$ vs. $1000/T$

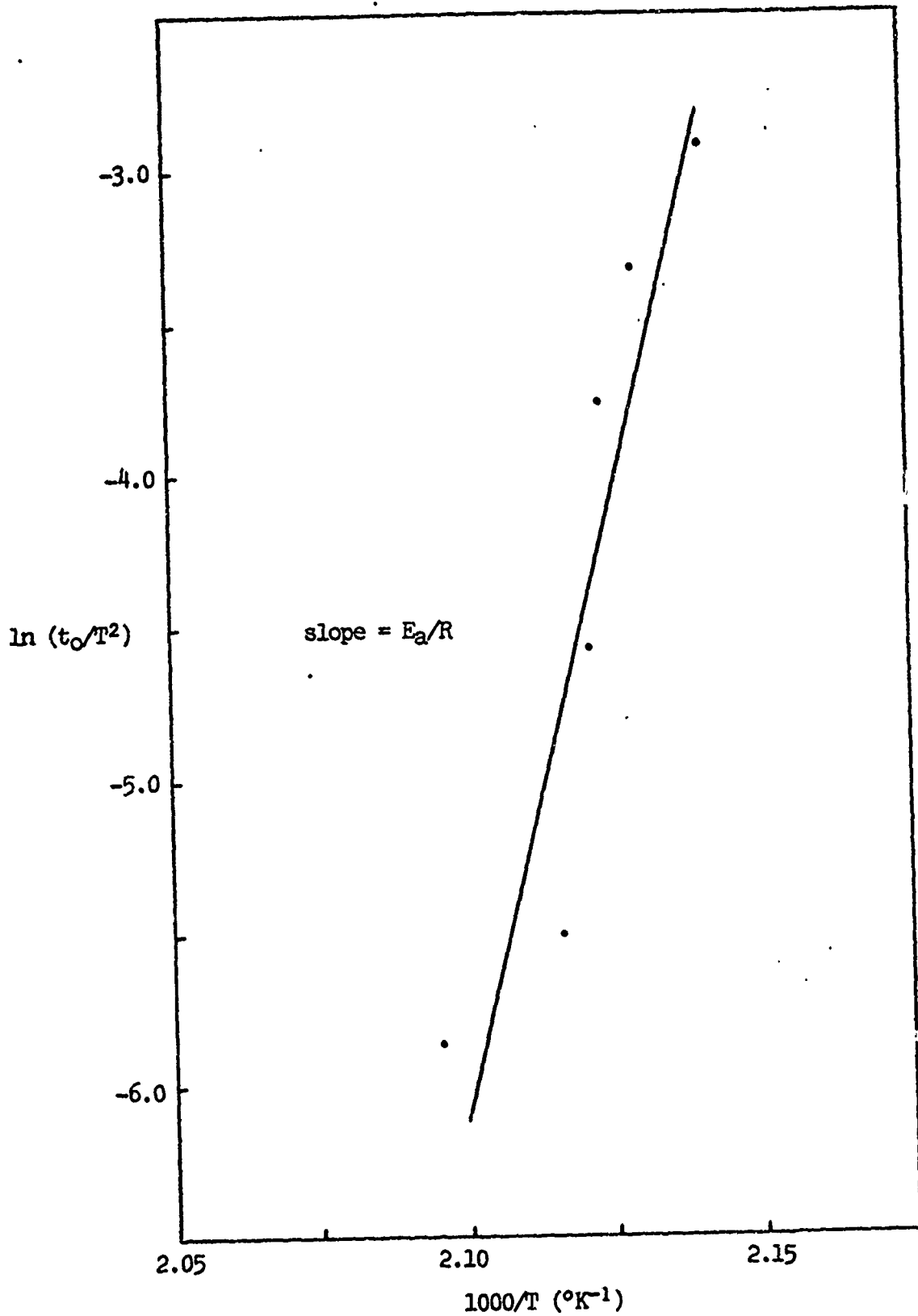


FIGURE 46: $\ln(t_0/T^2)$ vs. $1000/T$

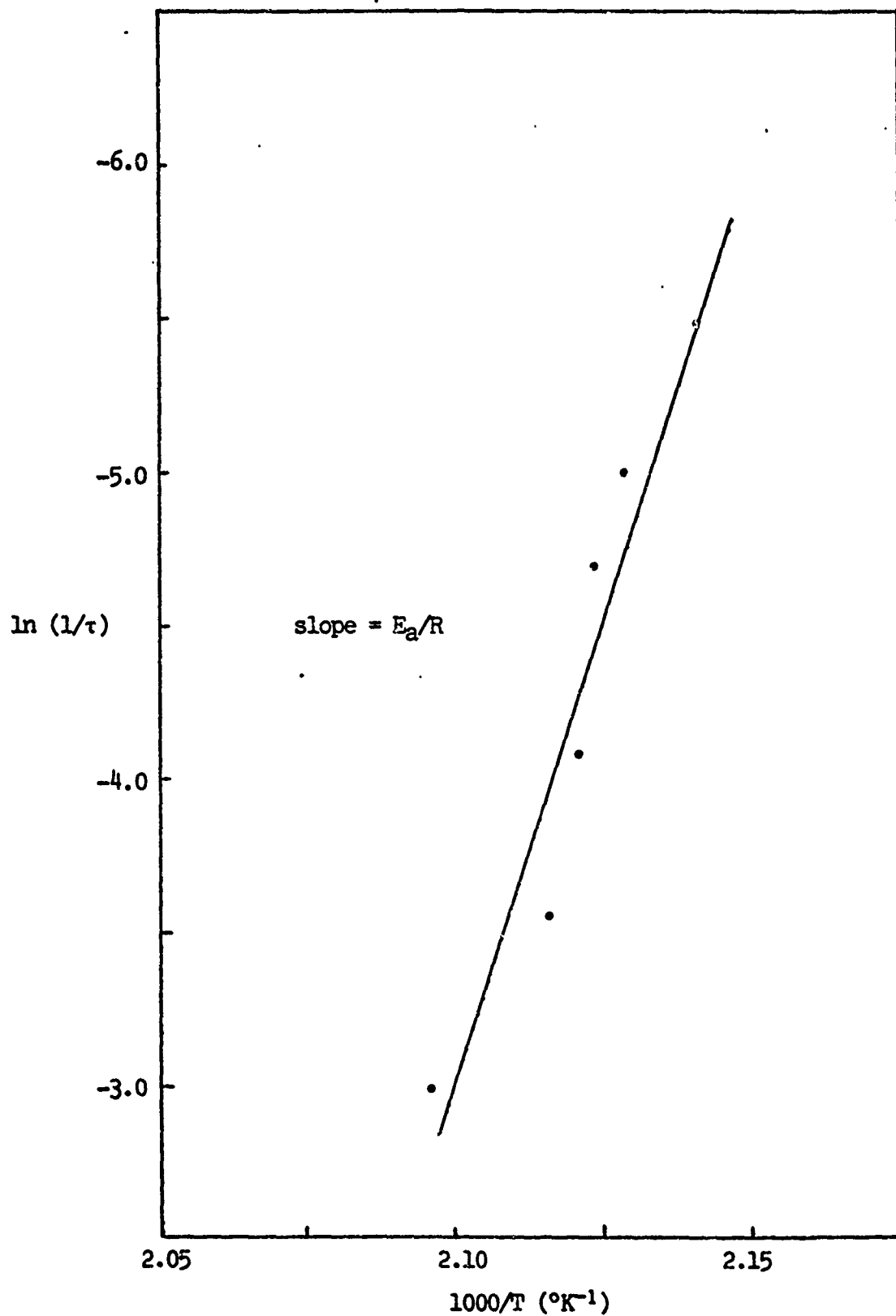


FIGURE 47: ln (1/τ) vs. 1000/T

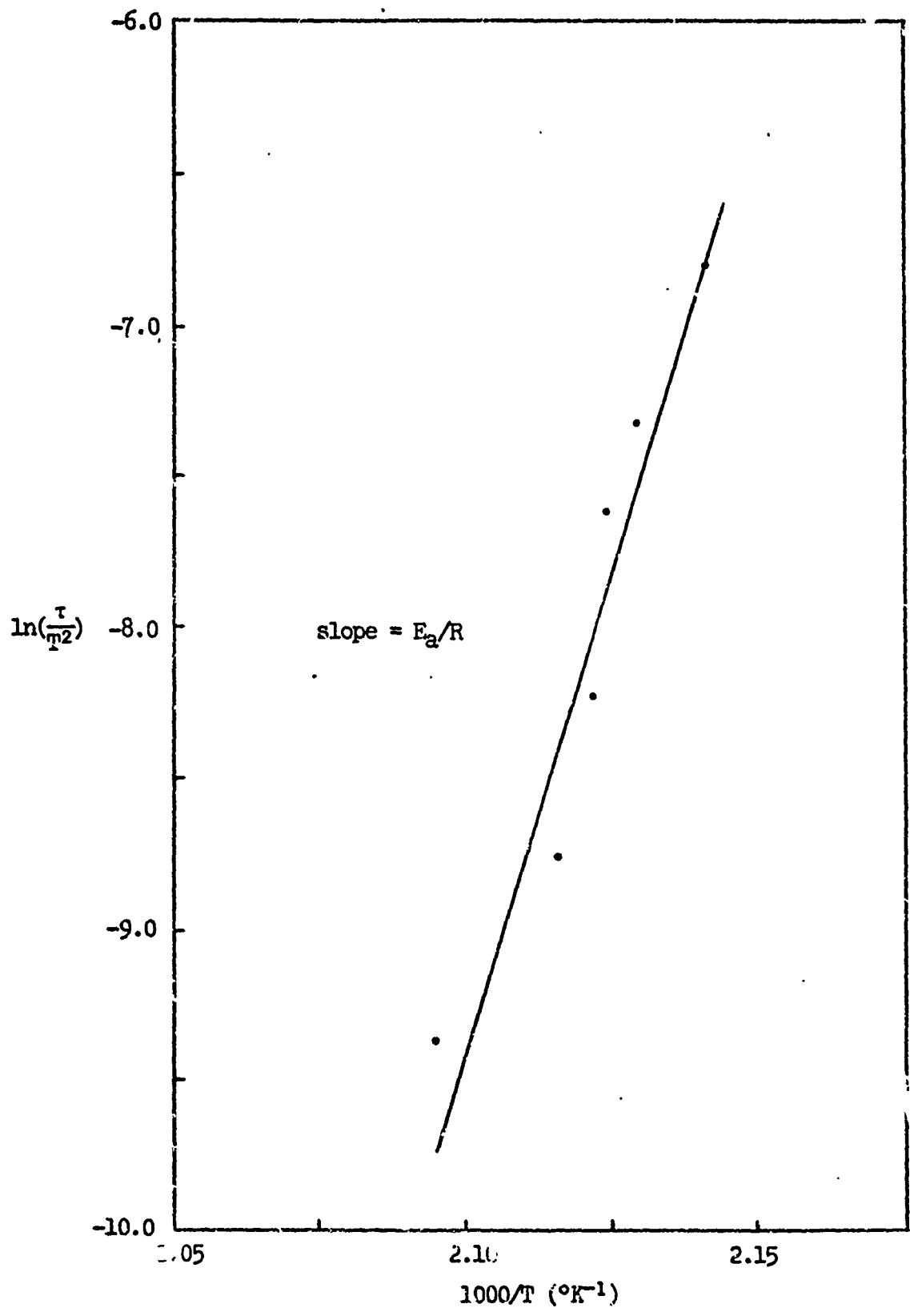


FIGURE 48: $\ln(\tau/T^2)$ vs. $1000/T$

APPENDIX A

HEATING RATE VS. PEAK TEMPERATURE, 500.00-530.50°K

$$\text{HEATING RATE} = \frac{A R T_m^2}{E_a} e^{-E_a/RT_m}$$

$$A = 6.91985 \times 10^{20}$$

$$E_a = 49,471.30 \text{ cal/mole}$$

$$R = 1.987 \text{ cal/mole } ^\circ\text{K}$$

TEMP. DEG K	RATE	TEMP. DEG K	RATE
500.00	1.64513	515.50	7.81557
500.50	1.73252	516.00	8.20592
501.00	1.82433	516.50	8.61496
501.50	1.92082	517.00	9.04354
502.00	2.02223	517.50	9.49271
502.50	2.12876	518.00	9.96309
503.00	2.24065	518.50	10.45597
503.50	2.35825	519.00	10.97224
504.00	2.48174	519.50	11.51268
504.50	2.61146	520.00	12.07884
505.00	2.74766	520.50	12.67184
505.50	2.89069	521.00	13.29251
506.00	3.04084	521.50	13.94250
506.50	3.19853	522.00	14.62290
507.00	3.36404	522.50	15.33508
507.50	3.53773	523.00	16.08067
508.00	3.72009	523.50	16.86069
508.50	3.91143	524.00	17.67717
509.00	4.11222	524.50	18.53172
509.50	4.32292	525.00	19.42580
510.00	4.54399	525.50	20.36110
510.50	4.77592	526.00	21.33943
511.00	5.01914	526.50	22.36304
511.50	5.27426	527.00	23.43390
512.00	5.54182	527.50	24.55339
512.50	5.82250	528.00	25.72473
513.00	6.11673	528.50	26.94904
513.50	6.42524	529.00	28.22940
514.00	6.74866	529.50	29.56830
514.50	7.08771	530.00	30.96779
515.00	7.44310	530.50	32.43098

APPENDIX B

HEATING RATE VS. PEAK TEMPERATURE, 500.00-530.50°K

$$\text{HEATING RATE} = \frac{A R T_m^2}{E_a} e^{-E_a/RT_m}$$

$$A = 1.70000 \times 10^{19}$$

$$E_a = 48,700.00 \text{ cal/mole}$$

$$R = 1.987 \text{ cal/mole } ^\circ\text{K}$$

TEMP. DEG K	RATE	TEMP. DEG K	RATE
500.00	0.08924	515.50	0.41415
500.50	0.09390	516.00	0.43452
501.00	0.09880	516.50	0.45585
501.50	0.10395	517.00	0.47818
502.00	0.10935	517.50	0.50156
502.50	0.11502	518.00	0.52603
503.00	0.12098	518.50	0.55165
503.50	0.12723	519.00	0.57847
504.00	0.13379	519.50	0.60654
504.50	0.14067	520.00	0.63590
505.00	0.14790	520.50	0.66665
505.50	0.15548	521.00	0.69880
506.00	0.16343	521.50	0.73244
506.50	0.17177	522.00	0.76763
507.00	0.18053	522.50	0.80446
507.50	0.18971	523.00	0.84296
508.00	0.19933	523.50	0.88323
508.50	0.20943	524.00	0.92535
509.00	0.22002	524.50	0.96939
509.50	0.23112	525.00	1.01545
510.00	0.24275	525.50	1.06359
510.50	0.25495	526.00	1.11392
511.00	0.26774	526.50	1.16653
511.50	0.28114	527.00	1.22153
512.00	0.29518	527.50	1.27901
512.50	0.30990	528.00	1.33906
513.00	0.32532	528.50	1.40185
513.50	0.34147	529.00	1.46742
514.00	0.35840	529.50	1.53594
514.50	0.37613	530.00	1.60753
515.00	0.39470	530.50	1.68233

APPENDIX C

RATE CONSTANT VS. ISOTHERMAL TEMPERATURE, 470.00-550.00 °K

$$k = A e^{-E_a/RT}$$

$$A = 6.91985 \times 10^{20}$$

$$E_a = 49,471.30 \text{ cal/mole}$$

$$R = 1.987 \text{ cal/mole } ^\circ\text{K}$$

TEMP. DEG K	K	TEMP. DEG K	K
470.00	0.00682	510.50	0.45627
470.50	0.00722	511.00	0.47857
471.00	0.00764	511.50	0.50191
471.50	0.00808	512.00	0.52634
472.00	0.00854	512.50	0.55192
472.50	0.00903	513.00	0.57868
473.00	0.00955	513.50	0.60666
473.50	0.01010	514.00	0.63599
474.00	0.01067	514.50	0.66664
474.50	0.01128	515.00	0.69871
475.00	0.01192	515.50	0.73225
475.50	0.01259	516.00	0.76733
476.00	0.01331	516.50	0.80402
476.50	0.01406	517.00	0.84239
477.00	0.01485	517.50	0.88252
477.50	0.01568	518.00	0.92446
478.00	0.01656	518.50	0.96833
478.50	0.01749	519.00	1.01416
479.00	0.01846	519.50	1.06209
479.50	0.01949	520.00	1.11218
480.00	0.02058	520.50	1.16454
480.50	0.02172	521.00	1.21923
481.00	0.02292	521.50	1.27640
481.50	0.02418	522.00	1.33613
482.00	0.02552	522.50	1.39852
482.50	0.02692	523.00	1.46371
483.00	0.02840	523.50	1.53179
483.50	0.02995	524.00	1.60290
484.00	0.03159	524.50	1.67718
484.50	0.03331	525.00	1.75475

APPENDIX C (continued)

TEMP. DEG K		K	TEMP. DEG K		K
485.00	--	0.03512	525.50	--	1.83574
485.50	--	0.03703	526.00	--	1.92029
486.00	--	0.03904	526.50	--	2.00858
486.50	--	0.04115	527.00	--	2.10077
487.00	--	0.04337	527.50	--	2.19696
487.50	--	0.04570	528.00	--	2.29741
488.00	--	0.04816	528.50	--	2.40220
488.50	--	0.05074	529.00	--	2.51157
489.00	--	0.05345	529.50	--	2.62573
489.50	--	0.05630	530.00	--	2.74482
490.00	--	0.05930	530.50	--	2.86910
490.50	--	0.06246	531.00	--	2.99872
491.00	--	0.06577	531.50	--	3.13397
491.50	--	0.06925	532.00	--	3.27501
492.00	--	0.07291	532.50	--	3.42214
492.50	--	0.07675	533.00	--	3.57555
493.00	--	0.08079	533.50	--	3.73556
493.50	--	0.08503	534.00	--	3.90243
494.00	--	0.08949	534.50	--	4.07638
494.50	--	0.09417	535.00	--	4.25776
495.00	--	0.09908	535.50	--	4.44687
495.50	--	0.10424	536.00	--	4.64402
496.00	--	0.10965	536.50	--	4.84947
496.50	--	0.11534	537.00	--	5.06354
497.00	--	0.12131	537.50	--	5.28675
497.50	--	0.12757	538.00	--	5.51929
498.00	--	0.13414	538.50	--	5.76161
498.50	--	0.14104	539.00	--	6.01412
499.00	--	0.14828	539.50	--	6.27721
499.50	--	0.15587	540.00	--	6.55121
500.00	--	0.16384	540.50	--	6.83666
500.50	--	0.17220	541.00	--	7.13399
501.00	--	0.18096	541.50	--	7.44369
501.50	--	0.19015	542.00	--	7.76624
502.00	--	0.19979	542.50	--	8.10215
502.50	--	0.20990	543.00	--	8.45181
503.00	--	0.22050	543.50	--	8.81602
503.50	--	0.23160	544.00	--	9.19509
504.00	--	0.24325	544.50	--	9.58973
504.50	--	0.25546	545.00	--	10.00054
505.00	--	0.26825	545.50	--	10.42831
505.50	--	0.28165	546.00	--	10.87339
506.00	--	0.29570	546.50	--	11.33659
506.50	--	0.31042	547.00	--	11.81863
507.00	--	0.32584	547.50	--	12.32022
507.50	--	0.34199	548.00	--	12.84212
508.00	--	0.35891	548.50	--	13.38532
508.50	--	0.37663	549.00	--	13.95021
509.00	--	0.39518	549.50	--	14.53783
509.50	--	0.41461	550.00	--	15.14928

APPENDIX D

RATE CONSTANT VS. ISOTHERMAL TEMPERATURE, 470.00-550.00 °K

$$k = A e^{-E_a/RT}$$

$$A = 1.7000 \times 10^{19}$$

$$E_a = 48,700.00 \text{ cal/mole}$$

$$R = 1.987 \text{ cal/mole } ^\circ\text{K}$$

TEMP. DEG K	K	TEMP. DEG K	K
470.00	0.00038	510.50	0.02398
470.50	0.00040	511.00	0.02513
471.00	0.00043	511.50	0.02634
471.50	0.00045	512.00	0.02760
472.00	0.00049	512.50	0.02892
472.50	0.00050	513.00	0.03030
473.00	0.00053	513.50	0.03174
473.50	0.00056	514.00	0.03325
474.00	0.00059	514.50	0.03483
474.50	0.00063	515.00	0.03647
475.00	0.00066	515.50	0.03820
475.50	0.00070	516.00	0.04000
476.00	0.00074	516.50	0.04188
476.50	0.00078	517.00	0.04385
477.00	0.00082	517.50	0.04590
477.50	0.00087	518.00	0.04805
478.00	0.00092	518.50	0.05029
478.50	0.00097	519.00	0.05264
479.00	0.00102	519.50	0.05508
479.50	0.00108	520.00	0.05764
480.00	0.00113	520.50	0.06031
480.50	0.00120	521.00	0.06310
481.00	0.00126	521.50	0.06601
481.50	0.00133	522.00	0.06905
482.00	0.00140	522.50	0.07222
482.50	0.00148	523.00	0.07553
483.00	0.00156	523.50	0.07899
483.50	0.00164	524.00	0.08260
484.00	0.00173	524.50	0.08637
484.50	0.00182	525.00	0.09030

APPENDIX D (continued)

TEMP. DEG K		K	TEMP. DEG K		K
485.00	-	0.00192	525.50	-	0.09440
485.50	-	0.00202	526.00	-	0.09868
486.00	-	0.00213	526.50	-	0.10314
486.50	-	0.00224	527.00	-	0.10780
487.00	-	0.00236	527.50	-	0.11266
487.50	-	0.00249	528.00	-	0.11772
488.00	-	0.00262	528.50	-	0.12301
488.50	-	0.00276	529.00	-	0.12852
489.00	-	0.00290	529.50	-	0.13427
489.50	-	0.00306	530.00	-	0.14026
490.00	-	0.00322	530.50	-	0.14651
490.50	-	0.00339	531.00	-	0.15303
491.00	-	0.00356	531.50	-	0.15982
491.50	-	0.00375	532.00	-	0.16690
492.00	-	0.00394	532.50	-	0.17427
492.50	-	0.00415	533.00	-	0.18196
493.00	-	0.00436	533.50	-	0.18998
493.50	-	0.00459	534.00	-	0.19833
494.00	-	0.00482	534.50	-	0.20703
494.50	-	0.00507	535.00	-	0.21609
495.00	-	0.00533	535.50	-	0.22553
495.50	-	0.00561	536.00	-	0.23533
496.00	-	0.00589	536.50	-	0.24562
496.50	-	0.00619	537.00	-	0.25629
497.00	-	0.00651	537.50	-	0.26741
497.50	-	0.00684	538.00	-	0.27899
498.00	-	0.00719	538.50	-	0.29104
498.50	-	0.00755	539.00	-	0.30359
499.00	-	0.00793	539.50	-	0.31665
499.50	-	0.00833	540.00	-	0.33026
500.00	-	0.00875	540.50	-	0.34442
500.50	-	0.00919	541.00	-	0.35916
501.00	-	0.00965	541.50	-	0.37451
501.50	-	0.01013	542.00	-	0.39047
502.00	-	0.01064	542.50	-	0.40710
502.50	-	0.01116	543.00	-	0.42439
503.00	-	0.01172	543.50	-	0.44238
503.50	-	0.01230	544.00	-	0.46110
504.00	-	0.01291	544.50	-	0.48058
504.50	-	0.01355	545.00	-	0.50084
505.00	-	0.01421	545.50	-	0.52192
505.50	-	0.01491	546.00	-	0.54383
506.00	-	0.01564	546.50	-	0.56664
506.50	-	0.01641	547.00	-	0.59034
507.00	-	0.01721	547.50	-	0.61501
507.50	-	0.01805	548.00	-	0.64065
508.00	-	0.01893	548.50	-	0.66731
508.50	-	0.01985	549.00	-	0.69502
509.00	-	0.02081	549.50	-	0.72384
509.50	-	0.02182	550.00	-	0.75378

LIST OF REFERENCES

1. Hondee, W., The Thermal Decomposition of β -HMX, Masters Thesis, U.S. Naval Postgraduate School, June 1971.
2. Kissinger, H. E., "Reaction Kinetics in Differential Thermal Analysis," Anal. Chem., v. 29, p. 1702-1706, 1957.
3. Navweps Report 7948, Effects of Thermal Aging on a Cast-Composite Propellant, by F. Kuletz and J. M. Pakulak, Jr., p. 1-3, October 1962.
4. Navweps Report 7646, Calculation of Critical Temperature and Time-to-Explosion for Propellants and Explosives, by P. A. Longwell, p. 1-3, March 1961.
5. Maycock, J. N. and Pai Verneker, V. R., "Characterization of Thermal and Photosublimation of Organic Explosives by Thermobarogravimetric Techniques," Thermochimica Acta, v. 1, No. 2, p. 191-198, 1970.
6. Navweps Report 7612, Thermal-Rate Studies on a Double-Base Propellant using a Derivative Differential Thermal-Analysis Technique, by J. M. Pakulak, p. 1-4, 17 January 1961.
7. Picatinny Arsenal Contract No. DAAA-2168-C-0334, Studies of Composition B-Final Report, by F. C. Rauch and R. B. Wainright, p. 21-32, February 1969.
8. Navweps Report 7769, Differential Thermal Analysis as a Research Tool in Characterizing New Propulsion Systems, by P. G. Rivette and E. D. Besser, p. 1-9, October 1961.
9. Robertson, A. J. B., "The Thermal Decomposition of Explosives," Trans Faraday Soc., v. 45, p. 85-92, 1949.
10. DuPont 900 Differential Thermal Analyzer Instruction Manual, E. I. DuPont de Nemours & Co. (Inc.), Wilmington, Delaware.